TELECOMMUNICATIONS

PROPERTY OF MELPAR, INC.

English Edition of

ЭЛЕКТРОСВЯЗЬ

No.2 February 1961

Published by the American Institute of Electrical Engineers
with the aid of a grant from the National Science Foundation

Translated and Produced by Royer and Roger, Inc.

AMERICAN INSTITUTE OF ELECTRICAL ENGINEERS

Established 1884

33 West Thirty-ninth Street
New York 18, New York

Warren H. Chase, President
N.S. Hibshman, Executive Secretary
C.E. Dean, Technical Vice President, Communications
W.F. Denkhaus, Director of Publications
L.G. Abraham, Chairman, Communications Division

The English edition of TELECOMMUNICATIONS is published by the American Institute of Electrical Engineers with the aid of a grant from the National Science Foundation. © 1961 by American Institute of Electrical Engineers. Also published under the same arrangement are the Russian electronic journals RADIO ENGINEERING AND ELECTRONICS and RADIO ENGINEERING.

TELECOMMUNICATIONS

(ЭЛЕКТРОСВЯЗЬ)

Publication of the
A.S. Popov Technical Society of Radio Engineering and Telecommunications

Translated and Produced
by
Royer and Roger, Inc.

Translation Editor: Jack Warren, Columbia University

AIEE REVIEW COMMITTEE FOR TELECOMMUNICATIONS
H.F. May
Bell Telephone Laboratories, Inc.
Chairman

A.G. Cooley
A.D. Fowler
A.E. Frost
F.G. Hollins
A.E. Joel
A.D. Moore
W.B. Quirk
L.L. Robinett
R.B. Shanck
D.L. Solomon
F.W. Smith
G. Worthen

Subscriptions to Telecommunications should be sent to AIEE
Special Subscription Department
41 East 28th Street
New York 16, New York

1961 Subscription rates:

	$	£
Individuals	14.25	5
Libraries, institutes, govt. agencies	28.50	10

12 issues per annum comprising approximately 1100 pages

PASSAGE OF FM OSCILLATIONS THROUGH APERIODIC AMPLIFIER

V.L. Rychka

The article examines the chief features of passage of FM oscillations through an aperiodic amplifier. It introduces the condition of amplifier quasistability and also derives a design formula for the quantity of nonlinear distortion of the FM signal during its passage through an aperiodic amplifier.

The works of our scientists [1, 2, 3] have examined the problem of passage of FM oscillations through tuned amplifiers and bandpass amplifiers as well as the distortion of FM signals in these amplifiers. To the best knowledge of the author, the chief regularities of FM signals passing through aperiodic amplifiers, have not been investigated, for until recently such a problem had not been confronted in practice — FM receivers used high intermediate frequency and tuned or bandpass amplifiers.

However, in recent years discriminators with pulse circuits have come into use, particularly a detector of the pulse-counter type [4, 5]. Without giving a description of the operation and analysis of the circuit, we will note that for normal operation of the detector the intermediate frequency of the FM receiver should be on the order of 200-300 kc; that is, in such a receiver it is necessary to use an aperiodic i-f amplifier.

In addition, the need for an aperiodic amplifier of FM signals may arise in various measuring devices and in automatic control units.

In this connection it is advisable to examine in detail the passage of FM oscillations through an aperiodic amplifier, employing the procedure already developed for tuned amplifiers and bandpass amplifiers.

SOURCES OF FM SIGNAL DISTORTION IN AN AMPLIFIER

In [2, 6] it is stated that the FM signal in an amplifier is distorted due to transient processes and slope of the phase characteristic.

If the transient process in the amplifier occurs much more rapidly than the signal varies, then the amplifier is quasistable and the effect of the transient process on the output voltage may be neglected. In tuned amplifiers the rate of the transient process is described in the well-known envelope theorem and the nature of the transient process consists in a gradual increase in amplitude of the voltages at the amplifier output with application of a radio pulse at its input. The known condition of quasistability of a tuned amplifier is derived from this statement.

In the same manner it is necessary to examine the transient process in an aperiodic amplifier and to deduce for it the condition of quasistability.

If the frequency at input of any quasistable amplifier varies sinusoidally, then the variation in frequency at the output obeys the following

rule [6]:

$$\omega_{out} = \omega_0 + \Delta\omega \sin \Omega t + \frac{d\tau(\omega)}{d\omega} \Delta\omega\Omega \cos \Omega t, \quad (1)$$

where ω_0 is the average frequency of input voltage, Ω is the modulating frequency, $\Delta\omega$ is the maximum frequency deviation at the input, $\varphi(\omega)$ is the phase response of the amplifier.

Presence of the third term in (1) indicates the possibility of frequency-amplitude and nonlinear distortion of the FM signal.

In fact, even if the phase characteristic is ideal (that is, $\varphi = k\omega$)

$$\omega_{out} = \omega_0 + \Delta\omega \sqrt{1 + \kappa^2 \Omega^2} \sin(\Omega t + \varphi).$$

Consequently, frequency deviation at the amplifier output, strictly speaking, does not remain constant but increases with the modulation frequency and slope of the phase characteristic. However, calculations show that in the multi-stage amplifiers commonly used, the total slope of the phase characteristic and the modulating frequency are not considerable and the mentioned distortions may be ignored. At the same time, in precise measurement of the frequency response of a transmitter (dependence of frequency deviation on modulating frequency) and in other special cases there arises the necessity of considering frequency-amplitude distortions of the FM signal in the amplifier.

If the phase characteristic is nonlinear, this leads to nonlinear distortion of the FM signal, depending on the slope of the phase characteristic and on the modulating frequency.

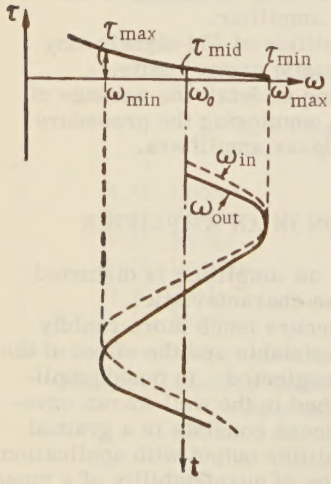

Figure 1

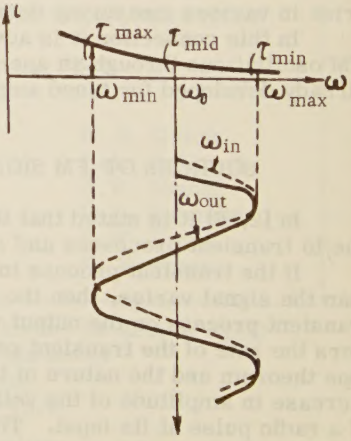

Figure 2

For proper selection of amplifier parameters and the required passband it is necessary to derive the equation of the phase characteristic, insert it into (1) and calculate the nonlinear distortion factor. This method is used in [3] for tuned amplifiers and is used here for aperiodic FM-signal amplifiers.

First, let us note that expression (1) was derived by formal, mathematical means. It is expedient to examine graphically the process of distortion in the amplifier due to the curve of the phase response.

If the phase characteristic is nonlinear, then the signal lag time $\tau = \frac{d\varphi}{d\omega}$ does not remain constant during modulation. For example, let τ vary as in Figures 1 and 2 while the frequency at the amplifier input varies sinusoidally from ω_{min} to ω_{max}. Figure 1 corresponds to a low modulating frequency and Figure 2 corresponds to a high modulating frequency. For a graphic plot of the curve of output-voltage frequency variation it is necessary to displace all points of the sinusoid to different segments along the time axes defined by the plot of $\tau(\omega)$. Because all these time segments are not identical, the sinusoid of frequency variation is distorted and, as is seen from comparison of Figures 1 and 2, the higher the modulation frequency, the greater the distortion.

TRANSIENT PROCESS IN AN APERIODIC AMPLIFIER

With a change in frequency at the input of any amplifier there arises in it a transient process, the voltage of which depends on the rate of change in frequency, according to the law of modulation. It is evident that the most significant transient process arises in the practical case of pulse-frequency modulation. Here the frequency at the amplifier input changes instantly from ω_1 to ω_2, wherein the initial phases of both oscillations, as well as the instant of change, may be arbitrary.

The study of transients is most simply performed by the operational method, for which the zero initial conditions are required. In the given case it is evident that they are not known. Hence, we shall use the artificial method. Let us assume that before and after the jump a continuous voltage of frequency ω_1 is applied at the amplifier input, but at the instant of change, two voltage pulses are applied: one with frequency ω_2 and arbitrary phase, the other with frequency ω_1 but with initial phase precisely opposite to the phase of the existing oscillations at the instant of change. It is also evident that the performed substitution is equivalent — on the basis of the principle of superposition. Hence, the real transient process in any amplifier with pulse-frequency modulation may be considered as the sum of two transient processes arising upon the application of two sinusoidal voltage pulses at the amplifier input.

Let us use this general method, described in [8], for the particular case of an aperiodic amplifier. We shall first examine the transient process upon application of a sinusoidal voltage pulse at the amplifier input

$$u_{in}(t) = \begin{cases} U_m \sin(\omega t + \varphi) & \text{with } t \geqslant 0 \\ 0 & \text{with } t < 0. \end{cases} \qquad (2)$$

As is known [2], the transform of the input-voltage function has the form

$$U_{in}(p) = \frac{U_m}{p^2 + \omega^2}(p \sin\varphi + \omega \cos\varphi), \qquad (3)$$

while the transfer function of the aperiodic amplifier

$$K(p) = \frac{K_0 p \tau_g}{1 + p\tau_g + p^2 \tau_g \tau_a}, \tag{4}$$

where τ_g and τ_a are the time constants of the grid and plate circuits of the amplifier stage, and K_0 is the amplifier gain at mid frequencies.

Applying the conventional method of Laplace transforms and the theory of residues in a complex plane, and omitting intermediate calculations, we obtain the following expressions for voltage at the amplifier output with $t \geqslant 0$:

$$u_{out}(t) = U_m K_0 \left\{ \frac{\sin(\omega t + \varphi + \alpha - \beta)}{\sqrt{1 + \left(\omega\tau_a - \frac{1}{\omega\tau_g}\right)^2}} - \frac{\sin(\varphi - \beta)}{\sqrt{1 + \omega^2\tau_a^2}} e^{-\frac{t}{\tau_a}} - \right.$$

$$\left. - \frac{\cos(\varphi + \alpha)}{\sqrt{1 + \omega^2\tau_g^2}} e^{-\frac{t}{\tau_g}} \right\}, \tag{5}$$

where

$$\operatorname{tg}\alpha = \frac{1}{\omega\tau_g}, \quad \operatorname{tg}\beta = \omega\tau_a.^*$$

The first term in parentheses obviously corresponds to the steady-state process of transmission of a sinusoidal voltage by an aperiodic amplifier, and the second and third terms describe the transient process.

From equation (5) there flow certain peculiarities of the transient process which proves to differ considerably from the transient process in a tuned amplifier.

One distinctive feature of the transient process lies in the fact that the output voltage is the algebraic sum of the sinusoidal signal and two exponential pulses, the rate of decay of which is determined by the time constants of the plate and cathode circuits of the amplifier. Amplitude of the sinusoidal oscillation during the transient process remains constant.

The initial value and polarity of the pulses depend on the instantaneous phase of the sinusoidal input voltage at the moment of connection and on the intermediate frequency.

In practice the time constant τ_g is sufficiently great, hence, the third term in (5) decreases rapidly and $\alpha \approx 0$.

At the initial moment

$$u_{out}(0) = U_m K_0 \left\{ \frac{\sin(\varphi - \beta)}{\sqrt{1 + \omega^2\tau_a^2}} - \frac{\sin(\varphi - \beta)}{\sqrt{1 + \omega^2\tau_a^2}} - \frac{\cos\varphi}{\sqrt{1 + \omega^2\tau_g^2}} \right\} \approx 0.$$

Consequently, whatever the phase of the input pulse, there arises in the amplifier such a transient process that the total output voltage is equal

---

*tg = tan (transl.)

to zero. This means that the maximum voltage of the transient process is equal to $U_m K_0$ (that is, the amplitude of the steady-state output voltage).

Neglecting the effect of τ_g on the transient process, we obtain the expression for output voltage

$$u_{out}(t) = U_m K_0 \frac{\sin(\omega t + \varphi - \beta) - \sin(\varphi - \beta) e^{-\frac{t}{\tau_a}}}{\sqrt{1 + \omega^2 \tau_a^2}}. \quad (6)$$

Let us turn now to the presented problem of pulse-frequency modulation.

If with $t < 0$ there is applied to the amplifier input for a sufficient length of time a voltage of the form

$$u_1(t) = U_m \sin(\omega_1 t + \varphi_1),$$

then at the moment $t = 0$ it is necessary to apply to the input the radio pulses

$$u_2(t) = U_m \sin(\omega_1 t + \varphi_1 + \pi) \text{ and } u_3(t) = U_m \sin(\omega_2 t + \varphi_2).$$

Then, with $t > 0$, the steady-state voltages from the first two terms cancel each other and the total output voltage has the form

$$u_{out}(t) = U_m K_0 \left\{ \frac{\sin(\omega_2 t + \varphi_2 - \beta) - \sin(\varphi_2 - \beta) e^{-\frac{t}{\tau_a}}}{\sqrt{1 + \omega_2^2 \tau_a^2}} - \right.$$

$$\left. - \frac{\sin(\varphi_1 + \pi - \beta)}{\sqrt{1 + \omega_1^2 \tau_a^2}} e^{-\frac{t}{\tau_a}} \right. . \quad (7)$$

The transient voltage is approximately equal to

$$u_{out}(t)_{trans.} = U_m K_0 [\sin(\varphi_1 - \beta) - \sin(\varphi_2 - \beta)] e^{-\frac{t}{\tau_a}}.$$

If the phase of an oscillation with frequency ω_2, applied at instant $t = 0$, is equal to the phase of an existing oscillation with frequency ω_1, then the transient process is absent (Figure 3).

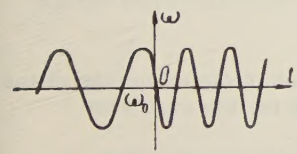

Figure 3

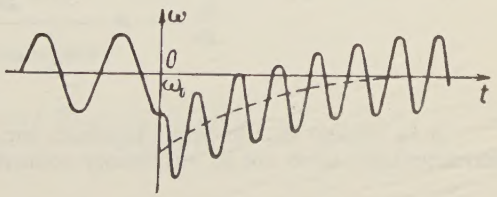

Figure 4

If the phases are opposed, then the transient process is more intense and the voltage at the initial moment in the case $\varphi_1 - \beta = \frac{\pi}{2}$ is equal to $2U_m K_0$ (Figure 4).

The amplifier is considered quasistable if the transient voltage becomes much smaller than the existing voltage during the minimum period of the modulating frequency. In the given case this condition reduces to the following:

$$2U_m K_0 e^{-\frac{T_{min}}{\tau_a}} < U_m K_0$$

or

$$2e^{-\frac{1}{\tau_a F_{max}}} < 1. \tag{7}$$

If, for example, the upper frequency of the amplifier passband is only 200 kc, then even with frequency F = 15 kc we obtain

$$e^{-\frac{1}{\tau_a F_{max}}} = e^{-60} \approx 0.$$

The condition of quasistability is fulfilled with a large margin. Thus, the aperiodic amplifier intended for amplification of FM oscillations may be considered quasistable and on this basis we may neglect the effect of the transient process on the FM signal.

NONLINEAR DISTORTION IN AMPLIFIER

Let us examine the influence of the slope of the phase characteristic of an aperiodic amplifier on the quantity of nonlinear distortion of the FM signal.

Let there be an n-stage amplifier without any compensation. The phase characteristic equation is

$$\varphi = -n \operatorname{arctg}\left(\omega\tau_a - \frac{1}{\omega\tau_g}\right). \tag{8}$$

In accordance with (1) it is necessary to calculate the frequency derivative from (8)

$$\frac{d\varphi}{d\omega} = -n \frac{\tau_a + \frac{1}{\omega^2 \tau_g}}{1 + \left(\omega\tau_a - \frac{1}{\omega\tau_g}\right)^2}.$$

It is evident that in order to obtain small values of distortion the phase characteristic must not be extremely contorted; that is, the argument

$$\omega\tau_a - \frac{1}{\omega\tau_g} < 1.$$

Hence

$$\frac{d\varphi}{d\omega} = -n\left(\tau_a + \frac{1}{\omega_0^2 \tau_g}\right)\left[1 - \left(\omega\tau_a - \frac{1}{\omega\tau_g}\right)^2\right], \tag{9}$$

or, considering that $\tau_a \ll \tau_g$

$$\frac{d\varphi}{d\omega} = -n\left(\tau_a - \omega^2\tau_a^3 + \frac{1}{\omega^2 \tau_g} - \frac{1}{\omega^4 \tau_g^3}\right).$$

But

$$\omega = \omega_0 + \Delta\omega \sin \Omega t,$$

$$\omega^2 \approx \omega_0^2 + 2\omega_0 \Delta\omega \sin \Omega t - \frac{1}{2}\Delta\omega^2 \cos 2\Omega t,$$

$$\frac{1}{\omega^2} \approx \frac{1}{\omega_0^2}\left(1 - 2\frac{\Delta\omega}{\omega_0} \sin \Omega t - \frac{3}{2}\frac{\Delta\omega^2}{\omega_0^2} \cos 2\Omega t\right),$$

$$\frac{1}{\omega^4} \approx \frac{1}{\omega_0^4}\left(1 - 4\frac{\Delta\omega}{\omega_0} \sin \Omega t - 5\frac{\Delta\omega^2}{\omega_0^2} \cos 2\Omega t\right).$$

Inserting these results into (9), transposing and omitting small terms of higher order, we obtain

$$\frac{d\varphi}{d\omega} = -n\left[\left(\tau_a + \frac{1}{\omega_0^2 \tau_g}\right) - 2\Delta\omega\left(\omega_0\tau_a^3 + \frac{1}{\omega_0^3 \tau_g}\right)\sin \Omega t + \right.$$
$$\left. + \frac{\Delta\omega^2}{2}\left(\tau_a^3 - \frac{3}{\omega_0^4 \tau_g}\right)\cos 2\Omega t\right]. \tag{10}$$

Let us insert (10) into (1):

$$\omega_{out} = \omega_0 + \Delta\omega \sin \Omega t + n\left(\omega_0\tau_a^3 + \frac{1}{\omega_0^3 \tau_g}\right)\Delta\omega^2 \Omega \cos 2\Omega t +$$
$$+ n\left(\tau_a^3 - \frac{3}{\omega_0^4 \tau_g}\right)\frac{\Delta\omega^3}{4}\Omega \cos 3\Omega t.$$

The second-harmonic distortion factor

$$K_2 = n\left(\omega_0 \tau_a^3 + \frac{1}{\omega_0^3 \tau_g}\right)\Delta\omega\Omega, \tag{11}$$

and the third-harmonic distortion factor

$$K_3 = n\left(\tau_a^3 - \frac{3}{\omega_0^4 \tau_g}\right)\frac{\Delta\omega^2 \Omega}{4}. \tag{12}$$

If the chosen intermediate frequency is high or τ_g is great, then distortion originating in the plate circuit of the amplifier is defined by factors

$$K_{2a} = n\omega_0 \tau_a^3 \Delta\omega\Omega,$$

$$K_{3a} = \frac{1}{4} n\tau_a^3 \Delta\omega^2\Omega.$$

It is evident that third-harmonic distortions are negligibly small and discussion may be limited to second-harmonic distortion, which increases in proportion to the intermediate and modulating frequencies.

If we neglect the effect of τ_a, then distortion originating in the grid circuit of the amplifier is

$$K_{2g} = \frac{n\Delta\omega\Omega}{\omega_0^3 \tau_g},$$

$$K_{3g} = \frac{3n\Delta\omega^2\Omega}{4\omega_0^4 \tau_g}.$$

In this case, too, the major role is played by second-harmonic distortion, which increases with decreasing intermediate frequency in cubic-hyperbola fashion.

The minimum nonlinear distortion occurs on the condition

$$\omega_{0\,opt} = \frac{1.3}{\tau_a} \sqrt[4]{\frac{\tau_a}{\tau_g}}.$$

In this case, third-harmonic distortion, as is easily shown, reverts to zero.

If we assume that $\Delta f = 50$ kc and $F_{max} = 15$ kc, then from (11) we obtain the following design formula:

$$K_2\,\% = 18.6 n\tau_a^2 \mu\,\text{sec.} \left(f_0 \tau_a + \frac{1}{1550 f_0^3 \tau_g \tau_a^2} \right). \qquad (13)$$

On the basis of (13) calculation of the nonlinear distortion factor was performed for one stage of amplification with various τ_g and τ_a. The results are given in the form of curves in Figure 5.

These results show that even with $\tau_a \leqslant 0.3$ μsec. $\tau_g \geqslant 80$ μsec. nonlinear distortion in the amplifier is small. The first inequality shows that steep slope of the frequency response curve to the 0.7-level is permissible at 500 kc; that is, in most cases an amplifier circuit without any upper-frequency compensation may be used. It follows from the second inequality that all frequencies below 2 kc may not be passed through the amplifier, which permits decreasing the coupling and bypass capacitors. This lowers the weight, cost and dimensions of the amplifier and increases its stability.

It should be mentioned that in practice [7] the passband of an aperiodic amplifier is increased considerably in both the low-frequency direction (to 30-50 cycles) and the high-frequency direction (to 2-4 Mc) by the use of frequency compensation circuits and low-resistance plate loads. The conclusions given here on the basis of observed regularities in passage of fm oscillations through an aperiodic amplifier show that these measures are

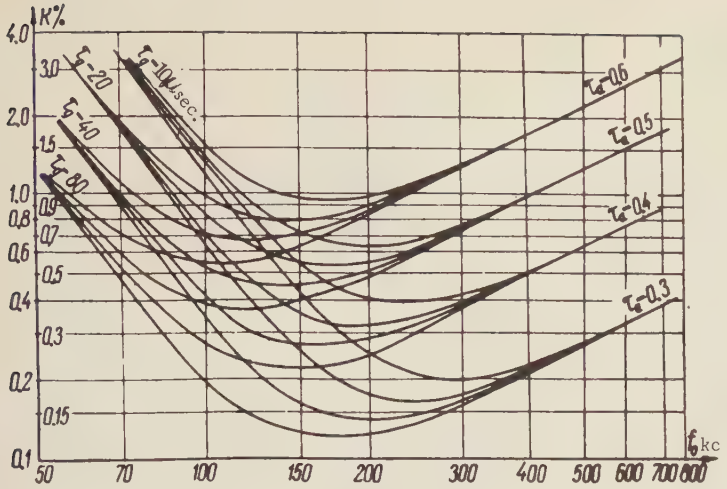

Figure 5

unnecessary.

Tests revealed the accuracy of the conclusions given here, with the result that there was developed an aperiodic i-f amplifier for an FM broadcast receiver with 6N15P dual triodes, without compensation of upper frequencies and with plate load resistance on the order of 27 kilohms.

It must also be pointed out that the phase characteristic and nonlinear distortion level of the FM signal in an aperiodic amplifier are stable in time and are relatively independent of tube replacements, supply fluctuations, and vibration. This represents a considerable advantage of aperiodic i-f amplifiers over tuned i-f amplifiers in FM operation.

In conclusion let us discuss the tolerance for increase in signal delay at given nonlinear distortion.

From (10) we find that the increment

$$\Delta\tau = \Delta\left(\frac{d\varphi}{d\omega}\right) = 2n\Delta\omega\left(\omega_0\tau_a^3 + \frac{1}{\omega_0^3\tau_g}\right),$$

or, on the basis of (11).

$$\Delta\tau = \frac{2K_2}{\Omega}. \qquad (14)$$

This is an extremely convenient design formula. If, for example, $K_2 = 1\%$ and $F_{max} = 15$ kc, then $\Delta\tau = 0.2\ \mu$sec. which for a frequency deviation of 50 kc corresponds to deviation of the phase characteristic from the linear by

$$\Delta\varphi = \Delta\tau\Delta\omega \approx 4^\circ.$$

This meets requirements with regard to irregularity of phase characteristic within a range of 50 kc.

CONCLUSION

Analysis of passage of an FM signal through an aperiodic amplifier has shown that this amplifier is usually quasistable (that is, the transient process therein occurs quite rapidly and may be disregarded.

It is not difficult to insure extremely low nonlinear distortion; hence, the amplifier circuit is simple and the parameters stable. This opens wide possibilities for use of aperiodic i-f amplifiers for FM signals on the condition that required selectivity is not high.

The author expresses cordial thanks to V.M. Sidorov and S.M. Khlytchiyev for their interest and assistance in working out the principal problems.

Article submitted to editors 17 February 1960

LITERATURE

1. S.I. Yevtyanov, Perekhodnyye protsessy v priyemno-usilitel'nykh skhemakh [Transient processes in receiver amplifier circuits]. Svyaz'izdat, 1948.
2. I.S. Gonorovskiy, Radiosignaly i perekhodnyye yavleniya v radiotsepyakh [Radio signals and transients in radio circuits]. Svyaz'izdat, 1954.
3. Ye. I. Manayev, "On the bandwidth required for absence of nonlinear distortion in FM reception." Radiotekhnika, No. 5, 1948.
4. Scroggie, "Low distortion FM discriminator." Wireless World, April, 1956.
5. Glaser, "Die Impulszahlschaltung als FM-Demodulator." Radio und Fernsehen, No. 22, 1958.
6. S.V. Person, "Nonlinear distortion in FM amplification." Radiotekhnika, No. 6, 1951.
7. A.V. Zen'kovich et al., "Modern methods and instruments for measuring frequency deviation." NTSb GKRE, No. 2 (6), 1958.
8. I.S. Gonorovskiy, Chastotnaya modulyatsiya i yeye primeneniye [Frequency modulation and its application]. Svyaz'izdat, 1948.

MINIATURE DELAY LINE WITH HIGH RESOLUTION

V.A. Solov'yev

The article presents analysis of a delay line with distributed constants. For compensation of characteristics, the line is divided into sections by means of short-circuited coils. A method of calculation is given which is based on time relationships and on the best approximation of the group propagation time to a constant value within a definite interval. A rule is given for determining the rise time of a spiral line from the amplitude-frequency characteristic.

INTRODUCTION

Delay lines are widely used in television, radar, measurement engineering and, especially, in electronic automation and computer engineering where they find mass application. The presently typical effort to increase the efficiency of electronic automation and computer engineering is associated with an increase in high-speed operation, an increase in the number of elements and a decrease in dimensions. The range of required characteristic impedances lies in the region from 1.5 kilohms to 0.3 kilohms, which is associated in particular with the use of semiconductor devices.

In this connection delay lines must meet the following requirements:

1. High resolution;
2. Miniaturization;
3. Simple construction, permitting mass production.

The requirement of high resolution, or small value of rise time, is wholly met only by delay lines with distributed constants. The method of design of delay lines with distributed constants discussed in this report permits obtaining structurally simple lines with volume $V < 1$ cm^3 with rise time of transfer characteristic $\tau_r \geqslant 20 \cdot 10^{-9}$ sec and characteristic impedance $Z_0 \geqslant 0.3$ kilohm for delay values of $T_d = (10 \text{ to } 15)\,\tau_r$. The core diameter D = 4 to 5 mm, wire diameter D = 0.05 mm, the number of slots in the core $N \geqslant 16$, that is, 30 to 60 times less than other existing designs of high-frequency delay lines with distributed constants [1].

A distinctive feature of this construction is division of the line into sections shielded by shorted coils. Thereby there is achieved adequate attenuation of coupling between sections. The parameters of each section are determined on the basis of its design equivalent in the form of an m-derived low-frequency mesh, which is permissible due to its short electrical length.

This insures better utilization of the passband and provides considerably more effective compensation of the line characteristics in comparison with other methods of compensation of delay lines with distributed constants [1].

Usually the use of m-derived sections leads to considerable increase in the size of the line due to the necessity for separating the sections from one another in order to avoid parasitic coupling. The use of shorted coils eliminates this disadvantage. The line sections are placed close together and represent a single continuous coil on an insulated conducting core. A substantial advantage of a line section with distributed parameters in comparison with an m-derived section with lumped L and C elements is the large passband. The miniature dimensions of this design are the result of the use of conductors of small diameter d = 0.05 to 0.1 mm.

SHIELDING OF DELAY LINE SECTIONS WITH DISTRIBUTED CONSTANTS BY SHORTED COILS

The shorted coils are positioned over a main winding on an insulating layer (Figure 1). The specifications for the shorted coils are determined by the shielding conditions of the section.

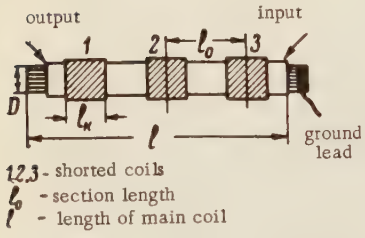

Figure 1

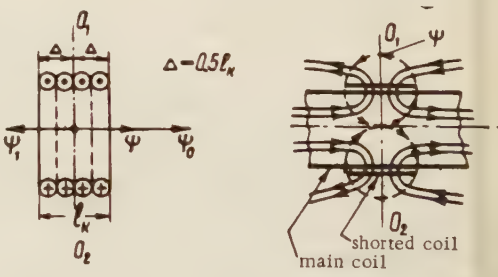

Figure 2

Let us designate the magnetic flux of the main coil of the line as $\bar{\psi}_0$, the flux created by current I_k in the shorted coil by $\bar{\psi}_1$, the resulting flux in the central section $0_1 - 0_2$ (Figure 2) of the shorted coil by $\bar{\psi}$

$$\bar{\psi} = \bar{\psi}_0 + L\bar{I}_к,$$

where L is the inductance of the shorted coil

$$\bar{I}_к = -i\omega \frac{\bar{\psi}}{r},$$

where r is the loss resistance of the shorted coil.

Now let us define the coefficient characterizing attenuation of the magnetic field in the central section of the shorted coil

$$n = \frac{|\psi_0|}{|\psi|} = \sqrt{1 + \left(\frac{\omega L}{r}\right)^2}.$$

This coefficient expresses the relationship between the parameters of the shorted coil. Since n $\gg$ 1 (in practice it is sufficient that n = 100), then

$$\frac{L}{r} \approx \frac{n}{\omega}. \qquad (1)$$

The formula for inductance of the coil may be expressed in the form [2]

$$L = L_0 W^2 D\, 10^{-9} \text{ h},$$

where $L_0 = \varphi\left(\frac{l}{D}\right)$, l is the coil length in cm, D is the coil diameter in cm, and W is the number of turns.

The loss resistance [2]

$$r = 5.25 \frac{DW}{d} \sqrt{f}\, 10^{-7},$$

where d is the conductor diameter in cm, f is the frequency in cps.

Using the last two expressions, we obtain

$$\frac{L}{r} = 1.9 \cdot 10^{-3} \frac{L_0 W d}{\sqrt{f}}. \qquad (2)$$

The length of the winding of the shorted coil is

$$l_к = \frac{W d q}{u},$$

where q is the winding density factor, u is the number of layers of the winding (u = 1 to 2).

Using expressions (1) and (2), we obtain

$$\frac{n}{2\pi \cdot f} = \frac{1.9 \cdot 10^{-3}}{\sqrt{f}} \frac{L_0 l_к \cdot u}{q}.$$

Let us introduce the designation

$$K = \frac{L_0 l_к u}{q}.$$

Hence,

$$K = \frac{n}{11.9\sqrt{f}},$$

where f is in Mc
and

$$l_к = K\frac{q}{uL_0} = \frac{K'}{L_0}, \tag{3}$$

where K' = Kq/u.

For a single-layer coil with l_k/D_k in the interval from 0.2 to 3 we may use for L_0 a formula given in [2] and yielding an accuracy of 1 percent.

$$L_0 = \frac{1000D_к}{101.7\,l_к + 45.6\,D_к},$$

which determines the following expressing for l_k:

$$l_к = \frac{45.6K'D_к}{1000\,D_к - 101.7\,K'}. \tag{4}$$

For a multi-layer coil (in practice, for a two-layer coil) with $0 < \frac{c}{D_к} < 0.25$ where c is the layer thickness of the coil, L_0 is determined with an accuracy of 2% from the formula

$$L_0 = \frac{1000}{45.6 + 101.7\,\frac{l_к}{D_к} + 85.3\,\frac{c}{D_к} + 65\,\frac{l_к c}{D_к^2}}.$$

Assuming that, on the average D_k = 4 to 6 mm and c/D = 0.08, we obtain

$$l_к = \frac{52.4\,K'D_к}{1000\,D_к - 107\,K'}. \tag{5}$$

Let us find the relationship between the diameters of the conductors of the main coil d and the shorted coils d_k. We shall use the formula for magnetic field strength at the center of a solenoid and along its axis, considering that $2l \gg D$. The shielding conditions are determined from the equality

$$\frac{W_к l_к}{\sqrt{D_к^2 + l_к^2}} = \frac{WI}{l},$$

where I is the current in the turns of the main coil.

Hence, considering that $W = W_0 l$, where W_0 is the number of turns per unit length, we obtain

$$\frac{l_к}{l} = \frac{W_0}{W_{0к}}\frac{\sqrt{D_к^2 + l_к^2}}{l_к}. \tag{6}$$

On the other hand,

$$\bar{I} \approx -i\omega \frac{\bar{\psi}}{r'},$$

$$\bar{I}_\kappa = +i\omega \frac{\bar{\psi}}{r'_\kappa},$$

which is applicable to that part of the main inductance coil and the shorted coil included in the total resulting magnetic flux ψ (Figure 2).

Whence

$$\frac{I_\kappa}{I} = \frac{W d_\kappa D}{W_\kappa d D_\kappa}.$$

On the basis of equality (6), let us write

$$\left.\begin{aligned} d_\kappa &= d \frac{W_0}{W} \frac{W_\kappa}{W_{0\kappa}} \frac{D_\kappa}{D} \frac{\sqrt{D_\kappa^2 + l_\kappa^2}}{l_\kappa} \\ d_\kappa &= d \sqrt{\left(\frac{D_\kappa}{l_\kappa}\right)^2 + 1} \end{aligned}\right\}, \qquad (7)$$

Let us examine the limitation on distance between the central sections of adjacent shorted coils (Figure 1) (or per length of section l_0) determined by the nonuniformity of the line. Associated with this distance is the amount of decay T_{do} of the section, determining the minimum frequency of the reflected signal arising at the butt of the sections

$$f_{\min \text{ ref}} = \frac{1}{2T_{do}}.$$

This frequency must lie beyond the passband of the delay line. In practice it will suffice if the level of the amplitude-frequency characteristic at this frequency is less than 0.1 of the level at mid-frequencies of the passband

$$\frac{1}{2T_{do}} > f_{0.1}. \qquad (8)$$

Conformity with this relationship insures the absence of distortion due to nonuniformity of the line caused by its separation into sections.

REQUIREMENTS FOR DELAY LINES IN HIGH-FREQUENCY PULSE CIRCUITS

(Pulse duration τ_u = (30 to 100) · 10^{-9} sec.)

Let us examine the most general pulse form (Figure 3).

Assuming $\tau_{\phi p} = \tau_{\phi z} = \tau_\phi$, let us express pulse duration as a coefficient, which we shall term the pulse-shape coefficient, A:

$$\tau_u = A\tau_\phi.$$

Let us find the maximum permissible rise time of the transfer

characteristic of the delay line τ_r at which transmission with maximum amplitude in matched operation is still obtained. For this purpose let us use the rise-time addition formula [3], considering the transfer characteristic of the delay line to be monotonic. (The formula affords an accuracy of 10% if the overshoot does not exceed 2%)

$$\tau_{r\,max} = \sqrt{(\tau_u - \tau_\phi)^2 - \tau_\phi^2} = \tau_\phi \sqrt{A(A-2)}. \qquad (9)$$

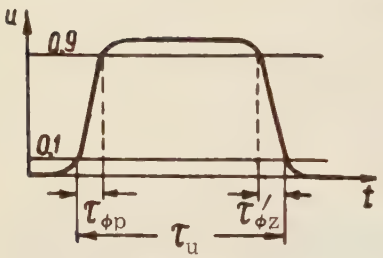

Figure 3

In practice, this formula may be used with sufficient accuracy on the condition that

$$\tau_L \leqslant 0.3\,\tau_r$$

where $\tau_L = \frac{2.3 R_L C_L}{2} = 1.15 R_L C_L$, R_L is the load resistance and C_L is the load capacitance.

With consideration of τ_L

$$\tau_{r\,max} = \tau_\phi \sqrt{A(A-2) - \left(\frac{\tau_L}{\tau_\phi}\right)^2}. \qquad (10)$$

In practice, for high-frequency circuits A = 2.5 to 3, while the pulse-shaping conditions and the requirements for reliability of operation lead to the inequality

$$\tau_{r\,max} < \tau_\phi \sqrt{A(A-2)}.$$

Let $\tau_{r\,max} = 0.9\,\tau_\phi \sqrt{A(A-2)}$.

Then, with A = 2.5, $\tau_{r\,max} = \tau_\phi$.

Calculation of shielding of the line sections with $B = \frac{T_d}{\tau_r} \ll 10$ to 12 must be performed for the upper frequency, basing this calculation on the pulse shape at the center of the delay line. (This value of B is characteristic for a line for mass application).

The pulse leading edge in the middle of the line

$$\tau_{\phi\,0.5} = \sqrt{0.5\,\tau_r^2 + \tau_\phi^2},$$

which permits determining the upper frequency required for calculation [3]

$$f_n = \frac{0.35}{\tau_{\phi\,0.5}} = \frac{0.35}{\sqrt{0.5\,\tau_r^2 + \tau_\phi^2}}. \qquad (11)$$

With $\tau_r = \tau_\phi$ $f_n = \frac{0.29}{\tau_\phi}$.

The lower frequency required for pulse transmission without distortion may be determined on the basis of spectral analysis as

$$f_L = \frac{1}{2\tau_m},$$

where, for evaluating the degree of shielding at the lower frequency of the pulse spectrum, it is necessary to insert the pulse duration at the center of the line in

$$\tau_{u\,0.5} = \tau_u + \tau_{\phi\,0.5} - \tau_{\phi}.$$

For $\tau_r = \tau_{\phi}$ and $A = 2.5$ $\tau_{u\,0.5} = 1.1\,\tau_u$.

DESIGN EQUIVALENT OF DELAY LINE WITH SHORTED COILS

Calculation of a delay line with shorted coils performed on the basis of the design equivalent of the section, for which there is chosen an m-derived low-frequency filter (Figure 4), where 2 (L + M) is the inductance with the shorted coils taken into account, and C is the total distributed capacitance of the section.

In addition, the parameters of the section are determined on the basis of the best approximation of the group propagation time to the constant value in the chosen interval [4]. Calculation of the operating transmission constant yields a bandpass efficiency $\eta = 0.7$. Let us determine the parameter of an m-derived section from the formula

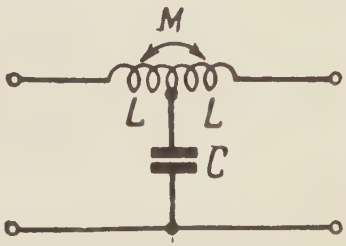

Figure 4

$$m = \frac{1}{\eta}\sqrt{\frac{1}{\sqrt{1-\eta^2}} + \eta^2 - 1},$$

$$m = 1.35.$$

The mean delay time of a section is

$$T_{do} = \frac{2m^3 + 3\sqrt{3(m^2-1)}}{2m^2\omega_0},$$

$$T_{do} = \frac{2.64}{\omega_0},$$

where ω_0 is the cutoff frequency of the passband

$$\omega_0 = \frac{2\pi f_c}{\eta}.$$

The passband cutoff frequency of the line is

$$f_c = \frac{0,35}{\tau_r},$$

where τ_r is determined from formula (9).

As a result

$$T_{do} = 0.84\,\tau_r. \tag{12}$$

The number of sections

$$p = \frac{T_d}{T_{do}} = 1,19\,\frac{T_d}{\tau_r}.$$

The number of shorted coils per unit is less than p' = p-1.

Improved matching of the line with load (compensation of the dependence of the section impedance on frequency) is achieved by division of one section into two parts. As a result the line begins and ends in a half-section and has p-1 whole sections (Figure 5). The total number of sections is

$$p_1 = p + 1. \tag{13}$$

In this manner distortions due to reflections from the load are almost completely eliminated. The remaining values are determined from the formulas

$$L = \frac{m^2+1}{2m}\,\frac{R_L}{\omega_0} = 0.33\tau_r R_L;$$

$$C = \frac{2m}{R_L\,\omega_0} = 0.86\,\frac{\tau_r}{R_L};$$

$$M = \frac{m^2-1}{2m}\,\frac{R_L}{\omega_0} = 0.098\,\tau_r R_L$$

where R_L is the load resistance.

For a given diameter of the core and wire of the main inductance coil, calculation of the parameters of the shorted coils, after selection of the type of winding (single-layer or two-layer), is performed from formulas (3), (4), (5) and (7). In addition, in formula (3) it is necessary to insert f_h [formula (11)] and n = 100, which insures adequate shielding.

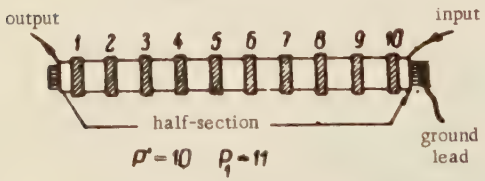

Figure 5

Acceptability of the idealization associated with calculation from an assumed section of the delay line with distributed constants is analytically evident due to its small electrical length ($T_{do} = 0.84\,\tau_r$) and was wholly justified by experiment.

QUALITATIVE INDEXES OF DELAY LINES AND EFFICIENCY OF COMPENSATION

The delay line indexes are: rise time of the transfer characteristic τ_r, delay time T_d, transfer constant K_{tran} and volume V cm^3. At identical values of T_d, K_{tran} and V, we may perform a comparative appraisal of lines by means of the coefficient

$$Q = \frac{T_d}{\tau_r},$$

which is known as the figure of merit of the line. The Q of the line is increased with a decrease in τ_r, which leads to an increase in resolution of the line. The minimum duration of a pulse which may be transmitted over a line in matched operation depends on the pulse-shape coefficient A:

$$\tau_u = \frac{\tau}{\sqrt{1 - \frac{2}{A}}}, \tag{14}$$

where $\tau = \sqrt{\tau_r^2 + \tau_L^2}$.

Resolution of the line may be characterized by the minimum-duration pulse which may be transmitted along a line under the above conditions and with A = ∞ (rectangular pulse). In addition, it is necessary to distinguish the intrinsic resolution ($\tau_L = 0$)

$$\tau_{u\,min} = \tau_r \tag{15}$$

and the operating resolution ($\tau \neq 0$)

$$\tau_{u\ min\ of} = \tau_r \sqrt{1 + \left(\frac{\tau_L}{\tau_r}\right)^2}. \tag{16}$$

This permits correct evaluation of the effect of a decrease in τ_r on $\tau_{u\ min\ of}$. The value of τ_r of a spiral line is influenced chiefly by phase distortions, thereby determining the merit of the line. For evaluation of the efficiency of compensation of a line with distributed constants let us determine the upper frequency at which deviation of phase from the linear characteristic β does not exceed 20° or 0.35 radian. At considerable amplitude distortion the phase distortion $\beta \leqslant 20°$ is insignificant [5] and is the critical distortion at which the formula defining the rise time of the transfer characteristic may be used,

$$\tau_r = \frac{0.35}{f_c}.$$

It defines the limit of the so-called phase passband — the "phase cutoff" frequency $f_{c\phi}$. (In the presence of amplitude distortion only, it is

necessary to insert into this formula the frequency corresponding to the 0.707-level — the attenuation frequency cutoff f_{cc}). Using an approximate formula showing the change in inductance of the spiral coil as a function of frequency [6],

$$\frac{L}{L_0} \approx 1 - 25\left(\frac{D}{2l}\right)^2,$$

where L_0 is the inductance per unit length at low frequencies, λ is the wavelength of the spiral.

(The formula gives excellent coincidence with $\frac{\pi D}{\lambda} < 0.5$).

In combination with the formula defining departure of the phase characteristic from the linear (we assume that C is independent of frequency),

$$\omega_c T_d\left(\sqrt{\frac{L}{L_0}} - 1\right) = \beta$$

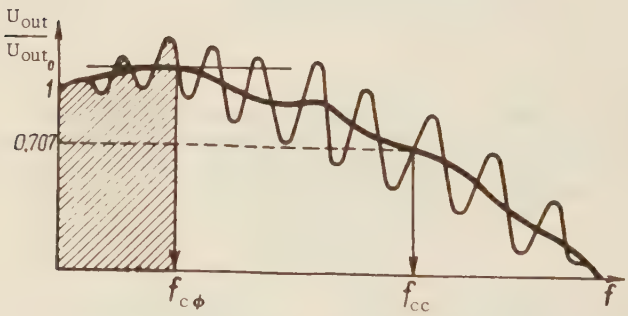

Figure 6

we obtain with $\beta = 0.35$

$$f_c = \frac{0.26}{T_d}\left(\frac{l}{D}\right)^{1/3}. \qquad (17)$$

The weighted amplitude-frequency characteristic of a spiral line ($\beta > 0.35$) has an ascent at the beginning of the characteristic and then an oscillating drop (Figure 6). The first inflection point, defined by the tangent parallel to the frequency axis, corresponds to the "phase cutoff" frequency $f_{c\phi}$ and may be recommended for determination of τ_r.

Now for the rise time of the spiral line ($\beta \leqslant 0.35$) we may write

$$\tau_r = 1.35\, T_d\left(\frac{D}{l}\right)^{1/3}. \qquad (18)$$

For a line with short-circuited coils we obtain from (15)

$$\tau_{r\kappa} = 1.19\, T_{do}. \tag{19}$$

As a result

$$\eta = \frac{\tau_r}{\tau_{r\kappa}} = 1.14\, p \left(\frac{D}{l}\right)^{3/5},$$

since $l = l_0 p$ (Figure 1), then

$$\eta = 1.14\, p^{1/5} \left(\frac{D}{l_0}\right)^{3/5}.$$

The coefficient η characterizes the efficiency of the method of compensation associated with the use of short-circuited coils from the point of view of increasing the resolution of the delay line.

It is known that $D/l_0 = 1.115(m^2-1)$ [7].

For our case (m = 1.35) we obtain

$$\eta = 1.05\, p^{3/5}. \tag{20}$$

Efficiency of compensation for extreme cases is

$$p_{min} = 2, \qquad \eta = 1.32,$$
$$p_{max} = 12, \qquad \eta = 2.4.$$

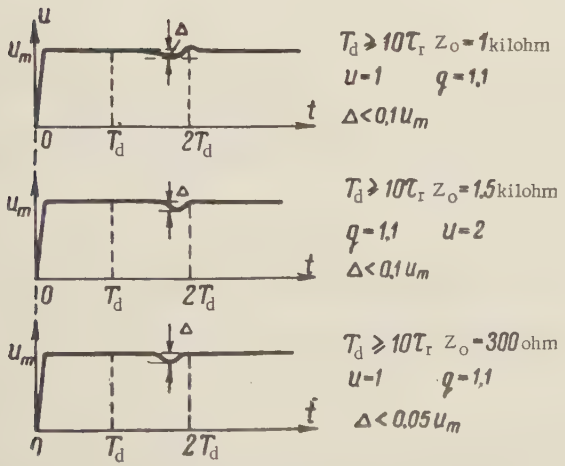

Figure 7

In the transmission of voltage changes (A > 30) through a line with shorted coils there arises an unusual distortion of the flat portion.

The voltages at the output of the line are represented in Figure 7. These distortions are maximum at large Z_o and minimum when $V < 1$ cm^3, wherein $\Delta_{max} < 0.1\ U_{max}$.

A great advantage of the discussed construction of delay line is the close spacing of the sections. In contrast to the usual improvement of quality by making delay lines with distributed constants in the form of sections, the use of delay lines with lumped constants of m-derived sections leads to a considerable increase in dimensions, which necessitates greater spacing between sections in order to avoid parasitic coupling.

MINIATURIZATION AND THE DELAY-LINE TRANSFER CONSTANT

Miniaturization of delay lines with distributed constants became possible due to the above-mentioned advantage in construction and the considerably higher efficiency of the method of compensation associated with use of shorted coils (20) in comparison with other existing methods [1] wherein $l/D \leq 15$ to 20. This is associated with the use of conductors of small diameter d = 0.05 to 0.1 mm. Realization of the greatest possibilities for reducing dimensions in this connection depends on the requirement for the transfer constant. The latter depends on the a-c resistance R of the inductance coil of the line. The value of R is determined by the skin effect and the proximity effect, the influence of the latter depending on frequency, conductor diameter and winding density.

For $f < 50 \cdot 10^6$ cps, with the use of such insulating materials as styroflex and teflon-4, the dielectric losses may be neglected and the following simple formula may be used for evaluation of the transfer constant:

$$K_{tran} = \frac{R_L}{R_L + R}. \qquad (21)$$

For pulses with duration τ_u = (30 to 100) $\cdot 10^{-9}$ sec typical values for the pulse edge τ_ϕ = (12 to 30) $\cdot 10^{-9}$ sec. For calculation from formula (21) it is necessary to take the value of the pulse edge at the center of the line. Let $\tau_\phi = \tau_r$, whence

$$\tau_{\phi\,0.5} = 1.22\,\tau_\phi,$$

$$\tau_{\phi\,0.5} = (15 \div 35) \cdot 10^{-9},\ \text{sec}.$$

These values for the pulse edge correspond to frequencies of

$$f = (23 \text{ to } 10) \cdot 10^6 \text{ cps}.$$

For a conductor diameter d = 0.05 the skin effect is practically absent [8], since the resistance increases by 3 to 6 percent. The resistance rises chiefly due to the proximity effect and may be estimated as

with U = 1 to 2 and q = 1.1, $R \approx 1.5\ R_0$,
with U = 1 and q = 1.5 $R \approx 1.1\ R_0$

here R_0 is the d-c resistance of the coil.

For a conductor diameter of d = 0.1 the skin effect increases the resistance by an average of 50 percent. In this case:

with U = 1 to 2 and q = 1.1 $R \approx 2R_0$,
with U = 1 and q = 1.5 $R \approx 1.6\ R_0$.

As a result, lines with Z_0 = 0.3 to 1.5 kilohms and τ_r = (20 to 50) · 10^{-9} sec and with $\frac{\tau_d}{\tau_r}$ = 10 to 12 and d = 0.05 have a volume of V < 1 cm^3 and K_{tran} = 0.0 to 0.85. With diameter d = 0.1 the volume does not exceed 2 cm^3, while K_{tran} = 0.9 to 0.95. In both cases the core diameter is D = 4 to 6 mm.

CONCLUSION

Delay lines with short-circuited coils are structurally simple and convenient for mass production. They are considerably smaller than other existing designs, possess higher resolution [τ_r = (20 to 50) · 10^{-9} sec] and, thus, are completely applicable for modern systems operating with extremely narrow pulses [τ_u = (30 to 100) · 10^{-9} sec] at maximum repetition frequencies.

Article submitted to editors 21 April 1960

LITERATURE

1. M.J. Di Toro, "Low-dispersion wired delay lines." IRE National Convention Record, Vol. 6, 2, 1958.
2. A.A. Kolosov, Rezonansnyye sistemy i rezonansnyye usiliteli [Resonant systems and tuned amplifiers]. Svyaz'izdat, 1949.
3. Lampovyye usiliteli [Vacuum-tube amplifiers]. Editor V.L. Sushkevich. "Sovetskoye radio," Part 1, 1950.
4. V.F. Golyshko, K.A. Sil'vinskaya, "Delay line with lumped parameters." Elektrosvyaz', No. 11, 1958.
5. L.A. Meyerovich, G.P. Tartakovskiy, "Calculation of time and frequency characteristics of multi-stage circuits." ZhTF, Vol. XII, No. 7, 1952.
6. L. Lewis, "Note on the variations of phase velocity in continuously wound delay lines." Proc. Inst. Electr. Eng., 98, III, 1951.
7. L.A. Meyerovich, L.G. Zelichenko, Impul'snaya tekhnika [Pulse techniques]. "Sovetskoye radio," 1953.
8. D. Ye. Vakman, "Impulse-current losses in conductors." Radiotekhnika, No. 6, 1959.

SYSTEM FOR CONTROL OF RADIATION PATTERN OF COMPLEX WIDEBAND ANTENNA WITH LOW SIDE-LOBE LEVEL

V.D. Kuznetsov, and V.K. Paramonov

The article describes a system for control of the horizontal radiation pattern of a wideband antenna in the form of a linear system of radiators by the Dol'f-Chebyshev method for the purpose of decreasing the side-lobe levels. A description is given and data are presented for a phasing unit and a transition unit — the chief elements of the radiation pattern control system in the receiver variant of the antenna. The article describes the results of experimental investigation of the transition and phasing units as well as the entire system as a whole. The system for control of the pattern in a transmitting antenna is examined.

Communications engineering is presently increasing the application of antennas with radiation patterns controlled in the horizontal plane. In short-wave operation the specifications for such antennas are determined by the necessity for maintaining communication either with a mobile correspondent or with several fixed correspondents.

In VHF communications systems employing ionospheric scatter propagation or propagation by ionized meteor trails it is convenient to use antennas with controllable radiation patterns wherein it is possible to select the most suitable path in accordance with the varying propagation conditions.

In the subsequent discussion we shall examine systems for control of the radiation pattern of the receiving and transmitting versions of a complex wideband antenna in the form of a linear network of radiators with low directivity (antenna elements in the receiver version) which may be fed with decreasing amplitude from the center of the antenna to its ends.

Figure 1 shows the feed diagram of a receiving antenna permitting multiplex operation of an antenna consisting of eight elements. Here E is an antenna element, Y is the wideband amplifier, PU is the phasing unit. The required number of phasing units as well as the number of outputs into the amplifiers are determined by the number of channels into which the amplifiers operate (two in duplex operation, three in triplex operation, etc). The required amplitude relationships are easily obtained by appropriaate regulation of the output voltages of the amplifiers. The circuit as shown permits, with one antenna, independent operation of several receivers at different frequencies (within the limits of the operating range) and with different radiation patterns, where each of these patterns may be controlled.

In simplex operation of the receiving antenna, control of the radiation pattern is also achieved by means of a phasing unit (Figure 2). In this circuit the required amplitude relationships insuring a low side-lobe level of

the pattern may be achieved either by means of attenuators or by transformation of resistances.

One of the principle parts of the circuit for feeding an antenna with controllable radiation pattern is the phasing unit (PU). The structural shape of the PU may differ, depending on the specific features of the given feed circuit. Below we describe a PU designed for an eight-element antenna with the feed circuit consisting of asymmetric coaxial cables with characteristic impedance W ≈ 75 ohms (RK-3, RKK-5/18, etc). The described PU is intended for operation over a two to one wavelength range (λ = 5-10 m), with an antenna base (that is, the distance between the centers of its extreme elements) of d = 38.5 m. It permits control of the radiation pattern within an angular range of $\varphi_0 = \pm 24°$.

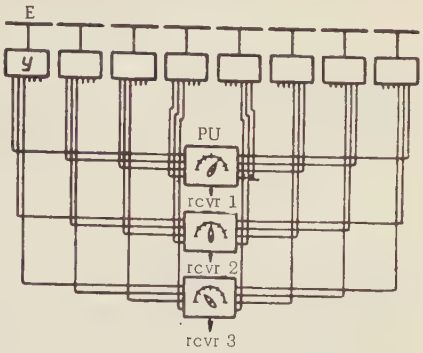

Figure 1

The PU circuit is shown in Figure 3. It consists of four asymmetric artificial lines AL with characteristic impedance

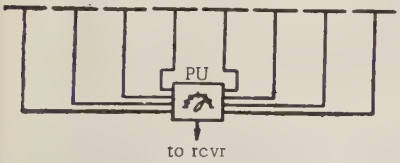

Figure 2

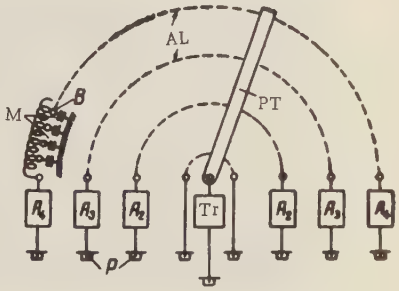

Figure 3

W = 75 ohms. The lines are formed from identical elementary π-sections M, and are arranged along the arcs of concentric semicircles with radii ratios of 1, 3, 5, 7. All the sections of the lines have taps B in the form of contact heads over which the wiper of a common sliding arm is moved — current pickoff PT. The sliding contact arm also represents an asymmetric line. In order to insure matching at the contact points the characteristic impedance of this line is varied stepwise at the contact positions: 37.5, 18.75, 12.5, 9.4 ohms.

Matching, of the receiver connection to the sliding contact at the axis of the wiper, is achieved by means of a special transformer Tr. This transformer is for transition from a line with characteristic impedance of 9.4 ohms (the result of parallel connection of eight 75-ohm lines) to a 75-ohm line.

In simplex operation of the antenna, between the ends of the artificial lines and the output connectors there are attenuators A which insure the required amplitude ratios between currents in the antenna elements.

The maximum equivalent length of the artificial line (l_e) is determined by the maximum angle of rotation of the radiation pattern φ_1 and the antenna

base

$$l_e = d \sin \varphi_1.$$

The elementary mesh parameters, L and C, are determined from the relationships

$$l_{e\,(cm)} = 3 \cdot 10^{10} n \sqrt{L_{(h)} C_{(fd)}}$$

$$W_{(ohm)} = \sqrt{\frac{L_{(h)}}{C_{(fd)}}},$$

where n is the number of elementary meshes of the line, W is the characteristic impedance of the line.

Actually, the inductances of the artificial lines are made in the form of helices of silver-plated copper wire; the capacitors of the meshes consist of the capacitances between the base plate and the housing, and the terminals fastened to the base plate by means of fluoroethylene washers.

A general view of the PU with housing and face plate removed is given in Figures 4 and 5.

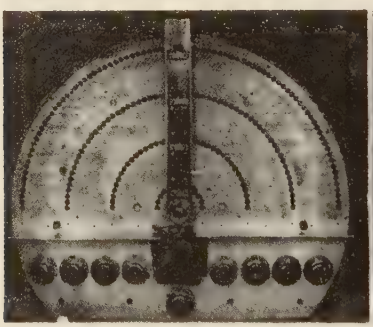

Figure 4

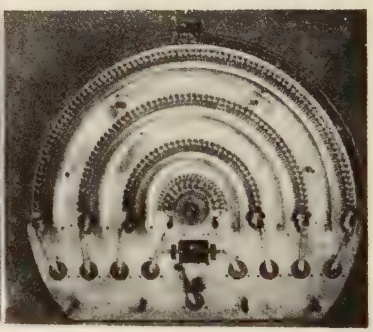

Figure 5

The 9.4-75-ohm transformer is made in accordance with the circuit shown in Figure 6. The procedure for calculation of such a transformer is described in [1]. Its design data are

$L_1 = 0.051$ μh, $L_2 = 0.405$ μh, $L_3 = 0.738$ μh,
$C_1 = 278$ pF, $C_2 = 34.8$ pF, $C_3 = 42.5$ pF, $K_c = 0.74$.

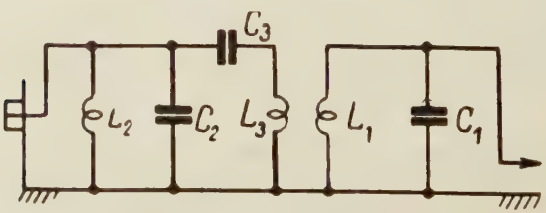

Figure 6

The transformer itself, consisting of inductances L_1 and L_3, is made in the form of a coil of several turns of insulated copper wire (L_3) above which, on a thin spacer of foamed plastic, there is one turn of copper strip (L_1). The inductance of the compensating circuit is a coil of several turns of enamel-coated wire.

Matching of the transformer made for the described PU was measured in the frequency range f = 25—70 Mc. The output load consisted of several parallel characteristic impedances with a total impedance of 9.4 ohms. The results of measurements are given in Figure 7. As is seen, within the limits of the operating frequency range (f = 30—60 Mc) the traveling-wave ratio at the transformer input did not drop below 0.85, which may be considered an extremely satisfactory result.

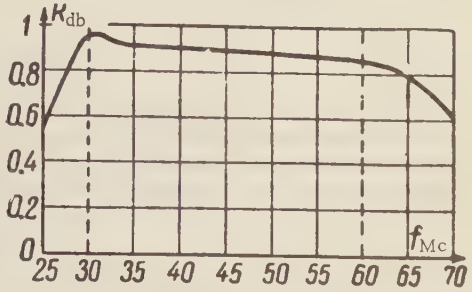

Figure 7

The elements (radiators) of the antenna, as a rule, have input impedances of the order of several hundred ohms. Therefore, for matching purposes, cables with characteristic impedance of 75 ohms require special matching units, that is, impedance transformers. In addition to the matching problem, upon connection of an asymmetric coaxial cable to symmetrical antenna elements (for example, to half-wave dipoles), it becomes necessary to solve the balancing problem. Solution of these problems in the centimeter range (tenths and hundredths of a meter) and in the relatively long-wave length range (hundreds and thousands of meters) presents no difficulty. In the first case the balancing and matching units are made of line segments with distributed constants, while in the second case they are made in the form of circuits containing lumped constants and transformers with air cores or magnetic cores.

The difficulties arise in the solution of these problems in the ultrashort wavelength region (meters and tens of meters). Here the use of segments of long lines becomes impractical due to the extreme increase in dimensions and the fact that circuits with transformers do not permit obtaining the required balancing due to the presence of capacitive coupling between the transformer windings.

There is given below a description of a phasing unit PU permitting wholly satisfactory matching over a wide range of short waves and ultrashort waves along with excellent balancing properties [2]. This unit has been developed on the basis of a short wave transformer described in the literature [1] and has the same equivalent diagram as this transformer. The operating diagram of the PU is presented in Figure 8a. As is seen from the figure, the PU is a balanced circuit and the following method is used for symmetrical introduction of emf into the circuit. The inductance of compensating circuit L_2 is divided into two equal parts (L_2') each of which is made in the form of a separate coil of thin 75-ohm coaxial cable. The coils are connected into the circuit at the braid ends, as shown in Figure 8c, and are interconnected by means of a tube segment with an opening in the center, through which the cable end is brought out (Figure 8b). The emf is introduced into the circuit along the inner conductor of this cable. As

calculations show, in units designed for operation in the short wave and ultra-short wave ranges, inductance L_2' is of the order of units or tenths of microhenries. In coils with such inductance made of a coaxial cable no particular difficulties are encountered.

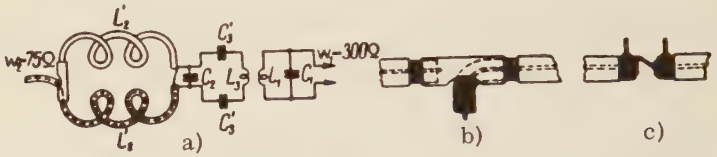

Figure 8

Calculation of the capacitance and inductance in the PU is performed by the method described in [1]. Thus, the PU for transition from a 75-ohm coaxial cable to a 300-ohm balanced line is intended for operation in the 30—60 Mc range (λ = 5—10 m) and has the following characteristics:

$$L_1 = 1.64\ \mu h, \quad L_2' = 0.205\ \mu h, \quad L_3 = 0.75\ \mu h,$$
$$C_1 = 8.6\ pF, C_2 = 34.4\ pF, C_3 = 83.2\ pF,$$

Figure 9 shows the results of measurements of the matching of a test model of a PU with the above data, loaded by a characteristic impedance of 300 ohms. As is seen, in the operating frequency range the traveling-wave ratio at the PU output does not drop below 0.9. Measurements revealed also that in this frequency range the asymmetry coefficient did not exceed 0.005 (0.5%). Both of these indexes may be considered excellent.

Experimental investigation of the system for radiation-pattern control was performed on an eight-element radiator of an antenna for communications by ionospheric scatter propagation [3].

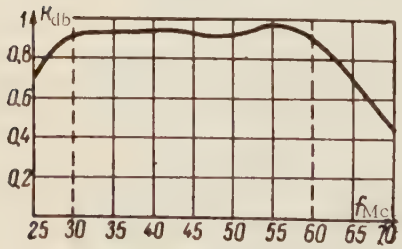

Figure 9

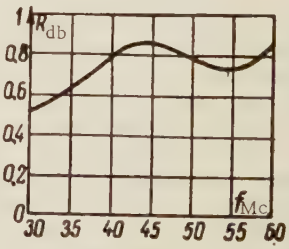

Figure 10

The radiator is a 90-degree corner reflector formed by the vertical wall of a unilinear wire mesh and a plated ground. In the bisecting plane of the corner reflector there is chain of eight half-wave dipoles with input impedances close to 300 ohms in the frequency range under study. The radiator base was d = 38.5 m.

The radiator feed circuit was based on cables of type RK-3 and contained the described balancing and phasing units. The PU units contained attenuators so calculated that the current amplitudes in the dipole pairs (beginning from the center of the radiator) were at ratios of 1, 0.825, 0.54, 0.305. According to the Dol'f-Chebyshev procedure, the mentioned relationships of amplitudes should insure attenuation of side lobes by not less than 28 db relative to the major-lobe level.

Figure 10 shows the results of measurement of matching at the input of the feed system. As is seen from the figure, for the most part, operating range lies at the 0.7—0.8 level and only in the long-wavelength fringe of the range drops to 0.5—0.6. Such matching may be considered adequate.

Investigation of the control of the radiation pattern in the horizontal plane was performed by plotting radiation patterns with different positions of the sliding contact of the phasing unit.

The radiation patterns were plotted by measuring the field strength at points on an arc with radius of 0.5 km, at the center of which was placed a radiator which served as a transmitting antenna. Measurement of the field strength was performed by use of a portable receiver with an output scale graduated in microvolts. The receiving antenna was a dipole with arms of variable length at 4 m above ground.

Local conditions permitted plotting the radiation pattern over a range from $\varphi = 30°$ in one direction to 60° in the other. Readings were made at 2-degree intervals.

The radiation patterns were plotted, both with cophasal feeding of the dipoles (the mean position of the PU sliding arm) and in antiphasal feeding, for the purpose of rotation of the pattern at different angles and in different directions. The measurements showed that the described phasing unit permits operational control of the radiation pattern over sufficiently great angular limits. By way of example, Figure 11 shows the radiation patterns plotted for frequencies of f = 35, 45 and 55 Mc in the mean position of the sliding arm as well as in the extreme positions corresponding to rotation of the pattern through 24°. The small increase in side-lobe level as well as a certain distortion in the major lobe of the patterns is explained chiefly by antiphasal operation of the radiator, caused by inaccuracies in lengths of the artificial lines of the PU and connecting cables.

In the transmitting version of the antenna, where the problems of efficiency and dielectric strength are of considerable importance, all the feeders are best made in the form of symmetrical lines so placed as to provide protection against precipitation, and to decrease the antenna effect of the transmission line in the shielding cages. The result is that the feed system for the transmitting antenna is extremely unwieldy. The problem of efficient power distribution in the operating range between radiators at the given ratios, matching, and dielectric strength, also presents particular difficulty. Hence, it is natural that operational control of the radiation pattern in the transmitting antenna may not be achieved as easily as in the receiving antenna.

The radiation pattern of a transmitting antenna in the form of a linear chain of eight radiators with nonuniform feed may be controlled by continuous or stepped displacement of feed points $C_1—C_4$ (Figure 12). As in the case of the receiving antenna, the values of feed-point displacements are determined by the angle of rotation of the pattern and the distances between centers of the corresponding radiators.

In practice, each of the movable feed points may be represented as a two-pole stepped switch, between the contacts of which are connected line segments with corresponding electrical lengths in the form of loops or

spirals (Figure 13).

The transformer designated in Figure 12 by Tr is a unit for nonuniform division of power between radiator pairs. For this purpose, circuits with parallel (Figure 14a) and series (Figure 14b) power division may be used. In both cases power division is performed at points corresponding to the change in characteristic impedance of the dividing networks. For example, if it is necessary to maintain a relation of a:b:c:d between four branched radiator pairs, then in a circuit with parallel power division the following relationships will apply:

$$W_0 = (a+b+c+d) = W_1 a = W_2 b = W_3 c = W_4 d.$$

Similarly, in a circuit with series division the following relationships will apply:

$$W_0 = (a+b+c+d) = W_1 a = W_2'(b+c+d),$$
$$W_2''(b+c+d) = W_2 b = W_3'(c+d),$$
$$W_3''(c+d) = W_3 c = W_4 d.$$

Calculation of the characteristic impedances of the branch lines is performed with the use of the above relationships and from a given or chosen value of characteristic impedance of one of two lines.

In order to insure adequate matching of the power divider in the operating frequency range we may, at portions of the divider circuit where the impedance is transformed (for example, $W_1 - Z_{m1}$, $W_2' - W_2''$), use multistepped quarter-wavelength transformers. The number of steps depends on the width of the operating band, the value of permissible mismatch, and the magnitude of the change in characteristic impedances.

The described circuit for

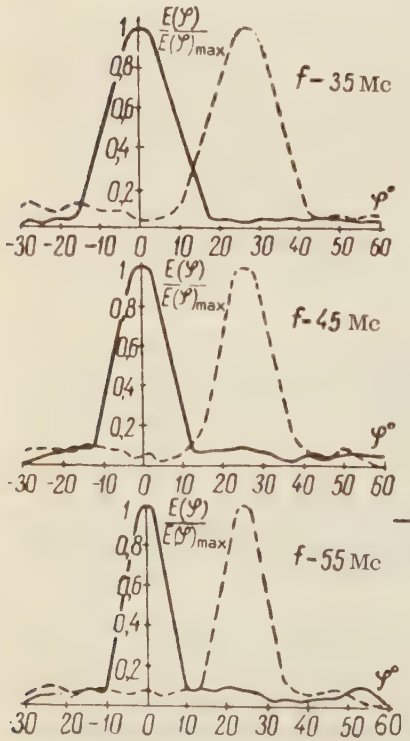

Figure 11

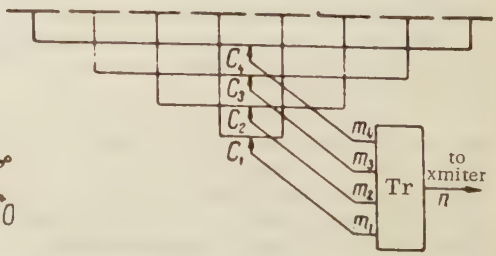

Figure 12

control of the radiation pattern of a transmitting antenna has a disadvantage.

This consists in the fact that in rotation of the radiation pattern, with inadequate matching of the radiators with the feedlines, there may arise disturbances of the assigned amplitude and phase relationships. The result may be an increase in the side lobes and distortion of the pattern.

Figure 13

Figure 15 shows the feed circuit for a transmitting antenna that eliminates this disadvantage. The circuit is based on the use of couplers [4] and operates as follows.

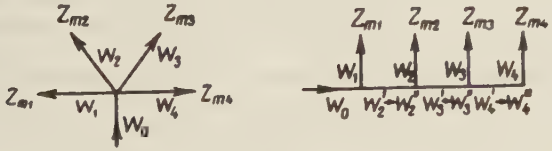

Figure 14

A radiator, or group of radiators, with maximum current amplitudes is connected to the generator by the main feeder. The remaining radiators are connected to the main feeder through directional coupler HO. The degrees of coupling of the HO with the main feeder determine the peak relationships between currents in the radiators, whereas the phase relationships between these currents are determined by the lengths of the coupling lines. In the terminating resistances of the HO (R) there is dissipated the power of the nonphasal wave components reflected by the radiators. This insures maintenance of the given distribution of amplitudes within the radiators even in the case where the latter are relatively poorly matched with the feeder lines. The

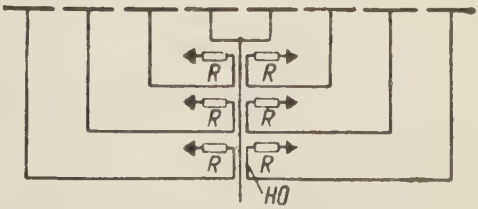

Figure 15

total value of power loss in the terminal resistances of the HO depends on the amplitude and phase relationships between the waves reflected by individual radiators. If all the radiators are identical, then in cophasal feeding their power will generally not be lost in the resistances. Moreover in any distribution of amplitudes and phases of currents in the radiators, the maximum value of power loss will not exceed $p^2 \cdot 100\%$, where p is the coefficient of reflection from a single radiator.

The circuit does not lose its properties in operation over a wide range of frequencies, since matching of the HO does not depend on frequency, and the transfer constant does not vary significantly with change in frequency. For example, with HO of length equal to a quarter of the average wavelength, the value of the voltage transfer constant, within the limits of the two to one frequency range, varies by not more than 10—12 percent.

Analysis of the operation and procedure for calculation of the HO will be given in a special report.

Phasing of the radiators, that is, control of the radiation pattern in the supply circuit using HO, may be achieved by varying the length of the feed lines by use of loops of variable length ("trombones").

Article submitted to editors 25 February 1960

LITERATURE

1. G. Z. Ayzenberg. Antenny dlya magistral'nykh radiosvyazey [Antennas for main radio links]. Svyaz'izdat, 1948.
2. V. D. Kuznetsov, V. K. Paramonov. Author's certificate No. 122784.
3. V. D. Kuznetsov, V. K. Paramonov. "High-efficiency VHF antenna with low side-lobe radiation and controllable radiation pattern." Elektrosvyaz', No. 7, 1960.
4. V. D. Kuznetsov, V. K. Paramonov. Author's certificate No. 122501.

NEGATIVE-RESISTANCE SEMICONDUCTOR DEVICES

M.A. Berg, and S.A. Garyainov

The article discusses negative-resistance semiconductor devices. It is established that the chief characteristic of such a device is not the amount of negative resistance but the amount of negative power delivered by the device over its negative resistance segment. Depending on its application, an attempt is made to establish the optimum shape of the volt-ampere characteristic of the device.

The last five years have seen the appearance of a new trend in

semiconductor electronics — a trend associated with the research and development of negative-resistance semiconductor devices.

At this time many countries are engaged in the development of these devices. The leading firms engaged in semiconductor production have already progressed to the mass production of negative-resistance devices.

The interest in negative-resistance semiconductor devices is not accidental but is associated with the prospects which they afford for application in telephony, telegraphy, automation, television and, especially, in high-speed electronic computers, wherein they may be used in counting circuits as memory elements, etc. It is also know that there is interest in use of negative-resistance devices in filters, in variable-signal relays and other special devices.

NEGATIVE-RESISTANCE SEMICONDUCTOR DEVICES, CHARACTERISTICS AND CLASSIFICATION

According to the number of electrodes, negative-resistance semiconductor devices are divided into two major groups: diodes and triodes. Triode devices with negative resistance are essentially the semiconductor analogs of thyratrons. The diode devices are best suited for use in the circuits of generators, amplifiers and various switching devices.

According to the shape of the volt-ampere characteristic, these devices may have a volt-ampere characteristic of class I (Figure 1) or a volt-ampere characteristic of class II (Figure 2). The characteristics may be discontinuous (Figures 3, 4) and continuous (Figures 1, 2). As an example of a discontinuous characteristic we present an oscillogram of the volt-ampere characteristic of a p-n-p device (abscissa value 60 v, ordinate value 30 ma).

In d-c operation, plotting of the points in the region of negative-resistance for a device with discontinuous volt-ampere characteristic of class I, presents difficulties associated with the necessity for using a current generator with infinitely large internal resistance, or a voltage generator in the case of a device with volt-ampere characteristic of class II. In devices with continuous volt-ampere characteristic these difficulties do not exist.

According to the mechanism whereby the conduction is changed, semiconductor devices may be divided into thermal, thermal-ionization, avalanche, tunnel, et al. In thermal devices the chief cause of change in conduction is the thermal generation of charge carriers. A typical example of such a device is the thermistor. In thermal-ionization devices the initial cause of change in conduction is the phenomenon of thermoelectronic ionization. Essentially, this phenomenon consists in the fact that the electric field applied to the semiconductor contributes to separation of an electron from the atom. This separation occurs as the result of thermal excitation. In avalanche devices the change in conduction occurs due to avalanche multiplication of the number of charge carriers, which is the result of impact ionization in the strong electric field of the p-n junction to which voltage is applied in the reverse direction. The change in conduction of tunnel devices is based on the tunnel effect, which consists in penetration of charge carriers through the potential barrier of the p-n junction.

It frequently happens that each of these mechanisms is accompanied by thermal generation. This occurs, for example, in point-contact germanium diodes of type DG-Ts4 through DG-Ts12, which have negative-resistance segments on the back branch of the volt-ampere characteristic.

Figure 5 shows an oscillogram of the volt-ampere characteristic of a point-contact diode of type DG-Ts4. The abscissa value is 120 v. On the

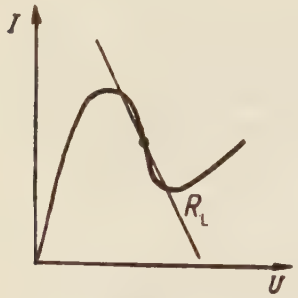

Figure 1

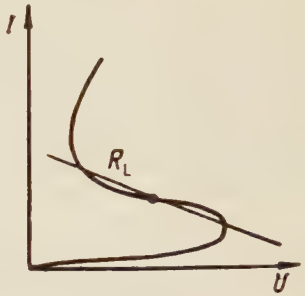

Figure 2

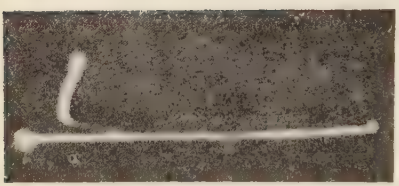

Figure 3

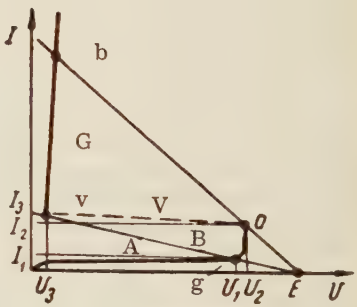

Figure 4

ordinate axis, on the righthand branch the value is 150 ma and on the back branch 105 ma. The region of generation is seen on the oscillogram. The leads and stray capacitance of the wiring serve as a tuned circuit.

Figure 5

Structurally, semiconductors are distinguished as follows: p-n-δ type, wherein δ will represent the thickness of semiconductor, the conductivity of which may vary under the influence of current, thermal or light effects or an applied voltage [1]; devices of the p-i-p type [2]; devices of the p-n-p type [4]; devices of the p-n-p-n type [5, 6, 7, 8]; devices of the p-n-p-m type, where m denotes metal [9]; devices of the n^+-p-i-p^+ type, where n^+ and p^+ are heavily doped regions with electron and hole conduction and i is a layer with intrinsic conductivity [10]; devices of the p-n type (tunnel diodes) [11].

Among these devices, only in the p-n and p-n-δ types (with the exception of the point-contact diodes DG-Ts4—Ts12) is the external voltage applied to the p-n junction in the forward direction. In all other devices the bias voltage is applied in the reverse direction to one or several p-n junctions. Classification of negative-resistance devices is shown in Figure 6.

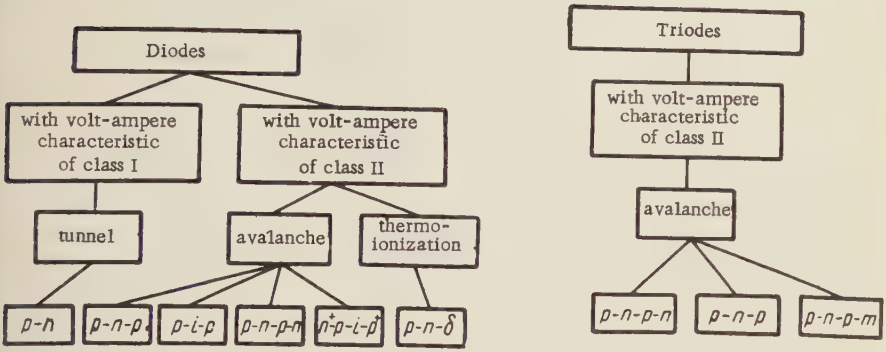

Figure 6

The mechanism of negative resistance in p-n-δ and p-n devices has been adequately described in the literature [1, 11]. We shall discuss devices which have p-n junctions with reverse voltage bias.

Devices of this type have a volt-ampere characteristic of class 2. Let us adopt the following symbols: I_1, current in the pre-breakdown state (Figure 4); I_2, forward switching current; I_3, reverse switching current; U_1, U_2 and U_3, voltages corresponding to currents I_1, I_2 and I_3; I_H and U_H are the rated values of current and voltage in the high-conductivity state; τ_1 is the forward switching time; τ_2 is the reverse switching time.

For existing devices with volt-ampere characteristic of class 2 the values of these quantities lie within the following limits:

$$U_1 \approx U_2 = 5 \text{ to } 200 \text{ v}; \; U_H \approx U_3 = 1 \text{ to } 5 \text{ v}; \; I_2 = 0.1 \text{ to } 10 \text{ ma};$$

$$I_3 = 0.5 \text{ to } 30 \text{ ma}; \; I_H = 30 \text{ ma to } 5 \text{ a}; \; \tau_1 = 0.08 \text{ to } 0.3 \; \mu\text{sec}; \; \tau_2 = (5 \text{ to } 10)\tau_1.$$

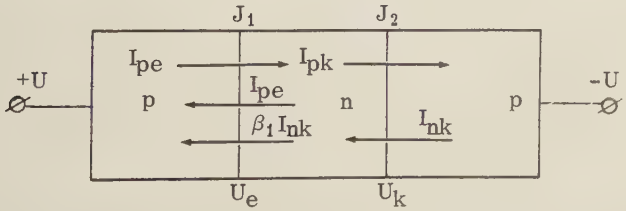

Figure 7

Let us examine the mechanism of negative resistance in such devices by the example of a device with p-n-p structure (Figure 7). Let us designate p-n junction J_1 as the emitter and J_2 as the collector. In such a device the negative resistance appears in the presence of positive internal emitter-collector feedback.

The result is that it sometimes happens that the beginning process of current increase will develop in avalanche fashion, which under certain conditions may lead to "flooding" of the collector [4, 14]. Essentially, the "flooding" consists in the accumulation of charge carriers in the depletion layer of the collector or regions immediately adjacent to it and compensation of the fixed space charge of the depletion layer by the dynamic space charge of accumulating carriers. Accumulation of carriers may occur in the case where the rate of filling of the depletion layer of the collector with carriers due to generation (thermal or light) of impact ionization or as a result of an avalanche increase in current due to the action of positive feedback exceeds the rate of their departure therefrom. Finally, the potential barrier of the collector is partially or wholly eliminated and the voltage at the collector, which before "flooding" was approximately equal to the voltage over the entire structure $U_k \approx U$, drops to a relatively small value and there appears a negative-resistance segment on the volt-ampere characteristic.

The initial increase in current in a p-n-p structure may occur due to a number of causes. For example, it may occur due to multiplication of the number of charge carriers as the result if impact ionization within the collector when the voltage therein reaches the value necessary for this $U_k \approx U_1$ (Figure 4). Multiplication with the collector increases the current of majority carriers reaching the middle n-region (base), which, in negatively charging the base, lower the potential barrier of the emitter. This increases the hole current of the emitter I_{pe} (Figure 7), which, in reaching the collector, takes part in the formation of electron-hole pairs and the increase in current flowing through the device, including the majority carrier current I_{nk}. In such a device there exists a clearly expressed current feedback which is increased with the beginning of collector "flooding." This occurs for the following reason. The voltage across the device U is equal to the sum of voltage drops at the emitter U_e and collector U_k. During "flooding" there occurs redistribution of the emitter-collector voltage. The voltage at the collector is decreased and at the emitter U_e is somewhat increased. There arises a corresponding increase in emitter current and further development of the process of collector "flooding" even after the voltage within the collector decreases to such extent that multiplication ceases.

The process develops in avalanche fashion, with the result that there occurs a rapid switching in the region of high conductivity (at point b, Figure 4). In this condition, the current is determined by the resistance of the device in the high conductivity state and the limiting resistance R, which resistance always exists in the circuit for plotting the volt-ampere characteristic. The voltage at the emitter is also such that the emitter current is in a state to maintain the required collector voltage. With a decrease in current below a certain value $I = I_e$ (for example, by increasing limiting resistance R, Figure 4), when the emitter current can not sustain the collector in the "flooded" state, the process develops in the reverse order and there occurs back switching into the low conductivity state (points d, Figure

4). The switching time will depend on the rate of development of the "flooding" process, which in turn depends on the degree of current feedback.

It may be shown that in any other structure with p-n junctions in which there is even only one p-n junction with external voltage applied in the reverse direction, the negative-resistance mechanism will have the general outlines described above: the structure will have not less than two sources of change in conduction, between which there is achieved positive current feedback; a decrease in voltage with an increase in current over the negative-resistance segment will occur as the result of "flooding" of the p-n junction to which voltage is applied in the reverse direction.

The presence of not less than two sources of conduction change embraced by positive current feedback or positive voltage feedback is characteristic for any device with negative resistance. By way of example, we may cite the tunnel diode, which has a volt-ampere characteristic of class I. The mechanism of negative resistance in the tunnel diode may be represented as follows. Usually, in an extrinsic semiconductor with electron conduction, the Fermi level occurs between the bottom of the conduction band and the donor levels. However, if the activation energy of the impurity levels is small but their number great, the Fermi level may approach the bottom of the conduction band and even cross it. For a p-type semiconductor the picture is the opposite — the Fermi level under the same conditions may lie within the limits of the valence-electron band. This condition occurs in the tunnel diode (Figure 8a). As a result, in the valence-electron band the p-regions above the Fermi level prove to be unoccupied by electrons of the level, while in the n-regions all levels of the conduction band lying below the Fermi level will be filled. If a forward voltage is applied to such a p-n junction, the Fermi levels in the p- and n-regions will be depleted at a value qU (Figure 8b). There will occur a coincidence of the unoccupied levels of the valence-electron band in the p-region with the filled levels of the conduction band in the n-region and there will flow across the barrier a current which we shall henceforth refer to as the tunnel current i_m. From Figure 8b it is seen that with an increase in applied voltage the tunnel current i_m will at first increase and then, upon reaching a maximum (when the bands with free and filled levels overlap), will decrease to zero.

Two sources of change in conduction of the device participate in the process of forming the negative-resistance segment on the volt-ampere characteristic of the tunnel diode. The first source is the presence of bands with filled (in the n-region) and free (in the p-region) energy levels, which together with an applied voltage, causes tunnel current to flow; that is, an increase in conductivity of the device. The second source of change in conduction of the device is the presence of a forbidden band leading to a decrease in conductivity of the device. This second source of change in conduction begins to act after the bands with free and filled levels overlap, which occurs at a certain voltage U_{min} (Figure 9). With $U > U_{min}$ reflection of electrons from the potential barrier begin, with the result that part of the previously overlapping energy levels of the n-region begin to coincide with the band of forbidden energy levels in the p-region. Both sources of change in conduction are related by voltage, which in the given case is an independent variable.

In addition to the tunnel current, through the p-n junction there will flow the usual forward current i_{np}, so that the total current is equal to $i(U) = i_m(U) + i_{np}(U)$.[1] From Figure 9 it is seen that in the absence of

[1] With $U = U_{max}$ (Figure 9) the current is greater than the sum of currents i_m and i_{np}. This phenomenon remains to be explained.

forward current i_{np} the negative-resistance segment would extend to the voltage axis.

The tunnel diode has extremely short forward and reverse switching times, which in oscillator operation insures frequencies of the order of tens of Mc. Moreover, it is distinguished by extremely high thermal stability of the parameters and low noise figure. These advantages of tunnel diodes derive from the fact that, due to the high concentration of impurities in p- and n-regions

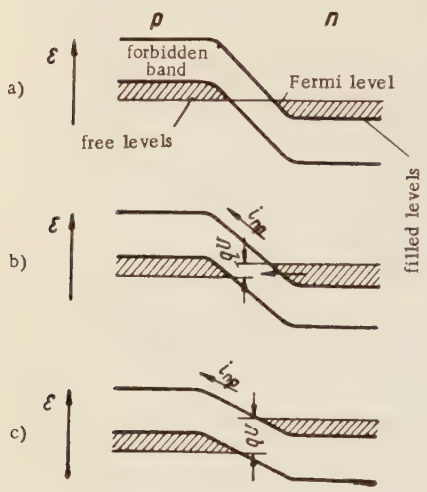

Figure 8

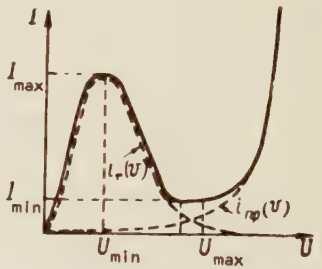

Figure 9

(of the order of $10^{19}/cm^3$), the electron gas therein is partially or wholly degenerated. Moreover, the electron energy, as in metals, is independent of temperature. Hence, the conduction of such a semiconductor is the same as in metals. This accounts for the advantages which tunnel diodes have over other semiconductor devices; high operating speed, excellent thermal stability, low noise figure, etc. It may be stated without exaggeration that tunnel diodes, along with other semiconductor devices with negative resistance, possess excellent prospects for future application.

However, the problem of the required shape of volt-ampere characteristic of such devices has still not been sufficiently studied. Elucidation of this point will require the examination of the possible areas of application of negative-resistance devices.

CONCERNING NEGATIVE RESISTANCE

Generation and amplification of electrical oscillations are possible due to the presence of a negative-resistance element in a circuit. In the circuits used in the past negative resistance was due to the presence of a nonlinear element, a source of power and circuits with external positive current or voltage feedback.

As a result, such a circuit possessed a-c or d-c negative resistance. The simplest example of this is the conventional self-excited oscillator. However, given an electronic device in which the volt-ampere characteristic possesses a negative-resistance segment, the problem is considerably simplified. In this case there is no need for circuits of external positive feedback since the feedback required for creation of negative resistance is achieved within the device. This considerably simplifies circuit problems for a whole series of radio engineering installations and explains the interest

which is presently focused on such devices. However, despite the fact that negative-resistance devices have long been known and the concept of negative resistance has found wide application in engineering practice, the theory of this problem has been inadequately developed. Since the time of introduction of the concept of negative resistance by M. A. Bonch-Bruyevich [12] and his followers and the discovery of the original work by P. P. Klimentov [13] the theory of negative resistance has not been given sufficient attention. As a result, on the basis of existing theory, it is difficult to state the technical requirements for negative-resistance devices and the shape of their volt-ampere characteristics. There is need for refinement of the very concept of negative resistance itself.

The power in any element of a radio circuit is defined by the expression

$$P = \frac{1}{T} \int iudt. \tag{1}$$

Usually, the phase shift between current and voltage is less than $\pi/2$ and the integral in (1) is greater than zero. Such an element is a power consumer. With $\pi/2 < \varphi < \pi$ or $\pi < \varphi < 3/2\,\pi$ the power becomes negative. This indicates that the element in this case is a power source capable of compensating for losses in the electrical circuit connected to it. The negative power $P^{(-)}$ is the equivalent of the negative value of instantaneous resist-

$$r^{(-)} = -\frac{u}{i} \tag{2}$$

ance $r^{(-)} = \frac{\partial U}{\partial I}$, if we refer to the negative-resistance segment of the volt-ampere characteristic of the device. However, losses in the electrical circuit may be compensated by other elements therein, for example, a battery. Nevertheless, a battery cannot be considered a negative resistance since it cannot make up for the energy losses in the connected circuit according to the applied signal. Let us further assume by the term negative resistance an element of the electrical circuit which is capable of converting the energy of the supply source into a-c energy and thereby compensate for losses in the circuit according to the applied signal.

REQUIRED SHAPE OF VOLT-AMPERE CHARACTERISTIC OF NEGATIVE-RESISTANCE SEMICONDUCTOR DEVICES ACCORDING TO APPLICATION

It was shown above that negative-resistance semiconductor devices may have a volt-ampere characteristic of class I or class II. The difference in shape of volt-ampere characteristics will naturally also determine the specific applications of devices of one or another group and will also affect the requirements placed on them. These differences, briefly stated, are as follows:

For devices with volt-ampere characteristic of class I:

1. Current is a single-valued function of voltage. Hence, in order to plot the volt-ampere characteristic it is necessary to use a voltage generator .

2. The negative-resistance segment is associated with a decrease in conductivity in proportion to the increase in voltage.

3. The mathematical description of negative resistance has the form

$$r^{(-)} = \frac{\partial U}{-\partial I} \approx \frac{\Delta U}{-\Delta I}. \tag{3}$$

4. Transition from the region of the volt-ampere characteristic where the differential resistance of the device is positive to the region with negative resistance occurs at the point where

$$r = \frac{\partial U}{\partial I} = \infty. \tag{4}$$

5. The internal feedback is voltage feedback.

6. On the basis of item 1, the load (an oscillator circuit) must be connected in parallel with the device.

7. The condition of excitation (Figure 1)

$$|r^{(-)}| < R_L. \tag{5}$$

For devices with volt-ampere characteristic of class II:

1. The voltage is a single-valued function of current. Hence, in order to plot the volt-ampere characteristic it is necessary to use a current generator.

2. The negative-resistance segment is associated with an increase in conductivity in proportion to the increase in current.

3. Mathematical description of the negative resistance is

$$r^{(-)} = \frac{-\partial U}{\partial I} \approx \frac{-\Delta U}{\Delta I}. \tag{6}$$

4. Transition from the region of the volt-ampere characteristic where the differential resistance of the device is positive to the negative-resistance region occurs at the points where

$$r = \frac{\partial U}{\partial I} = 0. \tag{7}$$

5. The internal feedback is current feedback.

6. The oscillator circuit and the negative-resistance device must be connected in parallel.

7. The condition of excitation (Figure 2)

$$|r^{(-)}| > R_L. \tag{8}$$

The required shape of the volt-ampere characteristic depends on the purpose of the device. For amplification it is convenient to use devices with volt-ampere characteristic of both class I and class II. Moreover, by appropriate choice of load and position of operating point on the negative-resistance segment it is possible to eliminate the likelihood of self-excitation in the absence of signal. In Figure 10, where a volt-ampere characteristic of class I is given as an example, it is seen that the gain will increase as the value of negative resistance decreases. Undistorted amplification is possible only in the case where the negative-resistance segment is linear. In order for the amplifier to consume minimum power in the absence of signal it is necessary that the negative-resistance segment be located as close

as possible to the axes so that the values of I_0 and U_0, in choosing the operating point at the center of the negative-resistance segment, will be as small as possible. Similar requirements apply to the volt-ampere characteristic of class II, the only difference being that the gain in this case will increase with an increase in negative resistance.[2] However, an increase in negative resistance is feasible only up to a certain level, since with an increase $r^{(-)} = \infty$ a signal with zero amplitude may be amplified without distortion. A similar result is obtained for devices with volt-ampere characteristic of class I with $r^{(-)} = 0$. Hence, at an optimum value of negative resistance it is necessary to strive to obtain that value at which the device provides maximum negative power on the negative-resistance segment. This is explained by the fact that the principal characteristic of any negative-resistance device is not the value of negative resistance $r^{(-)}$, but the value of negative power delivered by the device on the negative-resistance segment. In fact, it is easily demonstrated that with $r^{(-)} = \infty$ for devices with volt-ampere characteristic of class II, just as with $r^{(-)} = 0$ for devices with volt-ampere characteristic of class I, the negative power is equal to zero. Physically, this indicates that in this case the negative-resistance device is not capable of compensating for losses in a circuit connected to it; that is, the chief property of negative resistance is lost.

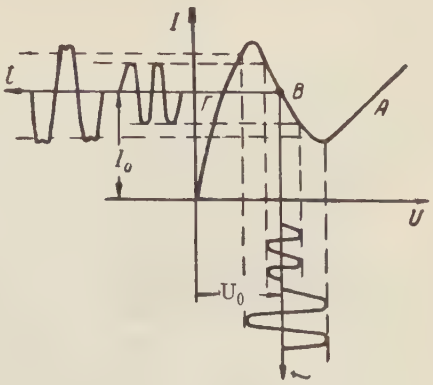

Figure 10

Devices with volt-ampere character of both class I and class II may also be used as oscillators. Requirements for optimum shape of the volt-ampere characteristic will be the same as above, with the exception that in order to meet conditions of self-excitation (5) and (8) it is necessary that the negative-resistance segment be nonlinear (Figures 1 and 2).

For switching operation the negative-resistance device must have a bistable characteristic with two stable regions: a region of large positive resistance A (Figure 4) and a region of small positive resistance G, separated by an astable region of negative resistance B. Moreover, the resistance of the device in region A must be as large as possible and in region G as small as possible. The negative-resistance segment must be as wide as possible. In addition, it is necessary to strive for a value of negative resistance $r^{(-)} \to \infty$ for devices with volt-ampere characteristic of class II and $r^{(-)} \to 0$ for devices with volt-ampere characteristic of class I.

The required shape of volt-ampere characteristic of negative-resistance devices intended for switching operation is given in Figure 11:

(a) for devices with volt-ampere characteristic of class I;

---

[2] It is possible to change the negative-resistance value by connecting an ohmic resistance in parallel or in series with the negative-resistance device.

(b) for devices with volt-ampere characteristic of class II.

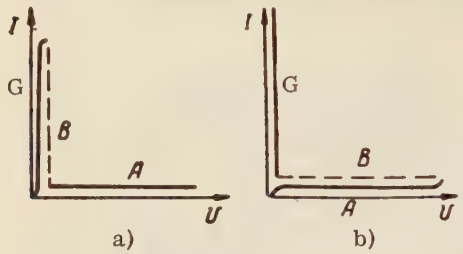

Figure 11

Such choice of shape of volt-ampere characteristic is explained by the fact that any intermediate slope of branches A and G, as well as another value of negative resistance may easily be obtained by various combinations of a negative-resistance device and an active resistance R. For example, in the series connection of a negative-resistance device and an active resistance R the value of negative resistance on the volt-ampere characteristic of the combination of "a device plus resistance R" will be less than value of the negative resistance of the device itself. The slope of branches A and G also changes. This is easily shown graphically (Figure 12). In parallel connection of a negative-resistance device and active resistance R the value of negative resistance on the volt-ampere characteristic of such a combination increases (Figure 13) in comparison with the value of negative

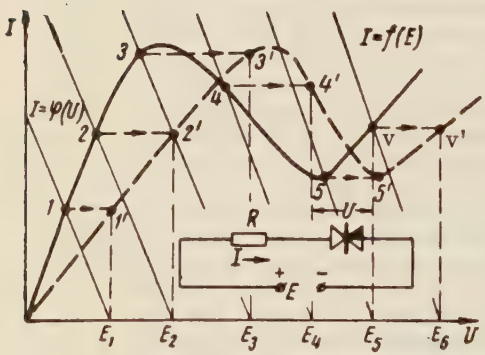

Figure 12

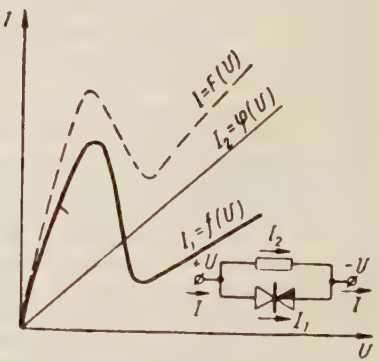

Figure 13

resistance of the device itself. The plots in Figures 12 and 13 are based on the fact that in the series connection of a negative-resistance device and an active resistance, there flows through the device and resistance R one and the same current, and in parallel connection the voltage is common. Figures 14 and 15 show the corresponding oscillograms for the combination of a device with volt-ampere characteristic of class II plus resistance R (Figure 14) and a negative-resistance device shunted by a resistance R (Figure 15). It is necessary to point out that whereas the value of negative resistance may increase as well as decrease, the value of negative power always decreases. This is further evidence that the value of negative power is the principal characteristic of a negative-resistance device, determining its amplifier and oscillator properties. Hence, in the design of negative-resistance

devices it is necessary that the value of negative power delivered by the device over the negative-resistance segment be as large as possible.

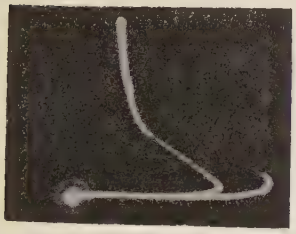

R = 0

R = ∞

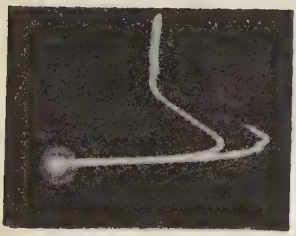

R = 200 ohms

R = 1000 ohms

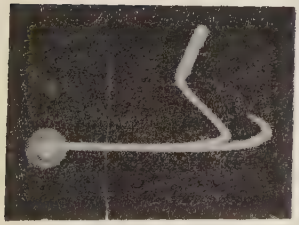

R = 600 ohms

Figure 14

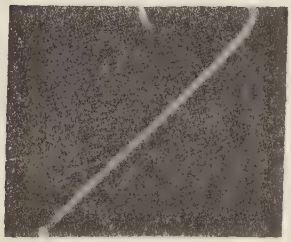

R = 200 ohms

Figure 15

CONCLUSION

The use of negative-resistance semiconductor devices in amplifiers, oscillators and switching circuits offers considerable advantages, which

enable these circuits to be made simpler and more reliable. The development of negative-resistance devices is an urgent problem. Negative-resistance devices show particular promise for application in computer engineering.

Negative-resistance devices have extremely short switching times; hence, their application may considerably increase the operating speed of electronic computers. For example, the forward and reverse switching time in tunnel diodes is of the order of thousandths of a microsecond. Moreover, considering that the parameters of tunnel diodes are relatively independent of temperature over an extremely wide range, it may be expected that further improvement of this device and its production will lead to a revolution in computer engineering.

Article submitted to editors April 27, 1960

LITERATURE

1. A. Lebedev et al., A few properties of germanium diodes with gold impurities. ZhTF, XXVI, No. 10, 1956.
2. Leblond, Contribution a etude de structures semiconductrices presentant des resistances dynamiques et des oscillations quelles peuvent entretenin. Annales de radioelectricite, Vol. XII, No. 4, 1957.
3. V. Stafeyev, Current multiplication of majority carriers in a non-ideal p-n junction. ZhTF, Vol. 27, No. 10, 1957.
4. M.A. Berg, S.A. Taryanov, Negative-resistance semiconductor diode. Radiotekhnika i elektronika, No. 2, 1960.
5. Mollu et al, P-N-P-N transistor switches. Proc. IRE, 44, No. 9, 1956.
6. Schenkel, Statz, Junction transistors with alpha greater than unity. Proc. IRE, 44, No. 3, 1956.
7. Shockley, Unique properties of the 4-layer diode. Electronic Industries and Tele-Tech, 76, No. 8, 1957.
8. Jounscher, P-N-P-N switching diodes. Journal of Electronics and Control, VIII, No. 6, 1957.
9. Phillips, Chang. Germanium power switching devices. IRE Transactions on electron devices. ED-5, No. 1, 1958.
10. Read, A proposedhigh frequency negative resistance diode. BSTJ, XXXVII, No. 2, 1958.
11. Sommers, Tunnel diodes as high frequency devices. Proc. IRE, 47, No. 7, 1959.
12. M.A. Bonch-Bruyevich, Osnovy radiotekhniki [Principles of Radio Engineering], Part II. Svyaz'izdat, 1936.
13. P.P. Klimentov, Measuring the negative resistance of vacuum tubes in transitron operation. Radiotekhnika, No. 4, 1949.
14. S.A. Garyainov, Negative-resistance semiconductor diodes and their application in radio circuits. Trudy VVIA im. N. Ye. Zhukovskogo, No. 790, 1959.

CALCULATION OF TRANSISTORIZED VIDEO AMPLIFIERS

A.A. Rizkin

The article presents the required design relationships for three types of transistorized video stages (with common emitter, common collector and common base). A video amplifier with a compound transistor and two video amplifer circuits with feedback are examined. The results are verified experimentally.

Modern high-frequency transistors permit construction of simple video amplifier circuits which in their qualitative indexes (gain-bandwidth product, signal-to-noise ratio) are not inferior to vacuum-tube circuits and with regard to reliability, miniaturization and low power requirements are considerably superior to them. In this connection the development of engineering procedures for calculation of semiconductor video amplifier circuits is a pressing problem.

In this report, on the basis of a well-known circuit for transistor conversion at high frequencies, the basic relationships required for calculation of three types of semiconductor stages (with common emitter, common collector and common base) are presented. There is presented an analysis of a video amplifier employing a compound transistor and two video amplifier circuits with feedback.

BASIC RELATIONSHIPS

The equivalent circuit for a common-emitter stage suitable for video-frequency regions is shown in Figure 1. Given a resistance R_e in the emitter circuit, it acquires the form shown in Figure 2.

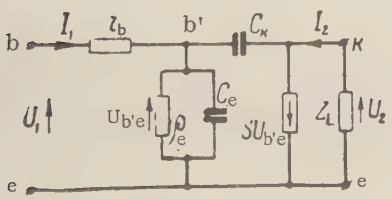

Figure 1

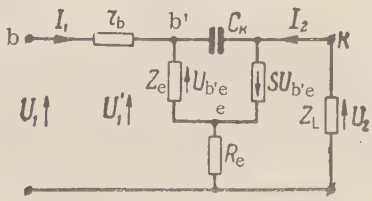

Figure 2

In accordance with the symbols given in the figure, we have the following equations:

$$I_c = (U_1' + I_2 Z_L)\, i\omega C_к;$$
$$I_2 + I_c = S U_{b'e};$$
$$U_1' = U_{b'e}\left[1 + \left(S + \frac{1}{Z_e}\right) R_e\right].$$

Solving these equations, we obtain the following expressions for current:

$$I_1 = U_1'\left[\frac{1}{aZ_e} + i\omega C_к \frac{1 + \frac{SZ_L}{a}}{1 + i\omega C_к Z_L}\right]; \quad (1)$$

$$I_2 = \frac{U_1'}{a} \frac{S - i\omega C_к a}{1 + i\omega C_к Z_L}, \quad (2)$$

In addition,

$$a = 1 + \left(S + \frac{1}{Z_e}\right) R_e. \quad (3)$$

Usually, the following inequalities are fulfilled:

$$\frac{1}{|Z_e|} \ll S; \quad \omega C_к |Z_L| \ll 1.$$

Then we will have approximately

$$a \approx 1 + SR_e \quad (4)$$

and

$$Y_{in}' = \frac{I_1}{U_1'} \approx \frac{1}{aZ_e} + i\omega C_к\left(1 + \frac{SZ_L}{a}\right). \quad (5)$$

Let us examine the expression for Y_{in}', which is evidently the input admittance of the circuit at point b'.

Inserting in this expression

$$Z_e = \frac{\rho_e}{1 + i\omega \rho_e C_e} \text{ and } Z_L = R_L + iX_L,$$

we obtain

$$Y_{in}' = \frac{1}{a\rho_e} - \omega C_к \frac{SX_L}{a} + i\omega\left[\frac{C_e}{a} + C_к\left(1 + \frac{SR_L}{a}\right)\right] = Y_0 + i\omega C_0,$$

where

$$Y_0 = \frac{1}{a\rho_e} - \omega C_к \frac{SX_L}{a} \text{ and } C_0 = \frac{C_e}{a} + C_к\left(1 + \frac{SR_L}{a}\right).$$

In connection with this, the equivalent of the input circuit of a stage with common emitter is given in Figure 3.

Within those limits where the load impedance Z_L of the stage may be considered active, the conductance of the input circuit Y_0 is constant and does not depend on frequency. Within these limits

$$Z_{in} = r_b + \frac{R_0}{1 + i\frac{\omega}{\omega_0}}, \quad (6)$$

where

$$\left.\begin{aligned} R_0 &= a\rho_e \\ \omega_0 &= \frac{1}{\rho_e[C_e + C_к(a + SR_L)]} \end{aligned}\right\}. \quad (7)$$

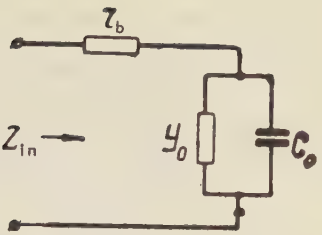

Figure 3

It must be pointed out that the value of ρ_e depends substantially on the operating conditions of the transistor, but for ordinary transistors the product $\rho_e C_e$ is relatively independent of operating conditions and is approximately equal to the reciprocal of the angular frequency at which the current gain in a common-emitter short-circuited configuration is lowered by 3 db.[1]

Approximately

$$\rho_e = \frac{26}{I_e}\frac{1}{1-\alpha_0}. \quad (8)$$

In this expression α_0 is the current gain in a common-base circuit at medium frequencies, I_e is the emitter current in ma, ρ_e is in ohms.

In accordance with formulas (1) and (2), the general expression for current gain of a stage with common emitter has the form

$$K_i = \frac{S - i\omega C_к a}{\frac{1}{Z_e}(1 + i\omega C_к Z_L) + i\omega C_к (a + SZ_L)}. \quad (9)$$

Usually, the value of $\omega C_k a$ in comparison with S may be neglected. Moreover, if inequality $\omega C_к |Z_L| \ll 1$ is fulfilled, then with an active load ($Z_L = R_L$) we will have

$$K_i = \frac{S}{\frac{1}{Z_e} + i\omega C_к (a + SR_L)} = \frac{S\rho_e}{1 + i\frac{\omega}{\omega_0}}. \quad (10)$$

In order to relate the introduced quantities to the current gain of a stage in short-circuited operation β_0 and its cutoff frequency ω_β, let us assume in this expression $R_L = 0$, $R_e = 0$ (that is, $a = 1$) and present it in the usual form

$$K_i\Big|_{\substack{a=1\\R_L=0}} = \beta = \frac{\beta_0}{1 + i\frac{\omega}{\omega_\beta}} = \frac{S\rho_e}{1 + i\frac{\omega}{\omega_0}\Big|_{\substack{a=1\\R_L=0}}}. \quad (11)$$

Consequently,

$$\beta_0 = \frac{\alpha_0}{1-\alpha_0} = S\rho_e; \qquad \omega_\beta = (\omega_0)_{\substack{a=1\\R_L=0}} = \frac{1}{\rho_e(C_e + C_к)}, \quad (12)$$

As for the voltage gain of the stage, this may be derived from the general formula

$$K = -K_i\frac{Z_L}{Z_{in}}, \quad (13)$$

---

[1]For drift transistors capacitance C_e shows complex dependence on the operating conditions and must be determined experimentally.

where k_i is the current gain of the stage, Z_{in} is its input impedance and Z_L is the load impedance.

Let us now discuss in brief a stage with common collector.

The circuit for conversion of this stage is given in Figure 4. Analysis thereof yields the following expressions for input impedance of a stage with common collector and its current gain:

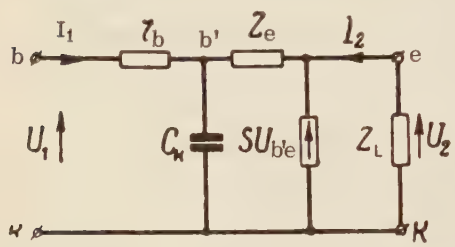

Figure 4

$$Z_{in} = r_b + \left(Z_0 \left\| \frac{1}{i\omega C_к}\right.\right) \qquad (14)$$

and

$$K_i = -\frac{1 + SZ_e}{1 + i\omega C_к Z_0}, \qquad (15)$$

where

$$Z_0 = Z_e + (1 + SZ_e) Z_L \approx Z_e (1 + SZ_L).$$

By means of the above expressions, the voltage gain of the circuit is easily determined from the general formula (13)

$$K = \frac{(1 + SZ_e) Z_L}{Z_0 + r_b (1 + i\omega C_к Z_0)}. \qquad (16)$$

In accordance with formula (14), the scheme for conversion of the input circuit of a stage with common collector is given in Figure 5.

In circuit calculation over a wide range of frequencies it is necessary to use the total expressions (14)-(16).

In those cases where r_b and C_k are sufficiently small but frequency is not extremely high, so that inequality $\omega C_к |Z_0| \ll 1$ is substantially fulfilled, it is permissible to use the following approximate expressions:

$$K_i \approx -(1 + SZ_e) \approx -\left(1 + \frac{S\rho_э}{1 + i\frac{\omega}{\omega_0}}\right) = -(1 + \beta)$$

and

$$K \approx \frac{(1 + SZ_e) Z_L}{Z_e + (1 + SZ_e) Z_L} \approx \frac{SZ_L}{1 + SZ_L}.$$

Since usually $|SZ_L| \gg 1$, then $K \approx 1$. In the same manner we may derive the necessary formulas for calculation of a stage with common base. Without dwelling on the calculations, let us present the final results.

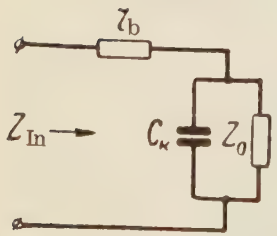

Figure 5

The current gain of a stage with common base is defined by the expression

$$K_i = -\frac{SZ_e' Z_к + r_b}{Z_к + Z_L + r_b}. \qquad (17)$$

The input resistance of such a stage is equal to

$$Z_{вх} = \frac{Z}{Z_к + Z_L + r_b}. \qquad (18)$$

The voltage gain of this stage, in accordance with formula (13) will be

$$K = (SZ_e' Z_к + r_b)\frac{Z_к}{Z}. \qquad (19)$$

In these expressions

$$Z_к = \frac{1}{i\omega C_к}; \quad Z'_e = \frac{Z_e}{1 + SZ_e}; \quad Z = Z'_e [Z_L + r_b + Z_к(1 - Sr_b)] + r_b (Z_L + Z_к)$$

In concluding the general section, let us examine the question of "Q" of a transistor from the point of view of its applicability to gain in the high-frequency region. By "Q" of a transistor stage we shall mean the product of the current gain of the stage at a frequency in the asymptotic region of extremely high frequencies. Let us determine this quantity for a multi-stage circuit in which all the transistors are connected in a common-emitter configuration. In such a circuit the input resistance in the region of extremely high frequencies approaches r_b, while the voltage gain approaches Sr_b. In accordance with formula (10), the modulus of current gain in this region is approximately equal to

$$|K_i| \approx \frac{\omega_0}{\omega} S\rho_e,$$

wherein, in accordance with (7), approximately

$$\omega_0 \approx \frac{1}{\rho_e [C_e + C_к S r_b]},$$

hence,

$$|K_i|\omega \approx \frac{1}{\frac{C_e}{S} + C_к r_b}.$$

Since

$$\rho_e C_e \approx \frac{1}{\omega_\beta} \approx \frac{1}{\omega_\alpha (1 - \alpha_0)}; \quad \rho_e = \frac{\beta_0}{S} \approx \frac{1}{(1 - \alpha_0) S},$$

the "Q" of the stage

$$Q = |K_i| f = \frac{1}{\frac{1}{f_\alpha} + 2\pi C_к r_b}. \tag{20}$$

Hence, the higher the cutoff frequency f_α and the smaller the $C_k r_b$ time constant, the higher the "Q" of a transistor with regard to its capacity for amplification at extremely high frequencies.

CIRCUITS WITH CASCADE TRANSISTORS

The use of cascade transistors permits obtaining high input resistance and, with small current of the first transistor, a low noise level.

One of the possible circuits of this type is shown in Figure 6.

As is seen from the diagram, its first stage is an "emitter follower" (that is, a stage with common collector), which insures high input resistance of the circuit.

The emitter of the first transistor is directly d-c coupled with the base of the second, as a result of which the emitter current of the first transistor is small. In order to reduce the collector voltage of the first transistor there may be introduced into the collector circuit a capacitance-shunted resistor. The low collector voltage and the low emitter current are advantageous from the point of view of lowering the noise figure.

D-C analysis of the circuit leads to the following approximate formula for the emitter current of the first transistor:

$$I_{e1} \approx \frac{I'_{k01} R_1 R_2 + \beta_{10} \left[E R_1 - I'_{k02} (R_1 + R_2) R_{e2} \right]}{R_1 R_2 + \beta_{10} \beta_{20} (R_1 + R_2) R_{e2}}.$$

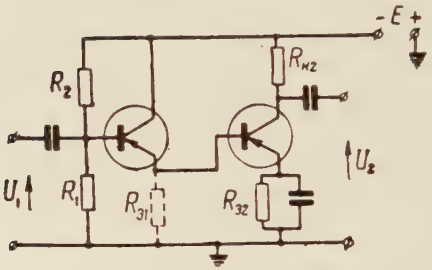

Figure 6

In this expression I'_{k01} and I'_{k02} are the initial currents of the transistors (with open-circuited bases) having values of the order of 100 microamperes. With resistances R_1 and R_2 of the order of 100 kilohms and supply voltages of the order of several volts, the emitter current of the first transistor has a value of the order of tenths of a milliampere.[2]

Let us turn now to evaluation of a-c operation of the circuit. Since the second transistor operates as a normal common-emitter amplifier, its input resistance may be determined from the conversion circuit shown in Figure 3.

Let us find the basic characteristics of the circuit shown in Figure 6. Since the input resistance of the circuit is somewhat large, it is also of interest to determine its voltage gain and frequency response.

The input resistance of the second stage at medium frequencies is $r_{b2} + R_{02}$, and has a value of the order of 1000 ohms and drops to a level of $\frac{1}{\sqrt{2}}$ of its initial value at a frequency close to ω_{02}. Moreover, the quanity Z_0 (defining, in accordance with formula (14), the input impedance of the first stage) is approximately equal to $S_1 Z_{e1} Z_{in2}$ and will at medium frequencies have a value of the order of 20-30 kilohms. The input impedance of the circuit at medium frequencies will also be of the same order.

Designating the voltage at the input of the circuit U_1, the voltage at the output as U_2, the current gain of the individual stages as K_{i1} and K_{i2} and their input impedances as Z_{in1} and Z_{in2}, we shall have

$$U_2 = -I_2 Z_{L2} = \frac{U_1}{Z_{in1}} K_{i1} K_{i2} Z_{L2}.$$

The voltage gain of the circuit is equal to

---

[2]With the indicated data, the terms in the expression for I_{e1}, depending on I'_{k01} and I'_{k02}, are relatively small, which indicates excellent thermal stability of the circuit.

$$K = \frac{U_2}{U_1} = \frac{K_{i1}}{Z_{in1}} K_{i2} Z_{L2},$$

where Z_{L2} is the load impedance of the second stage.

As is seen from formulas (14) and (15), with small r_b, approximately

$$\frac{K_{i1}}{Z_{in1}} \approx -\frac{1 + S_1 Z_{e1}}{Z_0} \approx \frac{-S_1 Z_{e1}}{S_1 Z_{e1} Z_{in2}} = -\frac{1}{Z_{in2}}.$$

Consequently,

$$K = -\frac{K_{i2}}{Z_{in2}} Z_{L2}.^3$$

With small r_{b2} the frequency relationships of K_{i2} and Z_{in2} are only slightly different and hence the frequency characteristic for gain of the circuit must be adequate. Using expression (6) and (10), it is easily shown that with an active load the voltage cutoff frequency for circuit gain is

$$\omega_{co} \approx \omega_{02} \left(1 + \frac{R_\omega}{r_{b2}}\right),$$

that is, considerably exceeds ω_{02}.

In the circuit in Figure 6 the emitter current of the first transistor may prove to be extremely small and this may have an unfavorable effect on the frequency characteristic. For an increase in current it is advisable to introduce the resistance R_{e1} shown in the figure by a broken line. The first stage in this case becomes an ordinary stage with common collector and may be calculated from formulas (14)-(16).

We will note that in cases where the emitter resistance of the second transistor is not capacitance-shunted it is best to introduce the resistor not between the emitter of the first transistor and ground but between the base and emitter of the second transistor. Moreover, the circuit of the second stage becomes similar to a vacuum-tube circuit containing a cathode resistor and a coupling resistor between the grid and cathode of the tube. Such a circuit, as is known, possesses high input impedance.

FEEDBACK CIRCUITS

Excellent results may be obtained by means of negative feedback and simple methods of compensation.

Figure 7 shows a single-stage circuit with parallel feedback in which compensation is achieved by introduction of a small inductance in the feedback circuit.[4]

Below we present in brief the theory of this circuit and the necessary design formulas.

On the temporary assumption that $L_0 = 0$ we may write the following equality for the circuit in Figure 7:

---

[3]This result indicates that, with the given assumptions, the voltage gain of the first stage may be taken to be equal to unity.

[4]Detailed analysis of such a circuit, based on the regeneration method, is given in the author's work [1]. The compensating inductor was introduced by Thomas [2]. We will note, incidentally, that the "Blackman method," widely used by Thomas for analysis of transistor circuits and the stability thereof, is none other than the regeneration method [1, 3].

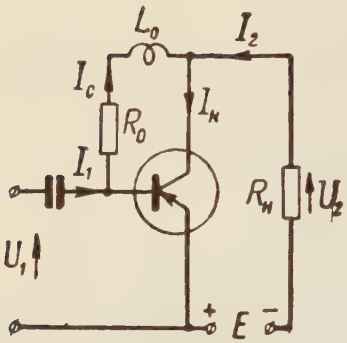

Figure 7

$$I_2 + I_0 = I_к = K_i I_b;$$

$$I_1 = I_b + I_0;$$

$$I_0 = \frac{U_1 - U_2}{R_0}; \quad U_2 = -I_2 R_L.$$

Moreover,

$$I_b = \frac{U_1}{Z_{be}},$$

where, in accordance with (6) and (7)

$$\left.\begin{aligned} Z_{be} &= r_b + \frac{\rho_e}{1 + i\frac{\omega}{\omega_0}}; \\ \omega_0 &\approx \frac{1}{\rho_e [C_e + C_к (1 + S R_{L0})]}, \end{aligned}\right\} \qquad (21)$$

whence

$$R_{L0} = \frac{R_L R_0}{R_L + R_0}.$$

Using these equations, it is easy to obtain the following results: the voltage gain of the stage

$$K = \frac{U_2}{U_1} = -\left(\frac{K_i}{Z_{be}} - \frac{1}{R_0}\right) R_{L0}; \qquad (22)$$

the current gain of the stage

$$A_i = \frac{I_2}{I_1} = \frac{-K}{(1-K)\frac{R_L}{R_0} + \frac{R_L}{Z_{be}}}; \qquad (23)$$

the input impedance

$$Z_{in} = \frac{U_1}{I_1} = \left(Z_{be} \left\| \frac{R_0}{1-K}\right.\right), \qquad (24)$$

If $R_L \ll R_0$, and $|K| \gg 1$, then approximately

$$A_i \approx \frac{K_i}{N}, \qquad (25)$$

$$Z_{in} \approx \frac{Z_{be}}{N}, \qquad (26)$$

where

$$N = 1 + K_i \frac{R_L}{R_0}. \qquad (27)$$

Introducing into the expression for A_i the complex value K_i, determined from formula (10), we obtain

$$A_i = \frac{A_{i0}}{1 + i\frac{f}{f_i}}, \tag{28}$$

wherein the current gain of the stage at medium frequencies A_{i0} and cutoff frequency f_i in this expression are defined by the expressions

$$A_{i0} = \frac{\beta_0}{N_0} \tag{29}$$

and

$$f_i = f_0 N_0, \tag{30}$$

where

$$N_0 = 1 + \beta_0 \frac{R_н}{R_0}. \tag{31}$$

As was to be expected, with the introduction of feedback the "Q" of the stage (that is, the gain-bandwith product) remains constant

$$A_{i0} f_i = \beta_0 f_0 \tag{32}$$

A further increase in bandwidth may be obtained by introducing a compensating inductance L_0.

If, upon introduction of the inductance, it is required that the feedback at that frequency where the gain drips to a value of $\frac{A_{i0}}{\sqrt{2}}$ be practically absent, then the frequency where the gain reaches this level (that is, the critical frequency of a stage with compensation ω_{com}) may be determined from the expression

$$\frac{A_{i0}}{\sqrt{2}} = \frac{\beta_0}{N_0\sqrt{2}} = \frac{\beta_0}{\sqrt{1 + \left(\frac{\omega_{com}}{\omega_0}\right)^2}},$$

whence

$$\omega_{com} = \omega_0 \sqrt{2N_0^2 - 1}.$$

The gain from introduction of compensation is

$$\frac{f_{com}}{f_i} = \sqrt{2 - \frac{1}{N_0^2}} \approx \sqrt{2}. \tag{33}$$

In choosing the value of inductance L_0 it is necessary to proceed from the requirement that the feedback at frequency f_{com} be practically absent. If we do not consider the stray capacitance in parallel with the compensating inductance, then in selecting the latter we may use the inequality

$$L \geqslant \frac{2\beta_0 R_н}{\omega_{com}}.$$

However, in practice, the effect of the mentioned stray capacitance on the upper frequencies may prove considerable and hence selection of the compensating elements is best performed by trial and error.

The input impedance of the compensated stage rises with frequency. Hence, in the creation of such stages in a multi-stage circuit the load of each stage, being equal to the input impedance of the following stage, will also rise with frequency. This will result in increasing the effect of compensation attainable by introduction of an inductance in comparison with that which is defined by formula (33). In such a circuit the current gain and voltage gain of the stage are numerically equal and may be determined by combined solution of equations (22) and (24), assuming therein that $R_L = Z_{in}$.

Thus we find that in the low-frequency region the gain of the stage is

$$K_0 = -A_{i0} = \frac{1 + mR_0}{2} - \sqrt{\left(\frac{1 + mR_0}{2}\right)^2 + nR_0},$$

where $m = \frac{1}{Z_{be0}} + \frac{1}{R_0}$; $n = \frac{\beta_0}{Z_{be0}} - \frac{1}{R_0}$; $Z_{be0} = r_b + \frac{r_e}{1 - \alpha_0}$.

For example, if $\beta_0 = 30$, $Z_{be0} = 500$ ohms, $r_e = 450$ ohms, $C_e = 60$ micromicrofarads and $C_k = 5$ micromicrofarads, then, assuming that $R_0 = 2500$ ohms, we find from the derived formulas that $A_{i0} = -K_0 = 9.3$ and $Z_{in0} = 164$ ohms.

Assuming in formula (21) $SR_{L0} = \frac{\beta_0}{\rho_e} R_{L0} = 10$, we find from our data that $f_0 \approx 3.2$ Mc and the critical gain frequency of a circuit with feedback (but without compensating inductance) from formula (32)

$$f_1 = \frac{\beta_0}{A_{i0}} f_0 = \frac{30}{9.3} 3.2 = 10 \text{ Mc}$$

It may be considered with an increase in compensating inductance and proper selection thereof the critical frequency of the circuit will rise by a factor of approximately 2.

Figure 8 shows a two-stage circuit with series feedback. In distinction from circuits with parallel feedback, this circuit has considerably higher input impedance. At the same time it can provide adequate gain in the bandwidth corresponding to the video channel[5].

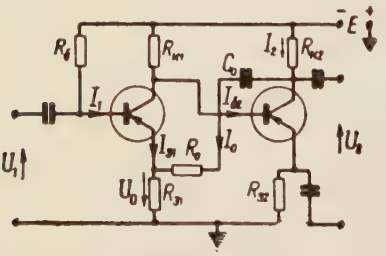

Figure 8

Let us find the principal quantities characterizing operation of this circuit.

The base current of the second transistor I_{b2} and load current I_2 are found from the expressions

$$I_{b2} = -K_{i1}\xi_1 I_1;\ I_2 = I_{к2}\xi_2 = \xi_2 K_{i2} I_{b2},$$

in which K_{i1} and K_{i2} are determined from formula (10) and ξ_1 and ξ_2 are determined from the expressions

[5] With appropriate choice of values we may eliminate coupling capacitor C_0 from the circuit. This will create negative d-c feedback in the circuit and will have a beneficial effect on its thermal stability. If this capacitor is not omitted it may be used for low-frequency compensation.

$$\xi_1 = \frac{R_{\kappa 1}}{R_{\kappa 1} + Z_{in2}}; \quad \xi_2 = \frac{R_0}{R_0 + R_{\kappa 2}}.$$

The current and voltage gains of the circuit are defined by

$$K_i = \frac{I_2}{I_1} = -K_{i1} K_{i2} \xi_1 \xi_2; \tag{34}$$

$$K = \frac{U_2}{U_1} = \frac{-I_2 R_{\kappa 2}}{I_1 Z_{in}} = -K_i \frac{R_{\kappa 2}}{Z_{in}}. \tag{35}$$

For the input current I_1 and feedback voltage we may write the following expressions:

$$I_1 = \frac{U_1 - U_{0c}}{Z_{be1}}; \quad U_{oc} = (I_{e1} + I_0) R_{e1},$$

in which $I_{e1} = I_1 (1 + K_{i1})$ and $I_0 = \frac{KU_1 - U_{0c}}{R_0}$,

while Z_{be1} is the emitter-base impedance of the input circuit of the first transistor.

From the presented relationships it is not difficult to derive the following expression for input impedance of the circuit:

$$Z_{in} = \frac{U_1}{I_1} = \frac{Z^\circ}{1 - Kb}, \quad \text{where} \quad Z^\circ = Z_{be1} + R'_{e1} (1 + K_{i1}); \; b = \frac{R_{e1}}{R_{e1} + R_0} = \frac{R'_{e1}}{R_0}. \tag{36}$$

Solving (35) and (36) simultaneously, we obtain

$$K = \frac{-K_i \frac{R_{\kappa 2}}{Z^\circ}}{1 - K_i \frac{R_{\kappa 2}}{Z^\circ} b} = \frac{K^\circ}{1 + K^\circ b}, \tag{37}$$

where

$$K^\circ = -K_i \frac{R_{\kappa 2}}{Z^\circ} \tag{38}$$

is the gain of the circuit in the absence of overall feedback.

Now, using (37), we reduce the expression for input impedance of the circuit as represented in formula (36) to the form

$$Z_{in} = Z^\circ (1 + K^\circ b). \tag{39}$$

Let us turn to evaluation of the frequency characteristics of the circuit.

Since the chief voltage gain of the circuit is concentrated in its second stage, this stage possesses the most unfavorable characteristic. For this reason, as is seen from formulas (34) and (38), the frequency dependence of K° will be determined chiefly by the frequency dependence of the current gain of the second stage K_{i2}. Hence, we may approximately consider that K° as well as K_{i2} has a cutoff frequency ω_{02} which may be determined from formula (7) with the data for the second stage.

As follows from classical feedback theory, the resulting gain K of the circuit, defined in formula (37), will also have a cutoff frequency exceeding ω_{02} by $(1 + K_0^\circ b)$ times, wherein K_0° is the gain of the circuit without feedback at medium frequencies.

In accordance with formulas (38) and (39), the input impedance of the circuit with a large amount of feedback is approximately equal to and has a

$$Z_{in} \approx K^{\circ} Z^{\circ} b = -K_i R_{\kappa 2} b \qquad (40)$$

frequency characteristic close to that of the current gain K_i of the circuit.

We will not dwell on the stability of these circuits, but will note only that this is solved, as in all feedback circuits, by Nyquist diagrams for their positive-feedback factor [1, 2, 3].

In order to check the principal conclusions, the circuits of Figures 7 and 8 were studied experimentally. Investigation showed excellent coincidence of the experimental and design data and affirmed the suitability of the derived relationships for practical calculations.

Thus, in close conformity with calculation, the circuit of Figure 8 was made with two P-403 transistors, battery voltage 22 v, collector currents 2.3 ma, and resistances:

R_b = 330 kilohms, R_{k1} = 6.8 kilohms, R_{e1} = 80 ohms, R_{k2} = 5.6 kilohms, R_{e2} = 3.0 kilohms, R_0 = 5.1 kilohms.

The circuit had a voltage gain, without feedback (when the lower end of resistor R_0 is connected to ground), equal to 560 with cutoff frequency of approximately 600 kc.

With the introduction of feedback the gain at medium frequencies decreased to 55, while the cutoff frequency rose to 6.2 Mc. Moreover, the input impedance at medium frequencies was 50 kilohms and dropped to 35 kilohms at a frequency of 450 kc.

APPENDIX

In calculations of the phase and transfer characteristics of semiconductor circuits it is possible to achieve considerably improvement in the results if into the circuit of Figure 1 there is introduced a transadmittance approximately allowing for the delay time t_d caused by the finite transit time of the minority carriers through the base layer.

Considering the delay time, the complex expression for current gain of a transistor in the short-circuited common-base configuration may be given as

$$a(i\omega) = \frac{\alpha_0 e^{-i\omega t_d}}{1 + i\frac{\omega}{\omega_\alpha}} = \frac{\alpha_0 e^{-i\nu\frac{\omega}{\omega_\alpha}}}{1 + i\frac{\omega}{\omega_\alpha}}. \qquad (A\,1)$$

Using the expansion

$$e^{-i\nu\frac{\omega}{\omega_\alpha}} = 1 - i\nu\frac{\omega}{\omega_\alpha} - \frac{\nu^2}{2}\left(\frac{\omega}{\omega_\alpha}\right)^2 + i\frac{\nu^3}{6}\left(\frac{\omega}{\omega_\alpha}\right)^3 + \dots$$

and limiting ourselves to frequencies for which $\nu\frac{\omega}{\omega_\alpha} < \frac{1}{3}$, we may

approximately[6] assume

$$\alpha(i\omega) \approx \frac{\alpha_0\left(1 - i\nu\frac{\omega}{\omega_\alpha}\right)}{1 + i\frac{\omega}{\omega_\alpha}}. \qquad (A\ 2)$$

The corresponding current gain in a common-base short-circuited configuration is expressed by the equation

$$\beta(i\omega) = \frac{\alpha(i\omega)}{1 - \alpha(i\omega)} = \frac{\alpha_0}{1 - \alpha_0} \frac{1 - i\nu\frac{\omega}{\omega_\alpha}}{1 + i\frac{\omega}{\omega_\alpha}\frac{1 + \alpha_0\nu}{1 - \alpha_0}}. \qquad (A\ 3)$$

The result expressed by formula (A. 3) may also be derived for the circuit in Figure 1 if we introduce into it the transadmittance

$$\bar{S} = \frac{\beta_0}{\rho_e}\left(1 - i\nu\frac{\omega}{\omega_\alpha}\right) \qquad (A\ 4)$$

and assume

$$\omega_\beta = \frac{1}{\rho_e(C_e + C_k)} = \frac{\omega_\alpha(1 - \alpha_0)}{1 + \alpha_0\nu}. \qquad (A\ 5)$$

In order to determine the value of ν it is necessary either to plot the effective voltage-gain transfer characteristic of the given transistor in a short-circuited common-base configuration in coordinates $\frac{\alpha(t)}{\alpha_0} = f(\omega_\alpha t)$ and determine the average abscissa distance $\nu = \omega_\alpha t_3$ between this curve and the origin of function α (p) plotted from equation (A. 2) with $\nu = 0$, or to measure the current gain cutoff frequencies in short-circuited common-base and common-emitter configurations (that is, the quantities ω_α and ω_β) and, knowing, α_0, to find ν from formula (A. 5).

Article submitted to editors 17 May 1960

LITERATURE

1. A. A. Rizkin. "Calculation of transistor stages by the regeneration method." Radiotekhnika, No. 5, 1956.
2. Thomas. "Some design considerations for high-frequency transistor amplifiers." BSTJ, XXXVIII, No. 6, 1959.
3. A. A. Rizkin. "On the positive-feedback coefficient and stability of circuits containing dependent sources." Elektrosvyaz', No. 5, 1960.

[6] For diffused-junction transistors $\nu \approx 0.2$. For drift transistors ν is close to unity. With the introduced limitation, maximum phase error in $\beta(i\omega)$ does not exceed 5°.

CALCULATION OF TWO-TERMINAL L-SECTION EQUALIZERS FOR AMPLIFIER GAIN CONTROL

O.F. Kosminskiy

The article sets forth the conditions for achieving variable two-terminal equalizing networks permitting any preassigned accuracy in reproduction of given control characteristics. Formulas are presented for determining the impedances of two types of L-section equalizers. An example is given for calculation of a variable equalizer which, for a given stray capacitance, permits a tenfold decrease in control error compared against a single active resistance and the same stray capacitance.

In the amplifier units used in communications equipment, it is frequently necessary to control frequency characteristics in a preassigned fashion. One of the means of controlling the amplifier characteristics lies in introducing into the amplifier circuit control networks, either in a feedback loop (Figure 1) or in the plate circuit of a tube (Figure 2).

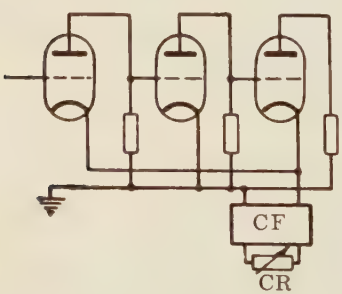

Figure 1

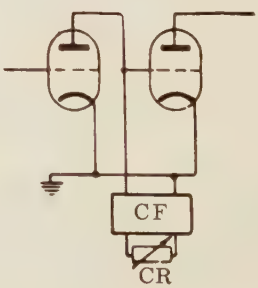

Figure 2

Since for the circuit in Figure 1 (with sufficient feedback) the gain is inversely proportional and for the circuit in Figure 2 (using pentodes) it is directly proportional to modulus of input impedance of the control network, in order to achieve gain control it is necessary to use networks whose modulus of input impedance may be varied in accordance with the assigned gain

control program.

The ensuing discussion deals with the method of calculation of such networks, which we shall refer to as two-terminal variable equalizers.

By a two-terminal variable equalizer we mean a circuit (Figure 3) possessing two terminals (1, 1) at which the modulus of input impedance varies as an assigned function of frequency with corresponding variation in a control resistance (CR) connected to the two other terminals (2, 2).

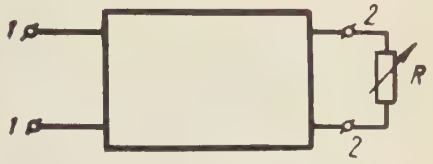

Figure 3

In the general form this is a four-terminal network with one of its terminal pairs connected to a variable resistor R.

By using four-terminal network analysis it is not difficult to show that the input impedance of the two-terminal variable equalizer is expressed by the formula

$$Z_{in} = Z_{c1} \frac{1 + \frac{R}{Z_{c2}} \operatorname{cth} g}{\frac{R}{Z_{c2}} + \operatorname{cth} g}, \qquad (1)$$

where Z_{c1} is the characteristic impedance of the four-terminal network at terminals 1, 1; Z_{c2} is the characteristic impedance of the four-terminal network at terminals 2, 2; g is the characteristic transfer constant of the four-terminal network.

Of great practical importance is the case of gain control of amplifiers over a range which is symmetrical relative to the assigned initial characteristic of amplification. Hence, all calculations herein refer only to equalizers with symmetrical control range.

For derivation of the basic formulas let us introduce the following symbols:

$|Z_{in\ 0}|$ — modulus of input impedance of the CF (controlled four-terminal network) loaded by resistance R;

$|Z_{in\ 1}|$ — modulus of input impedance of the CF loaded by resistance Rk, where $k > 1$;

$|Z_{in\ 2}|$ — modulus of input impedance of the CF loaded by resistance R/k;

$|F|$ — modulus of a function representing the required frequency dependence of the modulus of input impedance, with control resistance equal to Rk.

Then the required symmetry of the control range may be written as

$$\left|\frac{Z_{in\ 1}}{Z_{in\ 0}}\right| = |F| = e^{\alpha}, \qquad (2)$$

$$\left|\frac{Z_{in\ 2}}{Z_{in\ 0}}\right| = \left|\frac{1}{F}\right| = e^{-\alpha}, \qquad (3)$$

where α is a given function of control, the ordinate values of which are

---

*cth = coth (transl.)

expressed in nepers.

On the basis of (2) and (3) we find

$$\frac{Z_{in\,1}}{Z_{in\,0}} = \frac{Z_{in\,0}}{Z_{in\,2}}. \tag{4}$$

This condition may be written in the form

$$\frac{1+\frac{R_\kappa}{Z_{c2}}\operatorname{cth} g}{\frac{R_\kappa}{Z_{c2}}+\operatorname{cth} g}\,\frac{\frac{R}{Z_{c2}}+\operatorname{cth} g}{1+\frac{R}{Z_{c2}}\operatorname{cth} g} = \frac{1+\frac{R}{Z_{c2}}\operatorname{cth} g}{\frac{R}{Z_{c2}}+\operatorname{cth} g}\,\frac{\frac{R}{\kappa Z_{c2}}+\operatorname{cth} g}{1+\frac{R}{\kappa Z_{c2}}\operatorname{cth} g}. \tag{5}$$

It is not difficult to show that identity (5) will be valid only when $Z_{C2} = R$.

This justifies the following statement: in order to insure symmetry of the control range it is necessary that the characteristic impedance of the CF looking into the CR be equal to the mean value of CR.

With this in mind, the basic equation characterizing the CF may be written as

$$F = \frac{1+\kappa \operatorname{cth} g}{\kappa+\operatorname{cth} g}, \tag{6}$$

with $Z_{C2} = R$.

In equalizer calculations it is usually necessary to know one of the characteristics of the CF expressed as an assigned function of control F.

On the basis of (6) it is not difficult to find

$$\operatorname{cth} g = \frac{\kappa F-1}{\kappa-F} \tag{7}$$

and

$$e^{2g} = \frac{\kappa-1}{\kappa+1}\,\frac{F+1}{F-1}. \tag{8}$$

It is easily proved that the obtained functions satisfy the conditions of the problem. For this purpose, let us first determine the initial value of input impedance of the CF with load resistance $R = Z_{C2}$. On the basis of formulas (1) and (6)

$$Z_{in\,0} = Z_{c1}, \tag{9}$$

that is, the input impedance of the CF is wholly determined by its characteristic impedance as seen from the input terminals, which is as it should be according to the theory of characteristic parameters of four-terminal networks.

With the CF terminating in a load resistance equal to Rk,

$$Z_{in} = Z_{c1}\frac{1+\kappa\frac{\kappa F-1}{\kappa-F}}{\kappa+\frac{\kappa F-1}{\kappa-F}} = Z_{c1}F. \tag{10}$$

With the CF terminating in a load resistance of R/k

$$Z_{in} = Z_{c1} \frac{1 + \frac{1}{\kappa} \frac{\kappa F}{\kappa - F}}{\frac{1}{\kappa} + \frac{\kappa F - 1}{\kappa - F}} = Z_{c1} \frac{1}{F}. \tag{11}$$

Consequently, with variation of the control resistance over the range $R/k < R < Rk$ the modulus of input impedance of the CF will vary over the range $|Z_{c1}| \left|\frac{1}{F}\right| < |Z_{c1}| < |Z_{c1}| |F|$, which was required to be proven.

On the basis of the above discussion, the problem of determination of the CF circuit may be stated in the following theorem:

Theorem. In order to create a CF with given modulus of imput impedance varying over a symmetrical range as a given function of frequency (with change in CR over the range $R/k < R < Rk$) it is necessary to satisfy the following conditions:

1. The characteristic impedance of the CF as seen from the terminals to the CR must be constant and equal to the mean value of CR.
2. The hyperbolic cotangent of the CF transfer constant (or some other appropriate function) must satisfy relationship (7) considered as an assigned function of the modulus of input impedance and the range of variation of CR.
3. The modulus of characteristic impedance of the CF seen from the input terminals must have the assigned frequency dependence.

Using the theorem, let us derive the basic design formulas for several types of variable two-terminal equalizers.

L-SECTION EQUALIZER OF TYPE 1

The equalizer diagram is given in Figure 4.

For this circuit

$$Z_{c1} = \sqrt{Z_{oc1} Z_{sc1}} = \sqrt{Z_1 \frac{Z_1 Z_2}{Z_1 + Z_2}} = Z_1 \sqrt{\frac{Z_2}{Z_1 + Z_2}}, \tag{12}$$

$$Z_{c2} = \sqrt{Z_{oc2} Z_{sc2}} = \sqrt{Z_2 (Z_1 + Z_2)}, \tag{13}$$

$$\text{th}\, g = \sqrt{\frac{Z_{sc1}}{Z_{oc1}}} = \sqrt{\frac{Z_{sc2}}{Z_{oc2}}} = \sqrt{\frac{Z_2}{Z_1 + Z_2}}, \tag{14}$$

where Z_{oc1} and Z_{sc1} are, respectively, the open-circuit and short-circuit impedances of the four-terminal network looking into terminals 1, 1. Similarly, Z_{oc2} and Z_{sc2} are the open-circuit and short-circuit impedances looking into terminals 2, 2.

In accordance with the first condition of the theorem

$$Z_{c2} = R. \tag{15}$$

At the same time, on the basis of expressions

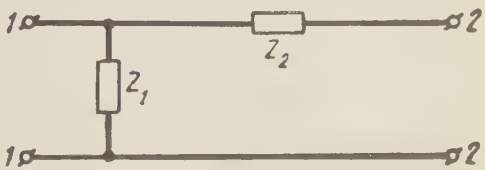

Figure 4

*th = tanh (transl.)

(13) and (14)

$$Z_{c2} = Z_2 \operatorname{cth} g. \tag{16}$$

Consequently, the formula for determining the series impedance will be

$$Z_2 = R \operatorname{th} g. \tag{17}$$

The hyperbolic cotangent of the CF transfer constant entering into this formula is found on the basis of expression (17). First there is determined the function F whose modulus must reproduce with the assigned accuracy the given frequency characteristic of control. Then, from function F and the chosen range of RCk, it is easy to find

$$\operatorname{th} g = \frac{\kappa - F}{\kappa F - 1}. \tag{18}$$

The shunt impedance Z_1 is determined on the basis of formula (14)

$$Z_1 = Z_2 (\operatorname{cth}^2 g - 1) \tag{19}$$

or

$$Z_1 = R (\operatorname{cth} g - \operatorname{th} g). \tag{20}$$

As follows from the principal design formulas (17), (18) and (20), in an L-section equalizer of type 1 it is possible to realize:

(1) the assigned frequency characteristic for variation of the modulus of input impedance of the CF and

(2) symmetrical limits of control.

The input impedance of this circuit is already derived as the function of the first two conditions

$$Z_{in} = Z_{c1} = Z_1 \operatorname{th} g = R (1 - \operatorname{th}^2 g). \tag{21}$$

In the calculation of wideband equalizers there arises the necessity for meeting an additional requirement: for the purpose of eliminating the influence of stray wiring capacitance there must be a derived capacitance of given value in the shunt arm of the equalizer. On the basis of formulas (18) and (20) it is easy to establish that the required condition for deriving the capacitance will be

$$\lim_{\omega \to \infty} F = 1. \tag{22}$$

L-SECTION EQUALIZER OF A. F. BELETSKIY

The canonic diagram of the two-terminal equalizer of A. F. Beletskiy is shown in Figure 5.

This circuit is divided in half along the dotted line of overlap of the T-section of an equalizer with constant characteristic impedance (Figure 6) and subsequent connection of impedance $Z_2/2$ at junction 1'.

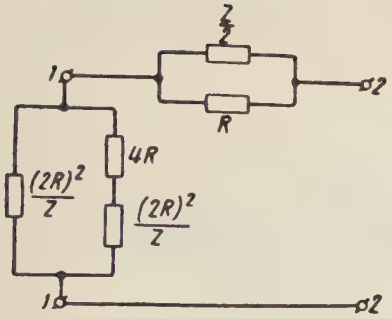

Figure 5

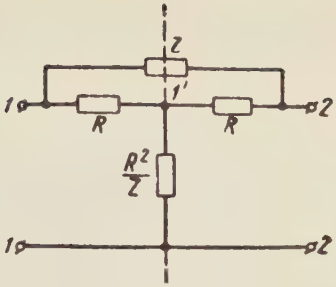

Figure 6

Let us derive the formulas for calculation of A. F. Beletskiy's circuit. For this purpose, we shall first determine the impedance of the series arm and the sum of the impedances of the series and shunt arms.

It is easily shown that

$$Z_1 + Z_2 = \frac{R}{2}(2R + Z) \qquad (23)$$

and

$$Z_2 = \frac{ZR}{2R + Z}.$$

Then

$$\operatorname{cth} g = \sqrt{\frac{Z_1 + Z_2}{Z_2}} = \sqrt{\frac{R}{2}(2R + Z)\frac{2R + Z}{ZR}} = \frac{2R + Z}{Z}, \qquad (24)$$

whence

$$Z = \frac{2R}{\operatorname{cth} g - 1}. \qquad (25)$$

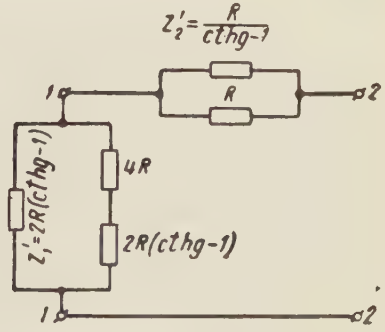

Figure 7

Consequently, A. F. Beletskiy's circuit will have the impedances shown in Figure 7.

It is easily ascertained that the initial characteristic of the modulus of input impedance and the conditions for derivation of capacitance in the shunt arm for this circuit coincide exactly with those for the preceding circuit (Figure 4). Circuit calculation is performed as in the preceding circuit, with the exception that instead of two functions it is sufficient here to determine only one

$$A = \operatorname{cth} g - 1, \qquad (26)$$

which must be a positive real function.

Since

$$F = \frac{1 + \frac{\kappa}{1+\kappa} A}{1 + \frac{1}{1+\kappa} A}, \tag{27}$$

it is easy to establish that this function must be a positive real function whose modulus may not be less than 1.

The same conditions of physical realizability apply also to the preceding circuit. By way of example, let us present calculations for the network for the circuit in Figure 2 which, over a frequency range of 0-8.5 Mc, provides continuous control of the frequency characteristic of gain within the limits of $\pm$ 0.3 neper with an accuracy of 0.005 neper.

In order to eliminate the effect of stray wiring capacitance it is necessary to have a derived capacitance of 10-20 micromicrofarads in the shunt arm of the network.

With consideration of (22) the square of the modulus of the given function of control, determined by the method of point by point interpolation, may be presented in the form

$$e^{2\alpha} = \frac{x^2 + 48.10893x + 206608.856}{x^2 + 9.70893x + 113405.5655}, \tag{28}$$

where

$$x = \left(\frac{\omega}{\omega_0}\right)^2 \text{ и } \omega_0 = 6.28 \cdot 1 \cdot 10^6 \frac{1}{\text{sec}}.$$

Inserting the values of the variable $0 < x < 72$, it is easily seen that deviations from the assigned characteristic do not exceed 0.005 neper. At a frequency of 9 Mc deviation is 0.00675 neper and at a frequency of 10 Mc it is 0.01 neper.

By means of the λ-transform, we convert $\lambda = 1\sqrt{x}$ to the function F and find

$$F = \frac{\lambda^2 + 30.95432\lambda + 454.78647}{\lambda^2 + 26.138550\lambda + 339.18465}. \tag{29}$$

With k = 4

$$\text{cth } g - 1 = \frac{8\lambda + 196.3084}{\lambda^2 + 24.53855\lambda + 297.49575}. \tag{30}$$

Resolving expression (30) into a continuous fraction, we obtain

$$Z_2' = R\left(0{,}125\lambda + \frac{1}{0{,}02689\lambda + 0{,}65987}\right) \tag{31}$$

and

$$Z_1' = \frac{2R}{0{,}125\lambda + \frac{1}{0{,}02689\lambda + 0{,}65987}}. \tag{32}$$

The corresponding circuit diagram of the network with component values is shown in Figure 8.

The modulus of input impedance of the network looking into terminals 1, 1 is approximately 318 ohms over the entire operating frequency range and with a change in CR by a factor of 4 rises to 429 ohms and decreases to approximately 235 ohms.

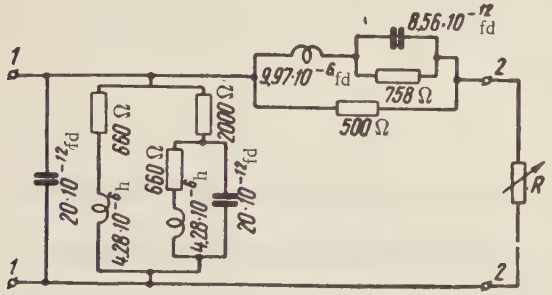

Figure 8

If instead of the network for continuous control we simply use one varying active resistance, then with a stray capacitance of 20 micromicrofarads and impedance of 318 ohms the error in reproduction of the characteristic at frequency of 8.5 Mc will be approximately 10 times greater than given under the conditions of this problem, while with an impedance increase to 580 ohms the error is approximately 0.2 neper.

With derivation of capacitance of not 20 but 10 micromicrofarads due to a twofold increase in characteristic impedance of the network as seen from terminals 2, 2 and corresponding recalculation of the elements, we may obtain a modulus of input impedance of the network at mean position of the CR which is equal to 636 ohms and at the other positions of the CR approximately 471 ohms and 859 ohms. Phase angle characteristics of input impedance obtained at the initial position and two extreme positions of the CR are given in Figure 9.

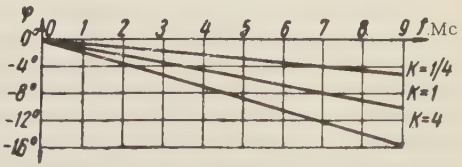

Figure 9

In conclusion, let us note that the premises formulated in the theorem permit solution of the problems of synthesis of equalizers with a given frequency dependence of initial attenuation, synthesis of four-terminal equalizing networks, synthesis of two-terminal networks and four-terminal networks, etc. Descriptions of these will be given in subsequent reports.

Article submitted to editors 17 June 1960

LITERATURE

1. O. F. Kosminskiy. Metody rascheta konturov dlya regulirovaniya

usileniya usiliteley [Methods of calculation of networks for gain control of amplifiers], NTS GSNII, No. 3, 1958.
2. A. F. Beletskiy, N. S. Kochanov. Teoreticheskiye osnovy elektroprovodnoy svyazi [Theoretical foundations of wire communications], Leningrad, 1956.
3. A. F. Beletskiy. Teoreticheskiye osnovy elektroprovodnoy svyazi. Leningrad, 1959.
4. By. Bode "Variable Equalizcis." BSTJ. Vol XVIV, 1938.

SYNTHESIS OF POLYNOMIAL BANDPASS FILTERS WITH CHEBYSHEV SELECTIVITY CHARACTERISTIC

G.I. Leviman, and O. I. Vostryakov

The article describes the procedure for synthesis of bandpass filters proposed by M. Dishal. On the basis of this procedure precise design relationships are derived for filters with three and four resonators, as well as relationships for filters with 3 to 6 reasonators which may be used with sufficient accuracy for wideband filter calculations or for calculation of filters with losses in certain resonators.

SELECTIVITY OF POLYNOMIAL BANDPASS FILTERS

Polynomial bandpass filters (characterized by a monotonic increase in attenuation of the filter with increasing distance from the passband limits) are most often made in the form of a system of coupled, identically tuned resonators and only for extremely wide passbands are made in the form of a system of symmetrically staggered resonators or a constant-k ladder filter. In this report we examine a filter with a system of n resonators (Figure 1) each of which is tuned (in common with the coupling elements joined with it) to the mid-frequency f_0 of the passband. The attenuation of resonators d_1, d_2, ..., d_n, their characteristic impedances ρ_1, ρ_2, ..., ρ_n and coupling coefficients k_{12}, k_{23}, ..., $k_{n-1, n}$ are arbitrary. As is known (for example, see [3]), the transfer admittance is

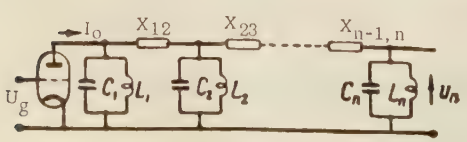

Figure 1

$$F(ix) = \frac{I_0}{U_n} = \frac{D}{\sqrt{\rho_1 \rho_n}\, \kappa_{12}\, \kappa_{23}, \ldots, \kappa_{n-1,\, n}}, \tag{1}$$

where the selectivity function is

$$D = \begin{vmatrix} d_1 + ix & i\kappa_{12} & 0 & 0 & 0 \ldots \\ i\kappa_{12} & d_2 + ix & i\kappa_{23} & 0 & 0 \ldots \\ 0 & i\kappa_{23} & d_3 + ix & i\kappa_{34} & 0 \ldots \\ \ldots & \ldots & \ldots & \ldots & \ldots \\ \ldots & \ldots & 0 & i\kappa_{n-2\,n-1} & d_{n-1} + ix \quad i\kappa_{n-1,\, n} \\ \ldots & \ldots & 0 & 0 & i\kappa_{n-1,\, n} \quad d_n + ix \end{vmatrix}. \tag{2}$$

Here $x = 2\frac{\Delta f}{f_0}$ is the relative detuning.

In accordance with (1) the selective properties of the filter are determined by the numerator, since it is assumed that a change in coupling impedances (x_{12}, x_{23}, ..., $x_{n-1,\, n}$) over the stagger range of interest to us may be neglected. Moreover, the selectivity of the filter depends only on the coefficient of coupling and attenuation of the resonators and does not depend on whether the coupling impedances are formed by capacitances, inductances or combinations thereof. In similar fashion, the choice of internal, external or combined coupling between resonators is of no importance. The quantities ρ_1 and ρ_n affect the value of transfer admittance.

If the current I_0 to the first resonator of the filter is the plate current of a pentode with transconductance S and sufficiently large internal resistance, then the maximum gain of this stage will be

$$K_{max} = \frac{U_{n\,max}}{U_g} = \frac{1}{D_{min}} S \sqrt{\rho_1 \rho_n}\, \kappa_{12}, \kappa_{23}, \ldots, \kappa_{n-1,\, n}. \tag{3}$$

Here U_g is the voltage at the pentode grid, D_{min} is the minimum value of D corresponding to maximum U_n.

The selectivity of the filter Se is

$$Se = \frac{|U_n|_{max}}{|U_n|} = \frac{|D|}{|D|_{min}}.$$

In the calculation of ladder filters wide use is made of the methods of network synthesis created by V. Cauer and S. Darlington, which permit determining the circuit and data for its elements on the basis of the chosen shape of the selectivity characteristic [1]. M. Dishal [2] applied this idea in revealing the possibility for synthesis of polynomial bandpass filters with dissipative elements.

However, the Dishal method does not yield a single-valued solution, since here certain preliminary conditions are assumed, the validity of which are then to be verified. Below we present a brief description of the Dishal procedure. This method may also be used for calculation of a series of networks.

If it is required to obtain the amplitude-frequency characteristic with maximum approximation to the ideal rectangular shape, then, as is known, this characteristic must be a Chebyshev response shape and is usually

written as [1, 2]

$$Se = \sqrt{1 + wT_n^2(\xi)} \quad . \tag{4}$$

Here

$$T_n(\xi) = \cos(n \arccos \xi) \quad \text{for} \quad |\xi| < 1,$$
$$T_n(\xi) = \operatorname{ch}(n \operatorname{arc\,ch} \xi) \quad \text{for} \quad |\xi| > 1 *$$

are Chebyshev functions of the nth order of argument $\xi = \frac{x}{x_P}$, where $x_p = P/f_0$, while P is the passband at the $\sqrt{1+w}$ level (Figure 2a). For odd n T_n (0) = 0, while for even n T_n (0) = $\pm$ 1. At the edge of the passband $\xi = \pm 1$ and $|T_n(\pm 1)| = 1$. Parameter ω characterizes the ripple of function Se within the passband. Ripple figures of 3 and 6 db correspond to $\omega = 1$ and $\omega = 3$, respectively. The extreme of Se (ξ) are associated with

$$\xi = \pm \sin\left(\frac{m}{2n}\pi\right),$$

where m = 0, 1, 2, ... n-1.

One of the equations of the Chebyshev filter synthesis appears as (see below, page 64 [original])

$$\sum_1^n d_\kappa = -\sum_1^n p_\kappa = \varepsilon R \sum_1^n \sin \frac{2\kappa - 1}{2n}\pi.$$

Using (11) and the known trigonometric relationship [10], we finally obtain

$$\sum_1^n d_\kappa = \frac{x_P \operatorname{sh}\left(\frac{1}{h} \operatorname{arc\,sh} w^{-\frac{1}{2}}\right)*}{\sin \frac{\pi}{2n}}. \tag{5}$$

The narrower the bandwidth and the greater n and ω, the smaller must be the attenuation of the resonators. Let the ordinate values on the selectivity curve at the edges of the passband represent Se_0 (Figure 2b). For the Chebyshev filter $Se_0 = \sqrt{1+w}$ (Figure 2a). However, of greater interest is the general case where $\sqrt{1+w} \leqslant Se_0$. In addition, it is again necessary to use relationship (4); however, here the bandwith P is a conditional value associated with the assigned value of bandwith P (at the Se_0 level) since:

$$Se_0 = \sqrt{1 + wT_n^2(P_0/P)} \quad . \tag{6}$$

---

*ch = cosh, sh = sinh (transl.)

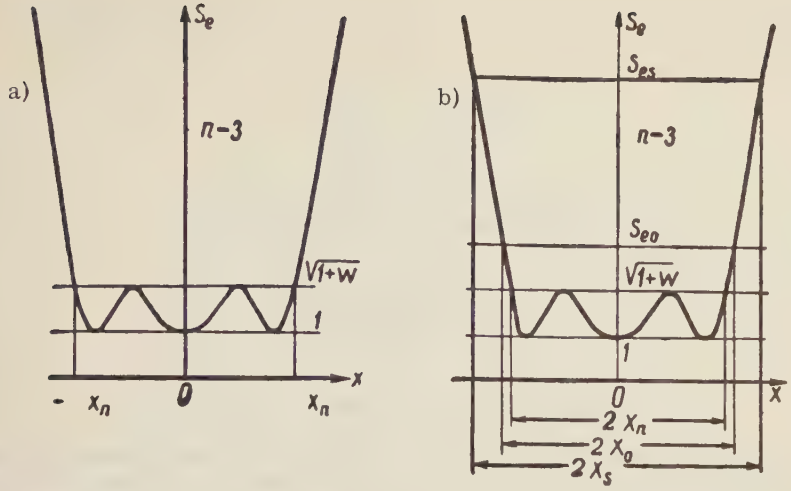

Figure 2

For example, with n = 3 a decrease in ω from 1 to 0.01 leads to a 35-percent decrease in P. However, with $\omega \to 0$, P also approaches zero.

Let us find the rectangularity ratio k_p of the selectivity characteristic of a filter iwth parameters P_0, Se_0 and ω (Figure 2b).

$$\kappa_p = x_s/x_0 = \xi_s/\xi_0.$$

Here x_0 and $\xi_0 = x_0/x_p = P_0/P \geqslant 1$ correspond to the edges of the passband, while x_s and $\xi_s = x_s/x_p$ are the frequency staggers for which the selectivity is equal to the assigned value of Se >> 1. Taking ξ_0 from (6) and ξ_s from (4), we obtain

$$\kappa_p = \frac{\operatorname{ch}\left(\frac{1}{n}\operatorname{arc\,ch}\frac{Se_s}{\sqrt{w}}\right)}{\operatorname{ch}\left(\frac{1}{n}\operatorname{arc\,ch}\sqrt{\frac{Se_0^2-1}{w}}\right)} \approx \frac{\sqrt[n]{\frac{2Se_s}{\sqrt{w}}}}{2\operatorname{ch}\left(\frac{1}{n}\operatorname{arc\,ch}\sqrt{\frac{Se_0^2-1}{w}}\right)}. \qquad (7)$$

If a Chebyshev filter with n resonators and ripple within the passband Se_0 is divided into k stages, each of which contains n/k resonators and ripple $w = Se_0^{2/\kappa} - 1$, then the rectangularity ratio of such a filter

$$\kappa_p = \operatorname{ch}\left[\frac{\kappa}{n}\operatorname{arc\,ch}\left(\frac{\sqrt[\kappa]{Se_s}}{\sqrt{Se_0^{2/\kappa}-1}}\right)\right].$$

If, for example, n = 6, $Se_0 = 1.41$, and $Se_s = 10^3$, then for a six-resonator filter (k = 1) we obtain $k_p = 2.01$, for two stages of three-resonator filters (k = 2) we have $k_p = 2.42$ and for three stages of two-resonator filters $k_p = 3.42$. Hence, it is evidently practical to lump all the resonators within one filter. It is also feasible because in adjusting the

passband of a Chebyshev filter by a factor of "a", its transfer constant varies by a^k.

Let us note that with $\omega \to 0$ from (7) we obtain

$$\varkappa_p = \sqrt{\frac{Se_y}{\sqrt{Se_0^2 - 1}}},$$

which corresponds to a filter with maximally linear response, as expressed by the following equation:

$$Se = \sqrt{1 + (Se_0^2 - 1)\left(\frac{x}{x_0}\right)^{2n}}.$$

SYNTHESIS OF CHEBYSHEV FILTERS

As stated above, calculation of an n-resonator filter reduces to determining the n of resonator attenuations and n-1 coupling coefficients. These 2 n-1 unknowns are determined from an expression which is an identity relative to x

$$\frac{|D|}{|D|_{min}} = \sqrt{1 + wT_n^2(\xi)}. \tag{8}$$

The polynomial $1 + wT_n^2(\xi)$, being a function of a real variable ξ, may be represented in the form of the function of a complex variable p = ix (for example, see [1], page 250 [original text]), where $e^{2\alpha b} - 1 = \omega$, and $\lambda = i\xi$ or [4])

$$1 + w\,T_n^2(\xi) = w\,2^{2(n-1)}\,x_p^{-2n}(p - p_1)(p - p_2)\ldots(p - p_{2n}). \tag{9}$$

Here $p_1 \ldots p_{2n}$ are the roots of the polynomial and may be written in general form as [4, 5]

$$p_\kappa = -\varepsilon R \sin\frac{2\kappa - 1}{2n}\pi + iR\cos\frac{2\kappa - 1}{2n}\pi. \tag{10}$$

Here $\kappa = 1.2\ldots\ 2n \qquad \varepsilon = \text{th}\beta$ *

$$R = x_p \operatorname{ch}\beta \qquad \beta = \frac{1}{n}\operatorname{arc\,sh}\, w^{-1}. \tag{11}$$

It is easily shown that the roots of the polynomial lie on an ellipse (Figure 3) the semi-axes of which are R and ϵR. With $\omega \to 0$ $\epsilon \to 1$, the ellipse degenerates into a circle with radius R. It may be shown that, with $\omega \to 0$ $R \to x_{0.707} = P_{0.707}/f_0$. The greater is ω, the closer R is to x_p. From (10) or Figure 3 it follows that for p = ix

$$|p - p_\kappa| = |p - p_{2n+1-\kappa}|. \tag{12}$$

Replacing in (8) $1 + wT_n^2(\xi)$ by the modulus of the right-hand side of (9)

---

*th = tanh (transl.)

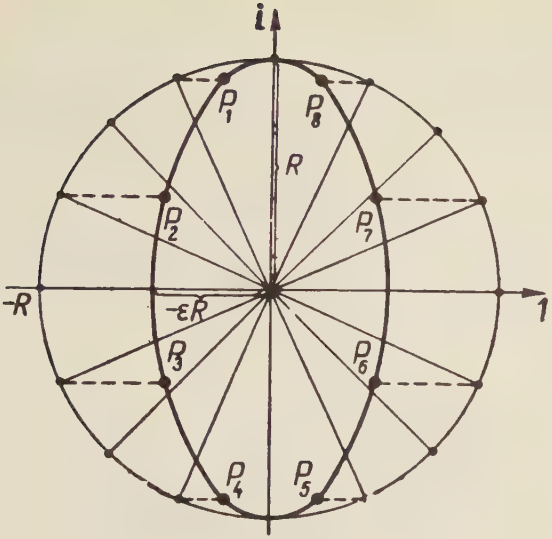

Figure 3

and considering (12), we obtain

$$|D| = |D|_{min} \sqrt{w}\ 2^{n-1}\ x_p^{-n} |(p-p_1)(p-p_2)\dots(p-p_n)|.$$

Since in the polynomial D the coefficient, with p^n, is 1, then

$$2^{n-1} \sqrt{w}\ x_p^{-n} |D|_{min} = 1. \tag{13}$$

Expression (13) is conveniently used for determining K_{max} (3). We may now write

$$|D| = |(p-p_1)(p-p_2)\dots(p-p_n)| \tag{14}$$

the n coefficients of the left-hand polynomial which contain 2n - 1 unknowns must be equated with the coefficients of the right-hand polynomial, which are easily determined from $p_1 \dots p_n$. Thus, we obtain n equations for 2n—1 unknowns, which permits superposition of n—1 supplementary conditions. If the number of these supplementary conditions is greater than n—1, then the determined unknowns must convert to identities lacking the equations which were not used in searching for them. If this does not occur, then it is necessary to abandon all the assumed conditions. Thus, calculation of the filter reduces to the trial-and-error method.

THREE-RESONATOR FILTER

From (1) for n = 3 we obtain

$$D(p)=\gamma_1\gamma_2\gamma_3+\kappa_{12}^2\gamma_3+\kappa_{23}^2\gamma_1, \tag{15}$$

where $\gamma_\kappa = d_\kappa + p$.

In accordance with (10) the roots of the polynomial will be

$$p_{1,3}=(-0.5\varepsilon \pm i0.5\sqrt{3})R,$$
$$p_2=-\varepsilon R.$$

Let us examine the case of symmetrical distribution of attenuation and coupling:

$$d_1=d_3=d,\quad d_2=0,$$
$$\kappa_{12}=\kappa_{23}=\kappa.$$

Figure (14) we obtain three equations for two unknowns:

$$d=\varepsilon R,\quad 2\kappa^2 d=0{,}25\,(3+\varepsilon^2)\,\varepsilon R^3,$$
$$d^2+2\kappa^2=1{,}25\,(\varepsilon^2+0{,}6)\,R^2.$$

Whence we find:

$$d=\varepsilon R, \tag{16}$$
$$\kappa=\sqrt{0{,}125\,(3+\varepsilon^2)}\,R. \tag{17}$$

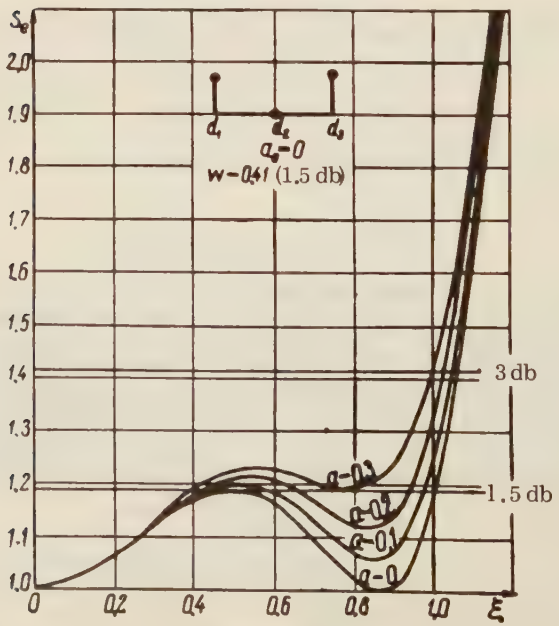

Figure 4

Inserting (16) and (17) in the unused formula, it is easily seen that it is transformed into an identity.

Condition $d_2 = 0$ was proposed by Dishal [6] for simplification of analysis. It has practical significance for wideband filters or in the compensation of losses in the second resonator [7]. The curves in Figure 4 show the difference in the selectivity characteristic of the filter from the Chebyshev with $d_2 = ad > 0$ (here $a < 1$). These curves were plotted from formula (15) with $d_1 = d_3 = d$ and $k_{12} = k_{23}$, chosen in accordance with (17). The slight contraction of the bandwidth and deformation of the curve shape may be disregarded in calculations.

Let us discuss the asymmetrical attenuation and coupling — $d_1 > d_2 = d_3$ and $k_{12} \neq k_{23}$ — investigated in 1939 by N. I. Chistyakov [8].

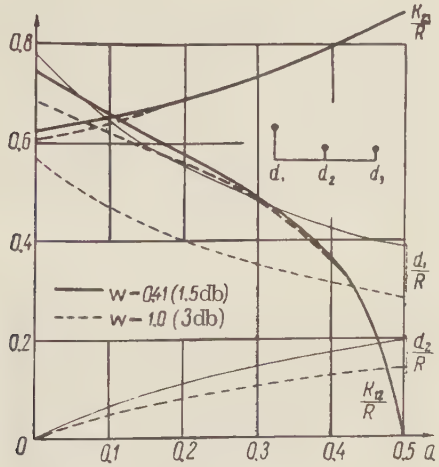

Figure 5

The method proposed below permits calculation for a given value of Se_0 (or ω). Designating $d_1 = d$ and $d_2 = d_3 = ad$ and solving the three equations into which formula (14) is analyzed, we obtain

$$d = \frac{2\varepsilon}{1+2a} R, \tag{18}$$

$$\kappa_{12} = \frac{R}{\sqrt{1-a}} \left\{0{,}375 + 1{,}125\,\varepsilon^2 - \left[0{,}75 + 0{,}25\,\varepsilon^2 + \frac{8\varepsilon^2}{(1+2a)^2}\right] a\right\}^{1/2}, \tag{19}$$

$$\kappa_{23} = R\left[0{,}75 + 1{,}25\,\varepsilon^2 - \frac{4(2+a)}{(1+2a)^2}\, a\varepsilon^2 - \kappa_{12}^2\right]^{1/2}. \tag{20}$$

With $0 \leqslant a \leqslant 0.5$ the filter is practicable, since k_{12} and k_{23} are real. The dependence of d/R, k_{12}/R and k_{23}/R on a at various ω is given in Figure 5. The curves in Figures 6, 7 and 8, calculated from formula (15) for $\omega = 0.41$, show the deviation of the selectivity curve of the examined filter from the Chebyshev response with deviation of a from the initial (normal)

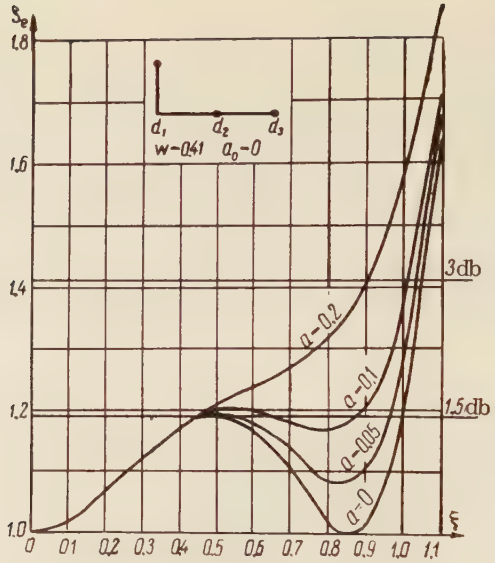

Figure 6

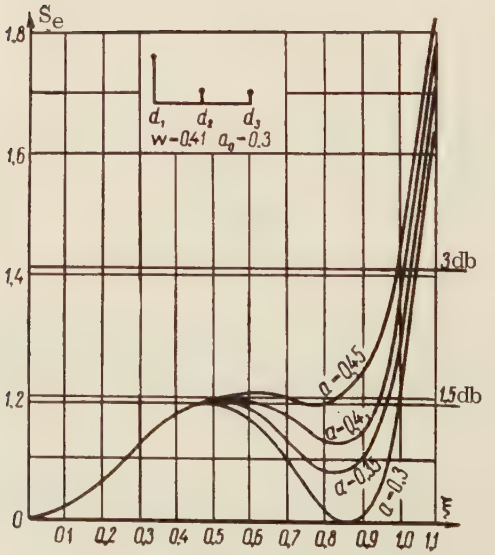

Figure 7

value a = 0 (Figure 6) and a = 0.3 (Figures 7 and 8); k_{12} and k_{23} were calculated from (19) and (20).

For comparison of filters with symmetrical and asymmetrical

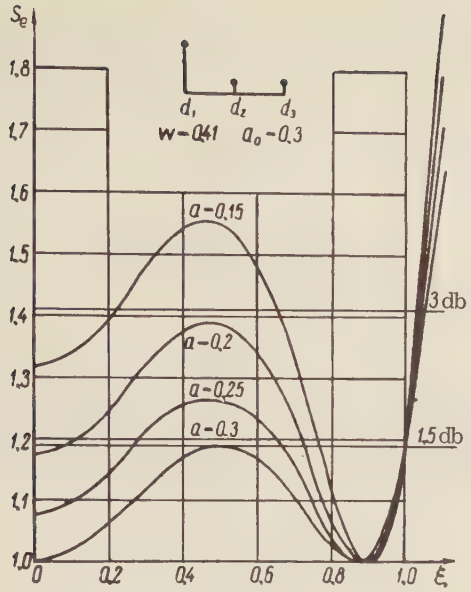

Figure 8

distribution of attenuation and coupling, which we shall designate as "filter 101" and "filter 100", let us rewrite (16) and (18) as

$$x_p = \frac{d}{\varepsilon \operatorname{ch} \beta}, \tag{16'}$$

$$x_p = (a + 0{,}5) \frac{d}{\varepsilon \operatorname{ch} \beta}. \tag{18'}$$

Hence it follows that in choosing a filter 100 with $a \to 0$, we provide half the bandwidth of filter 101 at the same attenuations d. Considering that in filter 101 the allowable value of $d_2 \leqslant \left(\frac{1}{3} \text{ to } \frac{1}{5}\right) d$ (Figure 4) and replacing d in (18a) with d_2/a, we obtain

$$x_p = \frac{3 \div 5}{\varepsilon \operatorname{ch} \beta} d_2, \tag{16''}$$

$$x_p = \left(1 + \frac{1}{2a}\right) \frac{d_2}{\varepsilon \operatorname{ch} \beta}. \tag{18''}$$

Hence it follows that in choosing a filter 100 with $a \to 0.5$, we may provide the same bandwidth with attenuations d_3 and d_2 1.5-2.5 times greater than in filter 101 and, moreover, obtain an ideal Chebyshev response curve. This is of considerable importance in employing compensation for losses in the resonators of the filter. A disadvantage of filter 100 is the marked dependence of the shape of the selectivity curve on the relationships between d_1 and $d_2 = d_3$ (Figures 6, 7 and 8). In filter 101 a decrease of d_2 to zero or even to a small negative value merely provides

approximation of the filter characteristic to the Chebyshev response. For adjustment of the bandwidth of filter 101 it is necessary to change attenuation $d_1 = d_3$ and to the same extent change $k_{12} = k_{23}$ [see (16) and (17)]. For this same purpose filter 101 would require a change in each of the values d_1, k_{12} and k_{23} in a rigidly prescribed manner. In addition, k_{12} must change by a greater factor than the passband (Figure 5). Hence, for adjustment of the passband filter 101 is more convenient.

FOUR-RESONATOR FILTER

From (1) for n = 4 we obtain

$$D(p) = \gamma_1\gamma_2\gamma_3\gamma_4 + \kappa_{12}^2\gamma_3\gamma_4 + \kappa_{23}^2\gamma_1\gamma_4 + \kappa_{34}^2\gamma_1\gamma_2 + \kappa_{12}^2\kappa_{34}^2. \tag{21}$$

Let us examine a filter with symmetrically distributed attenuation and coupling (filter 1001): $d_1 = d_4 = d$, $d_2 = d_3 = 0$ and $k_{12} = k_{34} \neq k_{23}$. As in the preceding example, (14) is analyzed into four equations, one of which is converted to an identity, while the others yield

$$d = 1{,}305\,\varepsilon R, \tag{22}$$

$$\kappa_{12} = 0{,}594\sqrt{1+\varepsilon^2}\,R^*, \tag{23}$$

$$\kappa_{23} = 0{,}544\,R. \tag{24}$$

Let us examine a filter with asymmetrical distribution of attenuation and coupling (filter 1000): $d_1 = d > d_2 = d_3 = d_4 = ad$ and $k_{12} \neq k_{23} \neq k_{34}$. The four equations resulting from substitution of these conditions are

$$d = \frac{2{,}61}{1+3a}\,\varepsilon R, \tag{25}$$

$$\kappa_{12} = \sqrt{\frac{(1+a)A - B}{1-a}}\,R, \tag{26}$$

$$\kappa_{23} = \sqrt{AR^2 - \kappa_{12}^2 - \kappa_{34}^2}, \tag{27}$$

$$\kappa_{34} = \frac{R^2}{\kappa_{12}}\sqrt{C + 6{,}82\,\frac{a\varepsilon^2(aA-B)}{(1+3a)^2} - 46{,}5\,\frac{a^3\varepsilon^4}{(1+3a)^4}}. \tag{28}$$

Here

$$A = 1 + \varepsilon^2\left[2{,}41 - 20{,}55\,\frac{(a+1)a}{(1+3a)^2}\right],$$

$$B = 0{,}647(1+3a) +$$

$$+ \varepsilon^2\left[0{,}354(1+3a) - 6{,}8\,\frac{3+a}{(1+3a)^2}\,a^2\right],$$

$$C = 0{,}125 + 0{,}75\,\varepsilon^2 + 0{,}125\,\varepsilon^4.$$

From Figure 9 it is seen that for $a \leqslant 0.27$ all the parameters of filter 1000 are real, which indicates its practicability.

Comparing (22) and (25), we note that with a = 0 and identical d in

---

*In literature [3] it was erroneously stated that $\kappa_{12} = 0.707\sqrt{1+\varepsilon^2}\,R$.

filter 1000 we may provide half the bandwith of filter 1001. With the given bandwidth an increase in a permits decreasing the Q of resonators 2, 3 and

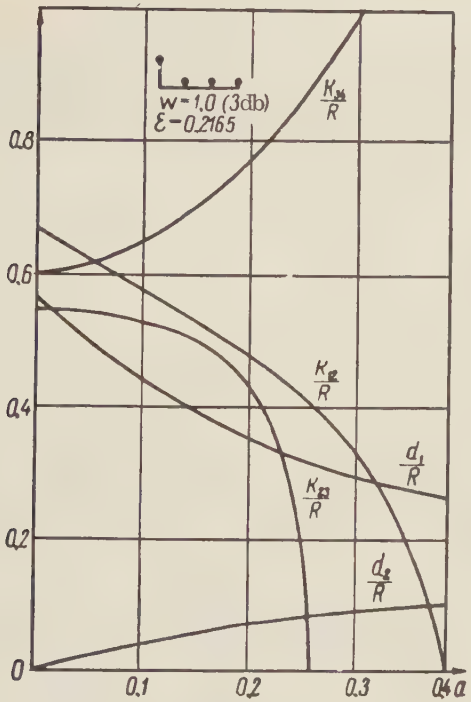

Figure 9

4. If a = 0.2, then $d_2 = d_3 = d_4 = 0.327\,\epsilon R$. In addition, the ideal Chebyshev response is insured, while in filter 1001 approximation to such response requires $d_2 = d_3 = \left(\frac{1}{3}\text{ to }\frac{1}{5}\right) d = (0.43 \text{ to } 0.26)\,\epsilon R$. For adjustment of the bandwidth filter 1001 is more suitable for the same reasons as for filter 101.

FIVE-RESONATOR FILTER

From (1) for n = 5 we obtain

$$D(p) = \gamma_1\gamma_2\gamma_3\gamma_4\gamma_5 + \kappa_{12}^2\gamma_3\gamma_4\gamma_5 + \kappa_{23}^2\gamma_1\gamma_4\gamma_5 + \kappa_{34}^2\gamma_1\gamma_2\gamma_5 + \kappa_{45}^2\gamma_1\gamma_2\gamma_3 + \\ + \kappa_{12}^2\kappa_{34}^2\gamma_5 + \kappa_{12}^2\kappa_{45}^2\gamma_3 + \kappa_{23}^2\kappa_{45}^2\gamma_1.$$

Let us examine a filter with symmetrical distribution of attenuation and coupling (filter 10001): $d_1 = d_5 = d$, $d_2 = d_3 = d_4 = 0$, $k_{12} = k_{45}$, $k_{23} = k_{34}$.

As before, (14) is analyzed into five equations, two of which are converted into identities, while the remaining equations provide

$$d = 1.612\,\varepsilon R, \quad \kappa_{12} = \sqrt{0.3452 + 0.6545\varepsilon^2}\,R,$$

$$\kappa_{23} = \sqrt{0.2798 + 0.02951\,\varepsilon^2}\,R.$$

Investigation was performed with a filter with asymmetrical distribution of attenuation: $d_1 = d > d_2 = d_3 = d_4 = d_5 = ad$, while the coupling coefficients were arbitrary. Solution of five equations with five unknowns shows that k_{34} for any a is an imaginary value, which indicates the unsuitability of the chosen attenuation distribution.

SIX-RESONATOR FILTER

From (1) for n = 6 we obtain

$$D(p) = \gamma_1\gamma_2\gamma_3\gamma_4\gamma_5\gamma_6 + \kappa_{12}\gamma_3\gamma_4\gamma_5\gamma_6 + \kappa_{23}\gamma_1\gamma_4\gamma_5\gamma_6 +$$
$$+ \kappa_{34}^2\gamma_1\gamma_2\gamma_5\gamma_6 + \kappa_{45}^2\gamma_1\gamma_2\gamma_3\gamma_6 + \kappa_{56}^2\gamma_1\gamma_2\gamma_3\gamma_4 + \kappa_{12}^2\kappa_{34}^2\gamma_5\gamma_6 +$$
$$+ \kappa_{12}^2\kappa_{45}^2\gamma_3\gamma_6 + \kappa_{12}^2\kappa_{56}^2\gamma_3\gamma_4 + \kappa_{23}^2\kappa_{45}^2\gamma_1\gamma_6 + \kappa_{23}^2\kappa_{56}^2\gamma_1\gamma_4 +$$
$$+ \kappa_{34}^2\kappa_{56}^2\gamma_1\gamma_2 + \kappa_{12}^2\kappa_{34}^2\kappa_{56}^2. \qquad (30)$$

Let $d_1 = d_6 = d$, $d_2 = d_3 = d_4 = d_5 = 0$, $k_{12} = k_{56}$, $k_{23} = k_{45}$. As above, we obtain six equations for four unknowns. The unused equations are transformed into identities:

$$d = 0.5(\sqrt{2} + \sqrt{6})\,\varepsilon R, \quad \kappa_{12} = \sqrt{0.125(1 - \sqrt{3})(1 + 3\varepsilon^2)}\,R,$$

$$\kappa_{23} = \sqrt{0.125(\sqrt{3} - 1)(3 + \varepsilon^2)}\,R, \quad \kappa_{34} = \sqrt{2 - \sqrt{3}}\,R.$$

CONCLUSION

The work was performed in 1958-1959 in conjunction with investigation of i-f filters of main-link receivers with adjustable passband at the Chair of the Radio-Receiver Section of the Odessa Electrical-Engineering Institute of Communications. Almost all the relationships were checked experimentally. Considerable attention was devoted to the use of compensation of losses in certain resonators of the filter by means of a transistorized circuit. From equation (5) it is evident that it is convenient to compensate losses in the greatest possible number of resonators. This idea was carried out in an i-f amplifier at frequency of 215 kc and with a continuously adjustable bandwidth (adjustable by means of ferro-variometers) from 2 to 12 kc. The rectangularity ratio (6 and 60 db) was not poorer than 2 at any bandwidth and the filter possessed thermal stability [9]. Even better results can be expected in employing compensation for losses at higher frequencies, which may permit elimination of dual frequency conversion in a main-link receiver.

Figures 10 and 11, by way of example, present experimental curves for 3- and 5-resonator filters with loss compensation.

Article submitted to editors 29 August 1960

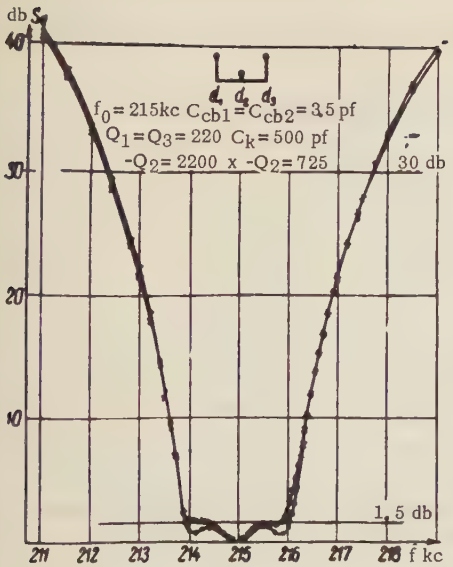

Figure 10

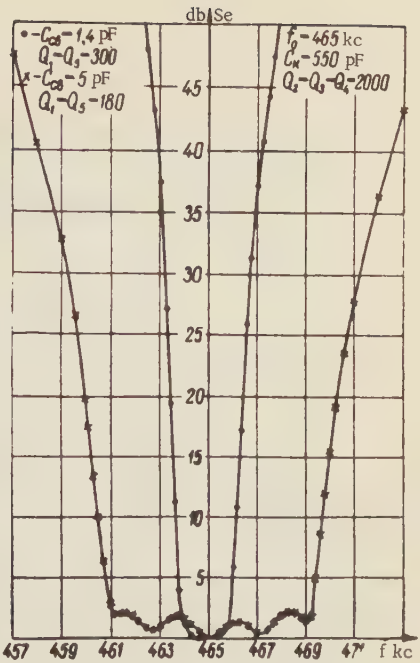

Figure 11

LITERATURE

1. A. F. Beletskiy. Teoreticheskiye osnovy elektroprovodnoy svyazi, chast' III [Theoretical fundamentals of wire communications, Part III]. Synthesis of reactive four-terminal networks and electrical filters. Moscow, 1959.
2. Dishal. "Design of dissipative band-pass filters producing desired exact amplitude-frequency characteristics." PIRE, 37. September 1949.
3. Drexler, Voss. Frequenz, 6, No. 11, 1952; 7, No. 1, 1953.
4. Lepage, Seely. General network analysis. Chapt. VII. McGraw-Hill Co. 1952.
5. A. F. Ufel'man. "General regularity in distribution of roots of the characteristic polynomial in the complex frequency plane in operating-parameter filter calculations." Elektrosvyaz', No. 7, 1959.
6. Dishal. "Exact design and analysis of double- and triple-tuned band-pass amplifiers." PIRE, June 1947.
7. I. L. Polyakov. "Transistor compensation of oscillator losses." Elektrosvyaz', No. 9, 1959.
8. N. I. Chistyakov. Rezonansyye usiliteli i predvaritel'nyye selektory [Tuned amplifiers and preselectors]. 1939.
9. Tekhnicheskiy proyekt UPCh magistral'nogo priyemnika s elektrichesko regulirovkoy polosy propuskaniya [Engineering project for i-f amplifier of main-link receiver with electrical passband regulation]. OEIS. Odessa, 1959.
10. P. P. Korovkin. Linenyye operatory i teoriya priblizheniy [Linear operators and the theory of approximations]. GIMFL. Moscow, 1959.

CONTACTLESS UNITS FOR TRUNK LINE WITH MULTIPLEX KRR-30/60

V.G. Bosenko, and G.Z. Maksimov

A KRR-30/60 [cable and radio relay] equipment for multiplexing of interoffice trunks of urban telephone systems has been developed and is now in production.

In order to decrease dimensions of the equipment, contactless units were developed for trunk lines multiplexed with the KRR-30/60 equipment. Below we describe the results of development of a unit designed for multiplexing of trunk lines between local offices of type ATS-47 [automatic exchange].

Each set consists of an incoming and an outgoing unit for installation at the respective ends of the channel. The basic diagrams of the semiconductor versions of the incoming and outgoing units are given in Figures 1 and 2. The transistors which are unblocked in the initial state are indicated by asterisks.

The outgoing unit (Figure 1) and associated channel are engaged in the hunting operation of the group selector [GI] of the previous selection stage. Upon travel of wiper c over the free-channel commutator position current flows through resistor R_1 and in the GI the busy relay closes. Due to the considerable increase in potential of point A the busy transistor TZ is blocked. Transistor T_1 and, through the circuit of I_1 and I_2, the transmit transistor TPer are unblocked by the signal from the TZ transistor. At the diodes of static relay StR there is created a positive bias and current of signal frequency $f_S = 3.8$ kc begins to enter the channel.

Upon access to the channel, there are two possible conditions:

(a) the high-frequency channel is operative;

(b) the high-frequency channel is inoperative.

If the channel is operative, as the result of action of the current of signal frequency in the incoming unit (Figure 2) a signal from the control signal receiver PSU switches the receive trigger TrPr. Busy transistor TZ is unblocked by the signal from the TrPr. Inverter transistor Inv is blocked, with the result that it unblocks key K_5 and to line c there is fed the battery plus. The next selector step engages the device at busy.

Simultaneously, through circuit I_1, transmit transistor TPer is unblocked by the signal from the inverter and a current of signal frequency begins to be transmitted from the incoming unit to the outgoing unit. Due to this, in the outgoing unit the receive transistor TPr is blocked by a signal from the PSU. Receive trigger TrPr is switched by a signal from the TPr.

The units are then ready to receive and relay the dialing pulses.

to hybrid system
to modulator
at transmitter input
PSU
Tr II
TS
Str
fs
TPer
TPr
To
Pr
Tr
TI
NL
P
Tz
Bl
hold
Tr I
"busy"
from ATX-47 (GI panel)
to channel-fault signalling

Figure 1

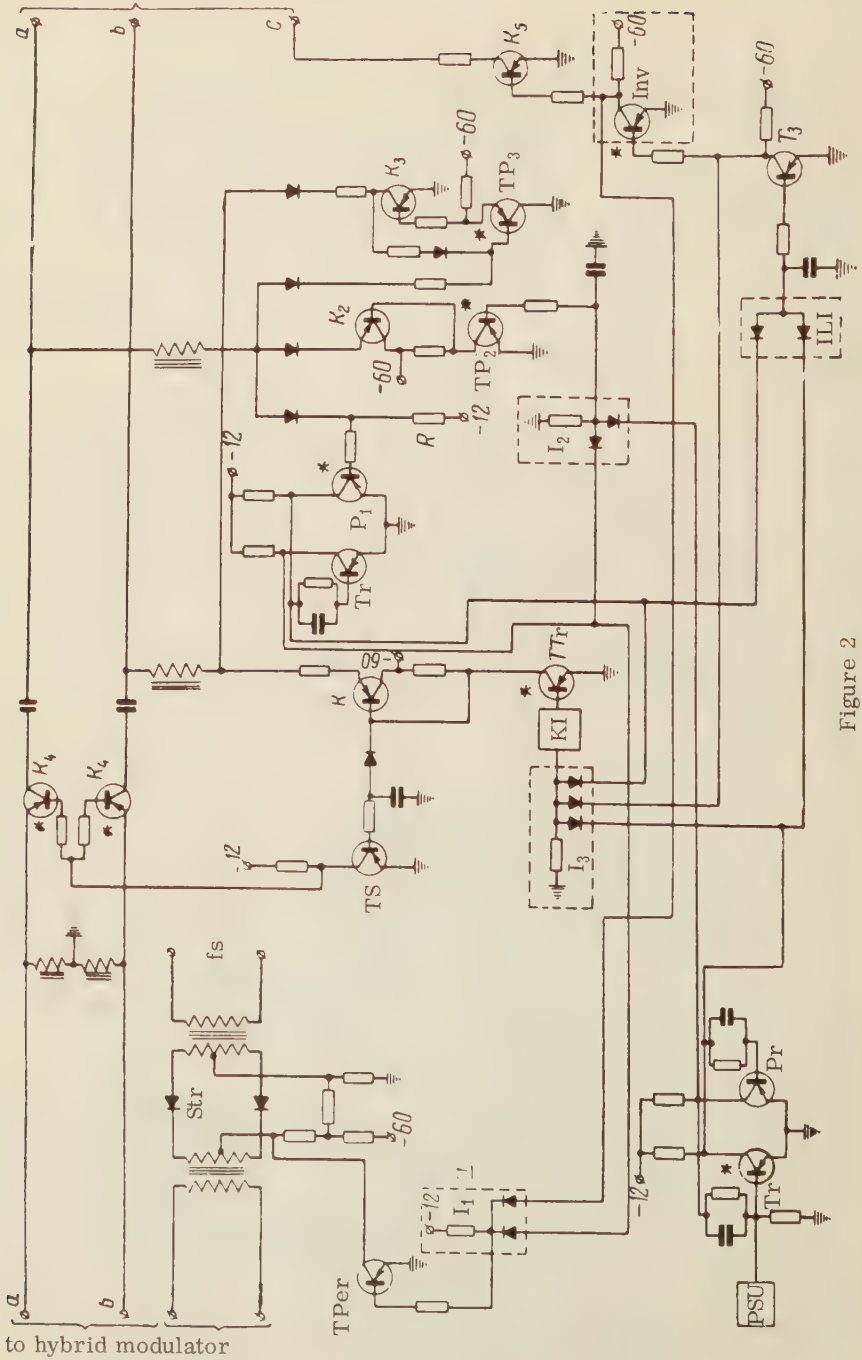
to ATs-47 (Input II/IV GI)
a
b
c
K_5
Inv
-60
T_3
K_3
TP_3
K_2
TP_2
R
-12
I_2
ILI
P_1
Tr
K_4
K_1
K
-60
TTr
KI
I_3
TS
fs
Str
I_1
TPer
Pr
Tr
PSU
to hybrid modulator

Figure 2

The dialing pulses in the outgoing unit are received by a section consisting of a neon tube NL and pulse transistor TI. Through circuits I_1 and I_2 the TPer transistor is blocked and unblocked by pulse-synchronous signals from the TI. Thus, the dialing pulses are relayed over the high-frequency channel by periodic interruption in the transmission of current of signal frequency from the outgoing unit to the incoming unit.

In the incoming unit, during each interruption in transmission of the current of signal frequency, the TrPr returns to the initial state. Through circuit I_3 and pulse corrector KI, relaying transistor TTr is switched by signals from TrPr. Key K_1 is switched synchronously with transistor TTr and the dialing pulses are d-c relayed along conductor b to the devices of the next steps in selection.

During each series of dialing pulses the series transistors TS of the sets are unblocked. Keys K_4 are blocked by signals from the TS, thereby isolating the channel inputs from the dialing pulses.

When the called subscriber answers, from the LI [line finders] in the IGI [group selectors] direction the battery plus is applied along conductor A, and the voltage drop across resistor R in the incoming unit increases. This results in switching of polarity-reversal trigger TrP_1 and polarity-reversal transistor TP_3. Transistor TPer is blocked and transmission of signal-frequency current from the incoming set to the outgoing set ceases. Key K_3 is unblocked by a signal from TP_3.

In the outgoing set transistor TPr is unblocked. Answer transistor TO is blocked by a signal from circuit I_5. Signals from TO unblock key K_3, switch polarity-reversal trigger TrP, and block key K_5. To conductor A in the direction of the IGI the battery plus is applied. A bypass circuit at the transmitter input prevents excitation of the channel before the called subscriber has answered.

A signal from trigger TrP interrupts transmission of current of signal frequency from the outgoing unit to the incoming unit. Thus the speech-current transmit state is established in the units.

Upon ring-off on the calling subscriber's side, current flows into the outgoing set along conductor A through resistor R_2 and key K_2. The potential created across the resistor unblocks transistor TPer and current of signal frequency begins to be transmitted in the channel.

In the incoming set trigger TrPr is switched. Through circuit I_2 polarity-reversal transistor TP_2 is blocked. Key K_2 is unblocked and the battery plus is applied to conductor A. In LI relay I operates and the busy signal is transmitted to the called subscriber.

When the called subscriber rings off, the battery plus is removed from conductor A at the LI. Trigger TrP_1 and transistor TP_3 return to the original state. Transistor TPer is unblocked and from the incoming unit into the channel the current of signal frequency is transmitted. In the outgoing unit transistor TPr is blocked and transistor TO is unblocked. Key K_2 closes and Key K_3 opens. In the IGI relay UR operates and clearing of the equipment begins.

After removal of wiper c from the channel commutator all transistors and triggers of the outgoing unit, with the exception of transistor TPr, return to the initial state. Transmission of current of signal frequency from the outgoing side of the channel ceases. This causes extension of the clearing process to equipment of the last selector steps and incoming unit returns to the initial state. Transmission of current of signal frequency from the incoming unit to the outgoing unit ceases and transistor TPr returns to the initial state. The unit is then ready for establishment of the next connection.

The unit also transmits all signals in the case where the called

subscriber rings off first and in the case of ring-off with an incomplete connection.

Moreover, the unit insures transmission of the "busy" signal to the calling subscriber in the event that the chosen channel is inoperative and also makes appropriate warning-signal connections.

An experimental model of the unit was tested at the Stalingrad Central Office in 1959. Operational tests showed positive results.

Size of the unit is 3—4 times less than that of an all-relay system, but they are approximately the same in cost.

The operational testing revealed high reliability of the transistorized unit. This was due to the fact that all the triggers in the unit are switched only through separate inputs. All switching in the units is static by means of directional and switching diodes. Such construction was adopted in the light of results of reliability studies of semiconductor switching devices and verification of the conclusions arising from these studies.

Improvement of the unit has concentrated on circuit simplification and increased reliability. One means of simplification is replacement of key K_4 in the speech section by upper-frequency filters with passbands from 300 kc and up. This will permit elimination of seven transistors from the unit.

Circuits for manufacture of industrial models of the unit have now been developed.

3 July 1960

LITERATURE

1. K. P. Yegorov, M. U. Polyak. "Design principles for simplified systems of multi-channel cable and radio-relay communications." Elektrosvyaz', No. 4, 1957.
2. V. G. Bosenko. "Transmission of control signals along high-frequency trunks in urban telephone systems." Sbornik nauchnykh trudov TsNIIS, 1958.

AUTHOR'S CERTIFICATES AND FOREIGN PATENTS*

Class 21g, 13_{17}. No. 123632. A. S. Tager. Method of generation, amplification and conversion of oscillations in the millimeter- and submillimeter-wavelength ranges.

Class 21g, 20_{01}. No. 122819. V. N. Sizov and P. N. Ivanov. Device for controlling distance between the styli of a facsimile receiver with chemical or thermal recording.

Class 21g, 38. No. 122823. Yu. V. Vvedenskiy. Nanosecond pulse generator.

Class 21g, 38. No. 122824. A. G. Konstantinovskiy. Relaxation oscillator.

Class 42b, 12_{03}. No. 123716. V. I. Gukov and B. M. Khalameyzer. Device for measuring thickness of magnetic materials.

Class 42d, 4_{01}. No. 124155. A. M. Yershov. Device for statistical processing of oscillograms.

Class 42d, 10. No. 124157. S. A. Doganovskiy. Adjustable-delay section.

Class 42g, 1_{01}. No. 122893. E. A. Bulokhov. Circuit for discrimination of basic speech tone.

Class 42g, 14. No. 122934. A. D. Talantsev. Analog-digital voltage converter.

Class 42m, 14. No. 122935. Ya. G. Koblents, D. A. Yakovenko and N. O. Morgacheva. Magnetic logical circuit.

Class 42 m, 14. No. 122983. L. I. Gutenmakher and G. G. Stetsyura. Device for optical recording and reading of binary-coded information.

Class 42m, 14. No. 122939. I. Ya. Lyamichev. Electroluminescent memory device.

Class 42m, 14. No. 122944. A. N. Radchenko and G. F. Yanbykh. Method of reversal of counting and coding devices and a device for this purpose.

Class 42m, 14. No. 122945. M. P. Sycheva and A. S. Fedorov. Memory device with ferrite elements.

Class 42m, 14. No. 122946. O. N. Dement'yev. Electronic device for squaring voltages of alternating sign.

Class 42m, 14. No. 122947. B. V. Serov. Multiplier device with ferrite matrix.

---

* Photocopies of patents (description in original language, drawings) may be obtained in person or C. O. D. from the All-Union Patent-Engineering Library of the Committee on Inventions and Discoveries attached to the Council of Ministers USSR. Moskva-tsentr, proyezd Serova, 4, pod"yezd 7a. For information phone B 8-64-52 and or B 3-09-57 — photo laboratory.

Class 42m, 14. No. 122948. N. I. Borodin. Arithmetic device.

Class 42m, 14. No. 122949. M. I. Petrukhin, L. A. Golubov and D. P. Losev. Single-cycle shift register employing ferrite-transistor cells.

Class 42m, 14. No. 123765. N. M. Sotina and Ya. A. Khatagurov. Diode-transformer gate with two transformers.

Class 42m, 14. No. 123767. B. I. Khazanov and L. S. Gorn. Reverse ring counter.

Class 42m, 14. No. 123768. Ye. M. Martynov. Switching-triode method for control of single-shift register with magnetic cores and a device for this purpose.

Class 42m, 14. No. 124202. K. A. Iyudu. Method of recording and reading information in a ferrite storage device.

Class 42m, 14. No. 124203. V. V. Chavchanidze, I. N. Bukareyev, Z. N. Mikeladze and V. A. Kumsishvili. Method of adding binary-coded numbers.

Class 42m, 14. No. 124204. Yu. I. Pivovarov. Static binary trigger.

Class $21a^4$, 8_{02}. No. 128059. D. A. Saf'yan. Crystal R-C oscillator.

Class $21a^4$, 10. No. 127293. V. G. Androsova and A. G. Pozdnyakov. Method for nickel-plating of crystal slabs.

Class $21a^4$, 16_{01}. No. 127294. N. V. Khrushcheva. Pulse generator.

Class $21a^4$, 29_{01}. No. 127706. V. M. Shkol'nik. Method of balancing with the reactive component of input bridges of tensometric amplifiers at carrier frequency.

Class $21a^4$, 35_{14}. No. 127295. L. N. Kiselev. Compensation stabilizer for d-c voltage.

Class $21a^4$, 35_{14}. No. 127296. V. K. Machinskiy and V. I. Shtil'man. Device for stabilization of ripple in rectified voltage.

Class $21a^4$, 35_{14}. No. 127707. G. Ya. Shkil'ko, S. M. Shevchenko, P. Z. Perel'man and I. A. Korsunskiy. Ferroresonant voltage stabilizer.

Class $21a^4$, 46_{03}. No. 127708. A. M. Pokras and A. M. Model'. Antenna with circular radiation pattern in horizontal plane and contracted vertical characteristic.

Class $21a^4$, 48_{68}. No. 127297. L. A. Semenov. Rectangular waveguide of large cross-section.

Class $21a^4$, 48_{75}. No. 128061. Ye. I. Kamenskiy. Ultrasonic delay lines.

Class $21a^4$, 70. No. 127709. S. N. Krize. Device for decreasing residual error in pulse systems for automatic control.

Class $21a^4$, 71. No. 127298. G. V. Korol'kov. Simulator of multibeam radio channel.

Class $21a^4$, 71. No. 127710. V. L. Vlasov and V. A. Potapov. Two-channel heterodyne phase-meter.

Class $21a^4$, 71. No. 128062. O. S. Poturayev. Method of determining the parameters of transistors in common-emitter switching operation.

Class $21a^4$, 71. No. 128063. V. A. Zotov. Semi-coaxial cavity resonator.

Class $21a^4$, 72_{04}. No. 127711. P. G. Surovov and Ye. V. Golitsyn. Antenna switch.

Class 21c, 7_{05}. No. 127714. Ya. I. Parkhomchuk. Tool for removing metal-hose shield from cable.

Class 21c, 7_{05}. No. 127715. T. K. Tsogoyev. Device for stripping insulation from ends of wire.

Class 21c, 46_{05}. No. 128067. L. M. Bernshteyn, Yu. M. Zbarskiy,

G. M. Karachun, I. I. Knyazhitskiy, O. G. Tenner and G. Ya. Pribluda. Program control system.

Class 21c, 47_{01}. No. 127307. I. I. Mikhaylov. Transformer decoder.

Class $21d^2$, 12_{03}. No. 128072. Ya. M. Chervonenkis. Method of controlling electron tubes in current converters.

Class 21e, 11_{10}. No. 127748. "First of May" Enterprise No. 828. Electromagnetic oscillograph.

Class 21e, 11_{12}. No. 127324. N. A. Uvarov, V. M. Gorbachev and L. L. Usenko. Method of reproducing images of electrical processes by means of twin-trace oscillograph.

Class 21e, 28_{02}. No. 127328. Yu. B. Shaub. Method for direct viewing of one or several electrical vectors on the screen of a cathode-ray oscilloscope.

Class 21e, 28_{02}. No. 127329. V. A. Baramidze. Generator of linearly rising voltage.

Class 21e, 29_{03}. No. 127751. A. V. Aleksandrov, L. Ya. Davidchuk, V. I. Sintsin and M. N. Chetverikov. Device for measurement of capacitance.

Class 21e, 36_{03}. No. 127332. V. S. Golub. Method of measuring the phase difference of two voltages.

Class 21e, 36_{03}. No. 127754. A. I. Fyurstenberg. Method for frequency comparison of two sinusoidal voltages.

Class 21e, 36_{10}. No. 127755. A. I. Il'yenkov. Method of reproducing the dynamic characteristic of nonlinear elements (e. g., voltage regulators) on an oscillograph screen.

Class 21e, 37_{03}. No. 127333. I. V. Kudryatsev. Method of testing stranded cables and deenergized circuits for insulation defects and a device for this purpose.

Class 21g, 11_{03}. No. 128081. P. P. Fomin. Full-wave phase-sensitive bridge rectifier.

Class 21g, 13_{06}. No. 127335. A. L. Lyam. Electron tube with two control grids.

Class 21g, 13_{50}. No. 127762. K. P. Ivanitskiy and N. I. Itkin. Method of measuring distortion factor in electronic tuning of klystrons.

Class 21g, 13_{50}. No. 127763. R. S. Medvedev. Method of testing dielectric strength of insulation of vacuum-tube electrodes.

Class 21g, 14_{20}. No. 127337. N. N. Chuzo. Method of extinguishing cold-cathode thyratrons.

Class 21g, 28_{02}. No. 128084. N. I. Sazonov. Power supply for devices and equipment.

Class 21g, 34. No. 128085. G. P. Bogdanovich. Band-elimination stage.

Class 21g, 36. No. 127340. V. F. Sikolenko, V. N. Rybin, A. S. Nasibov, Z. A. Yuzhaninova, Ya. R. Abas-ogly and I. S. Kurochkina. Electrical pulse generator.

Class 21g, 38. No. 128086. I. B. Grinberg and O. N. Mel'nikov. Converter for conversion of direct current into a pulse train.

Class 42d, 1_{12}. No. 127433. R. G. Karpov. Device for obtaining the sum of two pulse trains.

Class 42d, 3_{25}. No. 127829. O. K. Skikevich. Device for twin-beam photographic recording.

Class 42d, 3_{50}. No. 127830. O. K. Skikevich. Method of recording and reproducing electrical signals.

Class 42d, 10. No. 128160. S. A. Doganovskiy. Delay line.

Class 42g, 10_{01}. No. 127446. M. G. Arutyunov. Magnetic head for

sweep recording and playback.

Class 42g, 10_{01}. No. 128166. Pending decision on author's certificate No. 120928. S. P. Khlebnikov. Method of reproduction of varipolar pulse signals with increased signal-to-noise ratio.

Class 42g, 18. No. 127836. V. I. Pereverzev. Device for investigation of magnetic recording.

Class 42h, 1_{03}. No. 127447. D. T. Gaydayenko. Lens for magnification of television image.

Class 42l, 14. No. 127478. V. A. Afanas'yev. Ferrite-transistor decoder.

Class 42m, 14. No. 127859. I. A. Radkevich, V. V. Sokolovskiy and N. S. Rezvyakov. Method of decreasing "background noise" of magnetic drum.

Class 42m, 14. No. 127860. F. A. Truten'. Electronic computing unit.

Class 42m, 14. No. 127861. B. V. Anichkin. Magnetic head for recording of code pulses.

Class 42m, 14. No. 127864. M. I. Petrukhin, L. A. Golubev and G. F. Kucherov. Adder with ferrite-transistor cells.

Class 42m, 14. No. 128206. R. G. Karpov. Device for summation of several pulse trains.

Class 42n, 11_{03}. No. 127481. M. I. Kal'neko. Vacuum-tube model.

US Patent, Cl. 178-26, No. 2915585, 01.12.59. Zenner. (Teletype Corp.) System and apparatus for transmitting and phasing telegraph signals. Patenting a design of transmitter and reperforator for transmission of information in an eight-element code system with its transformation to a five-element teletype system.

British patent, Cl. 40(2), 100(1), No. 833549, 27.04.60. Willis, Skinner. (The Decca Record Co. Ltd.) Improvements in or relating to magnetic tape recording and or reproducing apparatus. Proposes an improvement in transport mechanism in electronic computers with magnetic memory.

US patent, Cl. 178-6.6, No. 2907818, 06.10.59. Wetzel. (Minnesota Mining and Manufacturing Co.) 24-channel system for magnetic recording of television signals.

US patent, Cl. 315-24, No. 2913623, 17.11.59. Studebaker. (International Telephone and Telegraph Corp.) Cathode-ray tube system. Scheme for correction of transcendental distortions of raster in memory tubes.

US patent, Cl. 178-5.1, No. 2909592, 20.10.59. Morris, Roschke. (Zenith Radio Corp.) Subscription television system.

US patent, Cl. 178-5.4, No. 2917574, 15.12.59. Single-tube pickup camera for color television.

US patent, Cl. 315-20, No. 2913621, 17.11.59. Luther, Baun. (Radio Corp. of America.) Protection system for cathode-ray tubes. Proposes a system which disconnects the power transformer upon overloading in order to protect the kinescope.

US patent, Cl. 178-6.6, No. 2921976, 19.01.60. Recording of color television signals on magnetic tape. Reproducing color television chrominance signals. (Minnesota Mining and Manufacturing Co.)

US patent, Cl. 179-6.5, No. 2921980, 19.01.60. (General Telephone Labs, Inc.) Prepay-postpay paystation telephone arrangement. Local calls paid before dialing, long-distance calls paid upon instruction from operator.

US patent, Cl. 315-39.63, No. 2897401, 28.07.59. Kumpfer. (United States of America as represented by the Secretary of the Army.) Magnetron amplifier. Proposes a two-cavity magnetron amplifier with high

gain and efficiency. May be used in pulse radar applications. Self-excitation is completely eliminated in input and output cavities and there is no reaction of output circuit on input.

US patent, Cl. 343-100, No. 2864204, 25.11.58. Henrici, Shaklin. (Collins Radio Corp.) Countermeasure system. Proposes a receiving system for determining the presence of radio signals over a wide range of frequencies with simultaneous indication of direction to the signal source.

West German patent, Cl. $21a^2$, 18/08, (H 03 f), No. 1055051, 01.10.59. Poppinger. (Siemens-Schuckertwerke Akt.-Ges.) Magnetischer Kippverstärker mit Gegentaktverhalten. Proposes a system similar to a differential vacuum-tube amplifier distinguished by high stability in the presence of power-line fluctuations. Employs the advantages of magnetic amplifiers, namely low input impedance.

US patent, Cl. 250-27, No. 2905819, 22.09.59. Kleinman. (Avco Manufacturing Corp.) Linear sawtooth wave generator. Linearity of output voltage is achieved by automatic control of voltage in cathode follower, insuring constancy of capacitor current charging.

US patent, Cl. 179-1, No. 2903515, 08.09.59. Smith. (United States of America represented by the Secretary of the Air Force.) Device for selective compression and automatic segmentation of speech. The relative level of consonants is raised by compression of vowels.

US patent, Cl. 178-19, No. 2919305, 29.21.59. Ridings. (The Western Union Telegraph Co.) Teleautograph system. Patents a device for two-wire transmission of written text, drawings, maps, etc.

BIBLIOGRAPHY

1. General problems of radio engineering
2. Radio communications
3. Radio-wave propagation
4. Antennas
5. Microwave techniques
6. Oscillators
7. Wire communications
8. Television
9. Radio broadcasting
10. Vacuum-tube devices
11. Semiconductor devices
12. Measurement techniques

---

1. GENERAL PROBLEMS OF RADIO ENGINEERING

Rouge, L. J. D. Electronic Progress — Circa 1960. IRE Internat. Convent. Record, 1960, Vol. 8, Part 6, pp. 158-164, ill.

Equations for certain nonlinear radio engineering circuits. Rizkin, I. Kh., "News of Higher Educational Institutions," Radiotekhnika, 1960, Vol. 3, VII-VIII, No. 4, pp. 501-505, ill., bibl. (5 titles).

The question of choice of initial frequencies in interpolation converters. Guk, I. M., "News of Higher Educational Institutions," Radiotekhnika, 1960, Vol. 3, V-VI, No. 3, pp. 342-349, ill., bibl. (6 titles).

Method for simplifying filter design. Lichtenfeld, K., Electronics, 1960, Vol. 33, V, No. 21, pp. 96-99, ill., bibl. (2 titles).

Phase-sensitive demodulation with interpolation. Johnston, J. S., Electronic Engineering, 1960, Vol. 32, VII, No. 390, pp. 488-490, ill., bibl. (3 titles).

Precise L-C comb filters packaged for reliability. Lisbin, D. M., IRE Trans. on Component Parts, 1960, Vol. CP-7, VI, No. 2, pp. 44-49, ill.

Broadband UHF distributed amplifiers using bandpass filter techniques. Thompson, E. C., IRE International Conv. Rec., 1960, Vol. 8, Part 2, pp. 139-148, ill., bibl. (10 titles).

2. RADIO COMMUNICATIONS

Providing communication and navigation for space probes. Hansen, R. C. and Spangler, E. R., Electronics, 1960, Vol. 33, VII, No. 28, pp. 43-47, ill.

Experiments set pattern for earth-based communication system. Teleph. Engr. Management, 1960, Vol. 64, V, No. 9, pp. 37-40, ill.

New VL to reach all Polaris subs. Electronics, 1960, Vol. 33, No. 29, pp. 34-35, ill.

Pacific scatter system completed. Electronics, 1960, Vol. 33, VI, No. 29, p. 39. ill.

The TJ radio relay system. Gammie, J. and Hathaway, S. D., Bell Syst. Tech. J., 1960, Vol. 39, VII, No. 4, pp. 821-877, ill., bibl. (14 titles).

Magnetostrictive ultrasonic delay lines for a PCM communication system. Aaronson, D. A. and James, D. B., IRE Internat. Convent, Rec., 1960, Vol. 8, Part 6, pp. 173-179, ill., bibl. (7 titles).

Common-aerial transmission and reception at VHF. Hyams, A. J., Electronic Engineering, 1960, Vol. 32, VIII, No. 390, p. 514, ill., bibl. (2 titles).

A personal two-way VHF radio communication system featuring modular construction. Yaffe, T. H., IRE Wescon Convent, Rec., 1960, Part 7, pp. 74-77, ill.

Lunar echoes received on space receivers at 106.1 Mc. Dyce, R. V., Proc. IRE, 1960, Vol. 48, V, No. 5, pp. 934-935.

Fire prevention or fire fighting. Yarbrough, L. A. and Worthington, J. W., IRE Internat. Convent, Rec., 1960, Vol. 8, Part 6, pp. 54-64, ill., bibl. (2 titles).

A general technique for interference filtering. Stirrat, W. A., IRE Trans. on Radio Frequency Interference, 1960, Vol. RFI-1, V, No. 2, pp. 12-17, Bibl. (4 titles).

3. RADIO WAVE PROPAGATION

Propagation of extremely long radio waves over the earth's surface. White, Zarubezh. radioelektronika [Foreign Radio Electronics], 1960, IX, No. 9, pp. 50-83, ill., bibl. (abbrev. translation).

On the mode theory of very-low-frequency propagation in the presence of a transverse magnetic field. Crombie, D. J., J. Res. of NBS, Sec D — Radio propag., 1960, Vol. 64D, V-VI, No. 3, pp. 265-267.

VLF propagation effects of D-region Layer produced by cosmic rays. Moler, W. F., J. Geophys. Res., 1960, Vol. 65, No. 5, V, pp. 1459-1468, ill., bibl.

On a method of measuring the coefficient of reflection from the earth and from inversion layers. Sazonov, A. I., "News of Higher Educational Institutions, Radiotekhnika, 1960, Vol. 3, VII-VIII, No. 4, pp. 517-518, ill., bibl. (7 titles).

Focusing, defocusing and refraction in a circularly stratified atmosphere. Toman, K., J. Res. of NBS, Sec D — Radio Propag., 1960, Vol. 64D, V-VI, No. 3, pp. 287-288, ill.

On the calculation of the Departures of radio wave bending from normal. Bean, B. R. and Dutton, E. J., J. Res. of NBS, Sec D — Radio Propag., 1960, Vol. 64D, V-VI, No. 3, pp. 259-263, bibl. (22 titles).

Experimental proof of focusing at the skip distance by backscatter records. Bibl. K., Proc. IRE, 1960, Vol. 48, V, No. 5, pp. 956-957, ill.

Polarization parameters of the downcoming radio wave. Murty, Y. S. N. and Khastgir, S. R., J. Geophys. Res., 1960, Vol. 65, V, No. 5, pp. 1149-1457, bibl.

Ionospheric backscatter observation at 440 Mc. Pineo, V. C. et al., J. Geophys. Res., 1960, Vol. 65, V, No. 5, pp. 1620-1621, ill., bibl.

On the theory of reflection of low- and very-low-frequency radio waves from the ionosphere. Johlir, J. R. and Walters, L. C., J. Res. of NBS, Sec D — Radio Propag., 1960, Vol. 64D, V-VI, No. 3, pp. 269-285, ill., bibl. (13 titles).

A preliminary study of radiometeorological effects on beyond-horizon

propagation. Ikegami, F., J. Res. of NBS, Sec D — Radio Propag., 1960, Vol. 64D, V-VI, No. 3, pp. 239-246, ill., bibl. (13 titles).

A theory of wavelength dependence in ultrahigh-frequence trans-horizon propagation based on meteorological considerations. Bolgiano, R., J. Res. of NBS, Sec D — Radio Propag., 1960, Vol. 64D, V-VI, No. 3, pp. 231-237, ill., bibl. (24 titles).

An analysis of propagation measurements made at 413 Mc/sec well beyond the radio horizon. Janes, H. B. et al., J. Res. of NBS, Sec D — Radio Propag., 1960, Vol. 64D, V-VI, No. 3, pp. 255-257.

4. ANTENNAS

The log-periodic antenna. Graf, C. R., Electronics World, 1960, Vol. 63, V, No. 5, pp. 100-101, ill., bibl.

A broadband 160-Mc colinear array. Yang, R. H. and Hansen, L. H., IRE Wescon Convent, Rec., 1960, Part 7, pp. 51-53, ill. bibl. (2 titles).

On the problem of decoupling of slot antennas by means of an impedance structure in the slot plane. Tereshin, O. N. and Belov, A. S., "News of Higher Educational Institutions," Radiotekhnika, 1960, Vol. 3, V-VI, No. 3, pp. 359-365, ill., bibl. (3 titles).

Antenna design for maximum L-F radiation. Monser, G. L. and Sabin, W. D., Electronics, 1960, Vol. 33, VI, No. 23, pp. 84-86, ill., bibl. (6 titles).

Design of corner reflector antennas. Technical News Bulletin of NBS, 1960, Vol. 44, V, No. 5, pp. 87-88, ill.

Determination of the optimum antenna pattern for a signal burst communication system. Lux, P. A., et al., IRE Wescon Convent. Rec., 1960, Part 7, pp. 17-26, ill., bibl. (titles).

Theory and performance of vehicular center-fed whip antenna. Brueckmann, H., IRE Wescon Convent. Rec., 1960, Part 7, pp. 40-50, ill., bibl. (4 titles).

On the problem of maximum attainable gain of a microwave antenna. Vorob'yev, Ye. A., "News of Higher Educational Institutions," Radiotekhnika, 1960, Vol. 3, VI-VIII, No. 4, pp. 471-476, ill., bibl. (5 titles).

Modern microwave antennas. Electronics, 1960, Vol. 33, VI, No. 26, pp. 74-77 ill.

Metal-plastic retarding lens. Polyanina, G. D. "News of Higher Educational Institutions," Radiotekhnika, 1960, Vol. 3, VII-VIII, No. 4, pp. 515-516, ill., bibl. (3 titles).

Effects of tower and guys on performance of side-mounted vertical antennas. Yang, R. G. H., and Willis, F. R., IRE Wescon Convent, Rec., 1960, Part 7, pp. 54-61, ill., bibl.

"Automatic Defrosting" for microwave relay antenna. Electrical Engineering, 1960, Vol. 79, V, No. 5, p. 434, ill.

5. MICROWAVE TECHNIQUES

Modern microwave components. Loaded waveguide. Electronics, 1960, Vol. 33, VI, No. 26, p. 82.

Modern microwave components. Circulators. Electronics, 1960, Vol. 33, VI, No. 26, pp. 82-83, ill.

Modern microwave components. Other ferrite devices. Electronics, 1960, Vol. 33, VI, No. 26, pp. 83-84, ill.

Certain problems in the propagation of electromagnetic waves in folded waveguides loaded by periodic structures. Morozov, B. N., "News of Higher Educational Institutions," Radiotekhnika, 1960, Vol. 3, VII-VIII, No. 4, pp. 495-500, ill., bibl. (10 titles).

Periodic and guiding structures at microwave frequencies. Harvey, A. F., IRE Trans. on Microwave Theory and Techniques, 1960, Vol. MTT-8, I. No. 1, pp. 30-61, ill., bibl. (293 titles).

Wideband phase shifter. Ahmed, A. A., Proc. IRE, 1960, Vol. 48, V, No. 5, p. 945, ill.

Electronically variable phase shifters utilizing variable capacitance diodes. Harden, R. H., et al., Proc. IRE, 1960, Vol. 48, V, No. 5, pp. 944-945, ill.

A new semiconductor microwave modulator. Jacobs, H., et al., IRE, Internat. Convent. Rec., 1960, Vol. 8, Part 3, pp. 155-159.

The diode-loaded helix as a microwave amplifier. Conrad, G., et al., Proc. IRE, 1960, Vol. 48, V, pp. 939-940, ill.

Noise figure of reactive converters and parametric amplifiers. Van der Zil, Zarubezh. radioelektronika, 1960, IX, No. 9, pp. 120-121, ill., bibl. (3 titles).

Bandwidth of lower sideband parametric up-converters and parametric amplifiers. Fisher, S. T., Proc. IRE, 1960, Vol. 48, V, No. 5, pp. 496.

Parametric phase distortionless L-band limiter. Sutherland, A. D. and Countiss, D. E., Proc. IRE, 1960, Vol. 48, V, No. 5, pp. 938-939, ill.

A ferromagnetic amplifier using longitudinal pumping. Denton, R. T., Proc. IRE, 1960, Vol. 48, V, No. 5, pp. 937-938, ill.

Modern microwave generators and amplifiers. Low-noise devices. Electronics, 1960, Vol. 33, VI, No. 26, pp. 78-79, ill.

Modern microwave generators and amplifiers. Klystron. Electronics, 1960, Vol. 33, VI, No. 26, p. 80.

The role of space-charge waves in modern microwave devices, Sims, G. D. and Stephenson, I. M., Electronic Engineering, 1960, Vol. 32, VII, No. 389, pp. 408-412; VIII, No. 390, pp. 499-503, ill., bibl.

On the large-signal aspect of the broadband multicavity klystron problem — theory and experiment. Yadavalli, S. V., Proc. IRE, 1960, Vol. 48, V, No. 5, pp. 953-954, ill.

On increasing the efficiency of microwave devices by retarding electrons at the collector. Gekker, I. R., "News of Higher Educational Institutions," Radiotekhnika, 1960, Vol. 3, VII-VIII, No. 4, pp. 440-447, ill., bibl. (8 titles).

GaAs reactance generates millimeter waves. Heilmeier, R. H., Electronics, 1960, Vol. 33, VII, No. 29, pp. 82-85 ill., bibl. (6 titles).

Noise measurements on an M-type backward-wave amplifier. Anderson, J. R., Proc. IRE, 1960, Vol. 48, V, No. 5, pp. 946-947, ill.

6. OSCILLATORS

Frequency control of crystal oscillator with series-controlled circuit. Servinskiy, Ye. G., "News of Higher Educational Institutions," Radiotekhnika, 1960, Vol. 3, VII-VIII, No. 4, pp. 477-484, ill., bibl. (3 titles).

Increasing the thermal stability of precision crystal resonators. Plonskiy, A. F., "News of Higher Educational Institutions," Radiotekhnika, 1960, Vol. 3, V-VI, No. 3, pp. 326-336, ill., bibl. (14 titles).

Piezoelectric excitation of quartz oscillations by means of a parallel

field. Bechmann R. Arch. elekt. Ubertragung, 1960, Vol. 14, VII, No. 8, pp. 361-365, ill., bibl. (6 titles).

Oscillator with gas-discharge tubes. Funkschau, 1960, IX, No. 18, p. 460, ill.

A low-frequency noise generator. Slater, N. T., Electronic Engineering, 1960, Vol. 32, VIII, No. 390, pp. 473-475, ill., bibl. (3 titles).

7. WIRE COMMUNICATIONS

Evaluation of message circuit noise. Aikens, A. J., and Lewinski, D. A., Bell System Tech. J., 1960, Vol. 39, VII, No. 4, pp. 879-909, ill., bibl. (16 titles).

A new measuring set for message circuit noise. Cochran, W. T., and Lewinski, D. A., Bell System Tech. J., 1960. Vol. 39, VII, No. 4, pp. 911-931, ill., bibl. (3 titles).

Telescriber aids plant department. Reed, J. S., Teleph. Engr. Management, 1960, Vol. 64, V, No. 9, pp. 52-65, ill.

Cable reliability in ground guided missile systems. Spergel, J., and Godwin, E. F., IRE trans. on Component Parts, 1960, Vol. CP-7, VI, No. 2, pp. 54-60, ill.

Pressure at the interface of inner conductor and dielectric of armorless ocean cable. Bhuta, P. G., Bell Syst. Tek. J., 1960, Vol. 39, V-II, No. 4, pp. 963-972, ill., bibl. (5 titles).

8. TELEVISION

Noise calculation in television channels. Ushakov, M. A. Tekhn. kino i televideniya, 1960, X, No. 10, pp. 57-60, ill., bibl. (4 titles).

Principal direction for further improvement of television receivers. Efrussi, Ya., I., Tekhn. kino i televideniya, 1960, X, No. 10, pp. 40-48, ill., bibl. (8 titles).

Origin and compensatibility of noise from flyback in TV cameras with vidicon. Schneider, H. D., Electron. Rundschau, 1960, IX, No. 9, pp. 367-368, 371, ill.

Choice of equisignal pedestal chrominance for color television system. Yefimkin, V. I., Tekh. kino i televideniya, 1960, IX, No. 9, pp. 62-64, ill., bibl. (15 titles).

Influence of image subject on choice of tint color of picture tube in black-and-white and color television. Novakovskiy, S. V. and Isayev, A. N., Tekh. kino i televideniya, 1960, IX, No. 9, pp. 58-62, ill., bibl. (6 titles).

Operating principles and advantages of SECAM color television system. Chaste, R. and Cassagne, P., Elektron. Rundschau, 1960, IX, No. 9, pp. 361-362, ill.

Single-gun vs three-gun tubes: their influence on color receiver design. Jackson, R. N., J. Telev. Soc, 1960, Vol. 9, IV-VI, No. 6, pp. 207-222, ill., bibl. (10 titles).

New process gives larger, squarer TV picture. Electrical Engineering, 1960, Vol. 79, V, No. 5, pp. 438-439, ill.

Heads for magnetic recording and reproduction of video signals. Vasilevskiy, Yu. A., Tekh. kino i televideniya, 1960, X, No. 10, pp. 30-39, ill.

9. RADIO BROADCASTING

Bilingual multiplex. Landon, N., Electronics, 1960, Vol. 33, VI, No. 23, p. 87, ill.

Technical requirements for FM stereophonic multiplex broadcasting. IRE Wescon Convent. Rec., 1960, Part 7, pp. 36-39.

On principles for construction of systems for automatic control of operating quality of broadcasting installations. Glukhov, A. A., "News of Higher Educational Institutions," Radiotekhnika, 1960, Vol. 3, VII-VIII, No. 4, pp. 463-470, ill., bibl. (9 titles).

Precision measurement of wow and flutter. Mullin, J. T., Electronics, 1960, Vol. 33, No. 26, pp. 100-102, ill.

10. VACUUM-TUBE DEVICES

New tube construction simplifies circuitry. Electronics, 1960, Vol. 33, VII, No. 28, pp. 70-73, ill.

High average power dissipation in helix tubes. Iverson, A. H., IRE Trans. on Electron Devices, 1960, Vol. ED-7, IV, No. 2, pp. 74-77, ill.

Low-wattage planar cathode. Chin, T. N., RCA Rev., 1960, Vol. 21, VI, No. 2, pp. 191-198, ill.

New pentode PL500 for horizontal sweep output. Radioschau, 1960, IX, No. 9, p. 336, ill.

New television tubes produced by West German firms. Kunze F., Radio und Fernsehen, 1960, VII, No. 14, pp. 450-451, ill.

New CRT provides advanced method of electronic reproduction. Electronics and Communications, 1960, VII, No. 7, pp. 34-35, ill.

New picture-tube designs. Kuzne, F., Radio und Fernsehen, 1960, IX, No. 17, pp. 536-537, ill.

11. SEMICONDUCTOR DEVICES

Tunnel diodes. Operation and Application Electronic Technology, 1960, Vol. 37, VI, No. 6, pp. 217-222, ill., bibl. (6 titles).

Frequencies of 4000 Mc claimed for tunnel diodes. Electronics and Communications, 1960, VI, No. 6, pp. 56-57, 70, ill.

Transient response of variable capacitance diodes. Schulz, D., IRE Trans. on Component Parts, 1960, Vol. CP-7, VI, No. 2, pp. 49-53, ill.

Gallium arsenide microwave diode at X band. Herndon, M., Proc. IRE, 1960, Vol. 48, V, No. 5, pp. 945, ill.

Noise figure of tunnel diode mixer. Breitzer, D. I., Proc. IRE, 1960, Vol. 48, V, No. 5, pp. 935-936, ill.

Approximate expressions for the alpha-cutoff frequency of the drift transistor. Aitchison, R. E., Proc. IRE Austr., 1960, Vol. 21, VI, No. 6, pp. 413-414.

On the frequency characteristics of alloyed-junction transistors. Paul, R., Nachrichtentechnik, 1960. VIII, No. 8, pp. 340-347, ill., bibl. (20 titles).

An NPN fusion alloy silicon transistor for "avalanche mode" operation. Wonson, R. C. and McCarthy, W. A., IRE Internat. Convent. Rec., 1960, Vol. 8, Part 3, pp. 10-16, ill., bibl. (4 titles).

15-watt microalloy diffused-base transistor. Miles, T. J. and Sluss, J. A., IRE Internat. Convent. Rec., 1960, Vol. 8, Part 3, pp. 3-9, ill.

Charge analysis of transistor operation. Baker, A. N., Proc. IRE, 1960, Vol. 48, V, No. 5, pp. 949-950.

On the use life of transistors. Radio und Fernsehen, 1960, VIII, No. 16, pp. 521-522, bibl. (4 titles).

Equivalent diagram of spacistor amplifier. Zakharov, A. Ya., "News of Higher Educational Institutions," Radiotekhnika, 1960, Vol. 3, V-VI, No. 3, pp. 309-318, ill., bibl. (2 titles).

On the frequency characteristics of the spacistor. Zakharov, A. L., "News of Higher Educational Institutions," Radiotekhnika, 1960, Vol. 3, VII-VIII, No. 4, pp. 431-440, ill., bibl. (5 titles).

12. MEASUREMENT TECHNIQUES

New line-impedance stabilization of networks for conducted radio interference measurements up to 100 megacycles. Oishi, K., IRE Trans. on Radio Frequency Interference, 1960, Vol. RFI-1, V, No. 2, pp. 2-6 ill.

High Q wavemeter design. Goodenough, E. F., Marconi Rev., 1960, Vol. 23, No. 137, pp. 85-98, ill.

Z-axis marker generator for bandpass circuit alignment. Odorizzi, D. J., Electronics, 1960, Vol. 33, VI, No. 26, pp. 108-110, ill.

UHF wobbler with passive marker. Bornträger, G., Funk-Technik, 1960, IX, No. 18, pp. 644-646, ill., bibl. (2 titles).

Feedback stabilizes signal generator. Fong, A., Electronics, 1960, Vol. 33, VII, No. 29, pp. 71-73, ill.

Distortion of pulse edge due to finite transit time between parallel deflecting plates (oscillograph). Lotsch, H., Frequenz, 1960, Vol. 14, VIII, No. 8, pp. 264-268, ill., bibl. (12 titles).

Heathkit Q meter. Funkschau, 1960, VIII, No. 15, pp. 397-398, ill.

TELECOMMUNICATIONS

1961

A.S. Popov Technical Society of Radio Engineering and Telecommunications
Svyaz'izdat, Moscow

EDITORIAL BOARD

A. Ch. Pukhal'skiy, Editor

B.F. Anosovich
S.V. Borodich
N.I. Chistyakov
A.D. Fortushenko
P.T. Gobets
I. Ye. Golubtsov
V.A. Kuz'min
G.A. Levin
Ye. V. Markhay
Ye. S. Medvedev
Ye. A. Rizkin
P.V. Shmakov
V.M. Shteyn
N.N. Shumskaya
V.I. Siforov
B.P. Terent'yev
G.S. Tsykin
N.B. Zeliger
E.V. Zelyakh

The English Edition of Telecommunications is mailed to subscribers within 18 weeks after the publication of the original Russian issue.

Russian Electronic Journals published by the
American Institute of Electrical Engineers
Translated by Royer and Roger, Inc.

	Subscription rates			
	Individuals		Libraries	
	$	£	$	£
Telecommunications	14.25	5	28.50	10
Radio Engineering and Electronics	28.50	10	57.00	20
Radio Engineering	14.25	5	28.50	10

Royer and Roger translates and produces
the following Russian scientific journals:

Biophysics
Entomological Review
Geochemistry
Geodesy and Cartography
Izvestiya, Academy of Sciences of the USSR, Geologic Series
Pavlov Journal of Higher Nervous Activity
Problems of Oncology
Radio Engineering
Radio Engineering and Electronics
Refractories
Sechenov Physiological Journal of the USSR
Soil Science
Telecommunications

Comments and inquires regarding *Telecommunications* and other translation journals should be sent to:

International Division
Royer and Roger, Inc.

1000 Vermont Avenue, N.W.
Washington 5, D.C.

41 East 28th Street
New York 16, New York

TELECOMMUNICATIONS
ЭЛЕКТРОСВЯЗЬ

NUMBER 2 1961

CONTENTS

Page

V.L. Rychka: Passage of FM Oscillations Through Aperiodic Amplifier 1

V.A. Solov'yev: Miniature Delay Line with High Resolution 11

V.D. Kusnetsov and V.K. Paramonov: System for Control of Radiation Pattern of Complex Wideband Antenna with Low Side-Lobe Level 24

M.A. Berg and S.A. Garyainov: Negative-Resistance Semiconductor Devices 32

A.A. Rizkin: Calculation of Transistorized Video Amplifiers 45

O.F. Kosminskiy: Calculation of Two-Terminal L-Section Equalizers for Amplifier Gain Control 58

G.I. Leviman and O.I. Vostryakov: Synthesis of Polynomial Bandpass Filters with Chebyshev Selectivity Characteristic 66

V.G. Bosenko and G.Z. Maksimov: Contactless Units for Trunk Line with Multiplex KRR-30/60 80

Author's Certificates and Foreign Patents 85

Bibliography 90